Aus dem Interfakultären Institut für Biochemie
der Universität Tübingen
Abteilung für Molekulare Medizin

NF-κB regulator IκB$_{NS}$ in macrophages and diffuse large B cell lymphomas

**Inaugural-Dissertation
zur Erlangung des Doktorgrades
der Medizin**

**der Medizinischen Fakultät
der Eberhard Karls Universität
zu Tübingen**

vorgelegt von

Keller, Ronald

2019

Dekan: Professor Dr. I. B. Autenrieth

1. Berichterstatter: Professor Dr. K. Schulze-Osthoff
2. Berichterstatter: Professor Dr. U. Lauer

Tag der Disputation: 12.03.2019

Table of contents

1. Figures

2. Tables

3. Abbreviations

ABC	Activated B cell-like
AIDS	Acquired immunodeficiency syndrome
AP-1	Activator protein 1
APC	Allophycocyanin
APS	Ammonium persulfate
BCL	B cell lymphoma
BCR	B cell receptor
Blimp-1	B-lymphocyte-induced maturation protein 1
CAPS	CIAS1-related auto-inflammatory syndrome
Cas	CRISPR-associated
CCL	C-C-chemokine ligand
CCR	C-C- chemokine receptor
CD	Cluster of differentiation
cDNA	Complementary DANN
CHIP	Chromatin immunoprecipitation
CIAS	Cold induced auto-inflammatory syndrome
CMV	Cytomegalovirus
cMyc	Cancer-related myelocytomatosis oncogen
CRISPR	Clustered regularly interspaced short palindromic repeats
CSF2R	GM-CSF receptor
CXCL	C-X-C-chemokine ligand
CXCR	C-X-C-chemokine receptor
DAMP	Damage associated molecular pattern
DC	Dendritic cell
DD	Death domain
DLBCL	Diffuse large B cell lymphoma
DMEM	Dulbecco's modified eagle medium
DMSO	Dimethyl sulfoxide
DNA	Deoxyribonucleic acid
Dox	Doxycycline
dsDNA	Double-stranded DNA
DSS	Dextran sulfate sodium
DTT	Dithiothreitol
DUSP	Dual-specificity phosphatase
ECL	Enhanced chemoluminiscence
EDTA	Ethylendiamintetraacetate
ELISA	Enzyme-linked immunosorbent assay
ERK	Extracellular-signal regulated kinase
FACS	Fluorescence-activated cell sorting
FADD	Fas-associated death domain
FCS	Fetal calf serum
FDC	Follicular dendritic cell
FITC	Fluorescein isothiocyanate
FoxP3	Forkhead-Box-Protein P3
GCB	Germinal center B cell-like
GFP	Green fluorescent protein
GM-CSF	Granulocyte and macrophage colony stimulating factor
HBS	2-(4-(2-Hydroxyethyl)-1-piperazinyl)-ethansulfonic acid -buffered saline

HEPES	4-(2-Hydroxyethyl)piperazine-1-ethanesulfonic acid
HEPES	2-(4-(2-Hydroxyethyl)-1-piperazinyl)-ethansulfonic acid
HIF	Hypoxia induced factor
HIV	Human immunodeficiency virus
IC	Inflammatory cytokines
IFNβ	Interferon-β
IFNγ	Interferon-γ
IgG	Immunoglobulin G
IKK	IκB kinase
IL	Interleukin
IL1RA	IL1 receptor antagonist
INK4-ARF	Inhibitors of CDK4-alternate reading frame
IRAK	Interleukin 1-receptor associated kinase
IRES	Internal ribosomal entry site
IRF	Interferon response factor
IκB	Inhibitor of κB
JAK	Janus kinase
KLF	Kruppel-like factor
LB	lysogeny broth
LDL	Low density lipoprotein
LPS	Lipopolysaccharid
LRR	Leucine-rich-repeat-motif
LTR	Long terminal repeat
MAPK	Mitogen-activated protein kinase
M-CSF	Macrophage colony stimulating factor
MHC II	Major histocompatibility complex II
MIF	Macrophage migration inhibitory factor
MyD88	Myeloid differentiation primary response protein 88
MZ B cell	Marginal zone B cell
NF-κB	'kappa-light-chain-enhancer' of activated B cells
NLS	Nuclear localization sequence
PAMP	Pathogen-associated molecular patterns
PBS	Phosphate-buffered saline
PCR	Polymerase chain reaction
PDL	Programmed death-ligand
PE	Phycoerythrin
PI-3K	Phosphoinositid-3-kinase
PMA	Phorbol 12-myristate 13-acetate
PMBL	Primary mediastinal B cell lymphoma
PTEN	Phosphatase and tensin homolog
Raf	Rat fibrosarcoma
Ras	Rat sarcoma
RelA	v-rel avian reticuloendotheliosis viral oncogene homolog A
RelB	v-rel avian reticuloendotheliosis viral oncogene homolog B
RHD	Rel-homology domain
RIP1	Serine/threonine kinase receptor-interacting protein 1
RNA	Ribonucleic acid
RPMI	Roswell Park Memorial Institute
RT	Reverse transcription
rtTA	Reverse tetracycline transactivator protein of TetOn-system
SD	Standard deviation

SDS	Sodium dodecyl sulfate
SDS-PAGE	Sodium dodecyl sulfate polyacrylamide gel electrophoresis
SOCS	Suppressor of cytokine signaling
ssRNA	Single-stranded RNA
STAT	Signal transducer and activator of transcription
TAD	Transactivation domain
TAK	TGF-β-activated kinase
TANK	TRAF associated NFκB activator
TBK	TANK-binding kinase
TCR	T-cell receptor
TEMED	Tetramethylenediamine
TIR	Toll-Interleukin 1 receptor domain
TIRAP	Toll-Interleukin 1 receptor domain containing adaptor protein
TLR	Toll-like-receptor
TNF-α	Tumor necrosis factor-α
TRAF	Tumor necrosis factor-α associated factor
TRAM	TRIF-related adaptor molecule
TRE	Tet-responsible element
Treg	Regulatory T-cell
TRIF	TIR-domain-containing adapter-inducing interferon-γ
Tween	Polysorbat 20
VEGFα	Vascular endothelial growth factor

4. Abstract

Innate immunity is one of our first lines of defense of the organism against invading pathogens. One cell type of the innate immune system consists of macrophages, which recognize a highly conserved set of structures on pathogens by specific receptors and initialize the unspecific and specific immune response by secreting signaling molecules with pro-inflammatory and chemotactic effects. A key signaling mediator of the primary immune response is the transcription factor NF-κB. NF-κB proteins are sequestered by classical IκB proteins in the cytoplasm of resting cells, but are released after cellular activation and degradation of the IκB. NF-κB is also regulated by atypical IκB proteins that can only be found in the nucleus of activated cells. One member of this atypical IκB protein family is $I\kappa B_{NS}$, which is the main focus here.

This project aimed to elucidate the effect of $I\kappa B_{NS}$ on the differentiation and activation of human macrophages, on macrophages infected with HIV and on DLBCL. Since two isoforms of $I\kappa B_{NS}$ exist, the effect of overexpression of each isoform was analyzed to uncover specific functions of these isoforms.

The analyses showed a conserved function of $I\kappa B_{NS}$ in murine and human cells. Moreover, $I\kappa B_{NS}$ isoform 1 and 2 showed marked different effects on macrophage activation. While $I\kappa B_{NS}$ isoform 1 mainly showed a suppressing effect, isoform 2 showed suppressing as well as activating effects on the expression of pro-inflammatory factors.

Overexpression of $I\kappa B_{NS}$ isoforms 1 and 2 resulted in a shift from macrophage to dendritic cell phenotype. During HIV expression, overexpression of $I\kappa B_{NS}$ isoform 1 resulted in reduced expression of antiviral factors, while overexpression of $I\kappa B_{NS}$ isoform 2 showed no significant effects.

In ABC DLBCL, no $I\kappa B_{NS}$-deficient cell line could be established, suggesting a crucial effect of $I\kappa B_{NS}$ on DLBCL survival and growth. This was confirmed in on the transcriptional level for $I\kappa B_{NS}$ isoform 1.

In summary, $I\kappa B_{NS}$ isoforms 1 showed no activating effect or even a suppressive effect on target gene expression, while $I\kappa B_{NS}$ isoform 2 overexpression showed a strong activation of chemotactic chemokines and type I interferons in macrophages. In DLBCL, $I\kappa B_{NS}$ isoform 1 overexpression resulted in a marked activation of chemotactic and angiogenetic chemokines and growth-promoting transcription factors, showing its importance in the development of negative prognostic factors.

5. Zusammenfassung

Das angeborene Immunsystem ist eine der ersten Verteidungslinien unseres Organismus gegen eindringende Pathogene. Ein Zelltyp des angeborenen Immunsystems sind die Makrophagen, die über spezifische Rezeptoren hochkonservierte Bestandteile von Pathogenen erkennen und anschließend über die Sezernierung von chemotaktischen und entzündungsinduzierenden Zytokinen und Chemokinen die unspezifische und spezifische Immunantwort einleiten können. Ein zentraler Mediator der primären Immunantwort ist der Transkriptionsfaktor NF-κB. In ruhenden Zellen sind die Proteine der NF-κB-Familie im Zytoplasma an klassische IκB-Proteine gebunden. Nach Aktivierung der Zelle werden die IκB-Proteine abgebaut, wodurch die NF-κB-Proteine in den Kern wandern und dort ihre transkriptionelle Aktivität ausführen können. Ein weiterer Regulationsmechanismus von NF-κB besteht aus atypischen IκB-Proteinen, die nur im Zellkern aktivierter Zellen gefunden werden können. Ein Mitglied der Familie der atypischen IκB-Proteine und Hauptfokus dieser Arbeit ist $I\kappa B_{NS}$.

Ziel dieses Projekts ist die Aufklärung des Effekts von $I\kappa B_{NS}$ auf die Differenzierung und Aktivierung von humanen Makrophagen, auf die Infektion von Makrophagen mit HIV und auf DLBCL. Da zwei verschiedene Isoformen von $I\kappa B_{NS}$ beschrieben sind, wird hier der Effekt beider einzelner Formen untersucht, um mögliche spezifische Funktionen der einzelnen Formen aufzudecken.

Unsere Experimente zeigten eine Konservierung der Funktion von $I\kappa B_{NS}$ in humanen und murinen Zellen. Isoform 1 und 2 von $I\kappa B_{NS}$ zeigten klare Unterschiede in ihrem Effekt auf die Aktivierung von Makrophagen: Während Isoform 1 einen indifferenten oder supprimierenden Effekt hatte, zeigte Isoform 2 abhängig vom untersuchten pro-inflammatorischen Faktor sowohl supprimierende als auch aktivierende Effekte.

Die Überexpression von $I\kappa B_{NS}$ Isoform 1 und 2 sorgte für eine Verlagerung der Differenzierung von Makrophagen weg hin zu dendritischen Zellen. Im Setting der Infektion mit HIV zeigten Zellen mit Überexpression von $I\kappa B_{NS}$ Isoform 1 eine Reduktion der exprimierten antiviralen Faktoren, während die Überexpression von $I\kappa B_{NS}$ Isoform 2 keine Reduktion der untersuchten Faktoren zeigte.

In den ABC DLBCL konnten wir keine $I\kappa B_{NS}$-defiziente Zellinie etablieren, was eine zentrale Rolle von $I\kappa B_{NS}$ auf das Überleben und das Wachstum der DLBCL suggeriert. Dies konnte in der Überexpression von $I\kappa B_{NS}$ Isoform 1 auf dem transkriptionellen Level bestätigt werden.

Zusammengefasst zeigte IκB$_{NS}$ Isoform 1 in Makrophagen keinen aktivierenden, sondern bei einigen Zielen auch suppressiven Effekt auf die Expressionslevel, während IκB$_{NS}$ isoform 2 hier eine ausgeprägte Aktivierung von chemotaktischen Chemokinen und Typ I Interferonen bewirkte. In den Lyphomzellen zeigte IκB$_{NS}$ isoform 1 eine starke Aktivierung von chemotaktischen und angiogenetischen Chemokinen sowie von wachstumsfördernden Transkriptionsfaktoren, was seine Schlüsselrolle in der Pathogenese und der Entwicklung negativ prognostischer Faktoren zeigt.

6. Introduction

6.1. Innate immune system

The bulk of invading pathogens expresses a stereotypical, conserved set of surface molecules and can thus be recognized and neutralized by an innate response system. Our innate immune system consists of humoral and cellular components such as dendritic cells, the different types of granulocytes, natural killer cells and macrophages (Delves and Roitt, 2000).

6.1.1. Macrophages in innate and adaptive immunity

Macrophages are a heterogeneous group of myeloid cells with multiple purposes that are part of the innate immune system. Their progenitors circulate in the blood stream, capable of recruitment to sites of inflammation and subsequent differentiation. However, macrophages are also scattered in the extravascular space as sentinels (Geissmann et al., 2003). Here, they recognize pathogens via a highly conserved set of receptors and neutralize them, attract additional cells of the immune response and activate the adaptive immune response.

The role as sentinel consists of the attraction and activation of the immune response, as well as a more direct reaction to the pathogens. This reaction covers the secretion of effector molecules, such as antimicrobial peptides, protease inhibitors and extracellular matrix degrading proteins. Additionally, the recognition of pathogen-associated molecular patterns (PAMPs) triggers phagocytosis of these molecules and structures connected to them, enabling macrophages to clear the organism from pathogens and cell debris (Yamasaki et al., 2008, Auffray et al., 2007). Following phagocytosis, fragments of the foreign molecule are mounted on MHCII complexes and presented on the cell surface of the macrophages. T-lymphocytes recognize these epitopes via their TCR and become activated, thus linking the macrophage function as part of innate immunity with the adaptive immune system (Armstrong and Hart, 1971, Flannagan et al., 2012, Soudja et al., 2014).

After the inflammatory response is triggered, macrophages remain key players of the regulation of the processes. Resident macrophages recognize the pathogens and secrete several chemotactic factors, which recruits neutrophilic granulocytes and monocytes from the blood into the tissue. The monocytes then differentiate to pro-inflammatory macrophages and dendritic cells (DCs). After neutralization of the pathogens, the neutrophilic granulocytes undergo apoptosis. This results in the abrogation of further influx of neutrophilic granulocytes and re-polarizes the macrophages from their pro-inflammatory classically activated (M1) to the anti-inflammatory alternatively activated state (M2). This shifts the immune response from an aggressive pro-inflammatory to an anti-inflammatory state with restoration of tissue homeostasis. The secretome of these M2-macrophages is dominated by anti-inflammatory factors (Levy et al., 2001, Freire-de-Lima et al., 2006, Bellingan et al., 1996).

The processes described above show three central aspects of the properties of macrophages:

(I) The secretome of macrophages has a strong impact on the local microenvironment, enabling them to precisely regulate subsequent immune reactions.

(II) Macrophages can adopt different polarization states, depending on the context of their activation. This enables them to initiate several reactions that differ fundamentally, for example the initiation of inflammation and wound healing. Thereby, macrophages are capable of triggering multiple highly differentiated reactions, depending of the kind of threat and progression of the response.

(III) Other than differentiated T lymphocytes, polarized macrophages retain their plasticity, which allows a reaction depending on changes in the local microenvironment.

Since activated macrophages are the main focus of this project, the next chapters concentrate on macrophage activation and the receptors and two major pathways involved in macrophage activation.

6.1.2. Macrophage activation

The ability of macrophages to respond to different exogenous activating and quenching stimuli was first delineated by (Mackaness, 1962). He described a macrophage population showing enhanced antimicrobial and anti-tumoral properties as a response to listeria-induced monocytogenesis (Mackaness, 1962). Subsequent studies could elucidate that certain treatments can lead to different modes of activation:

(I) Classical activation/M1 state: Induced by treatment with IFNβ, IFNγ or LPS (lipopolysaccharide) *in vitro*. Classically activated macrophages are pro-inflammatory, associated with a reduction of pathogens and show anti-tumoral effects. They display an enhanced response to pro-inflammatory agents.

(II) Alternative activation/M2 state: Commonly induced by IL4. Alternatively activated macrophages are anti-inflammatory and associated with wound healing and tumor growth. They exhibit a reduced response to pro-inflammatory stimuli.

(III) Innate activation: After contact with PAMPs, specific receptors like TLRs are ligated, leading to the production of pro-inflammatory cytokines, interferons and antimicrobial peptides.

(IV) Deactivation: Mostly induced by IL10. It is characterized by an anti-inflammatory cytokine profile and a reduced expression of MHC-class II proteins (Gordon and Taylor, 2005).

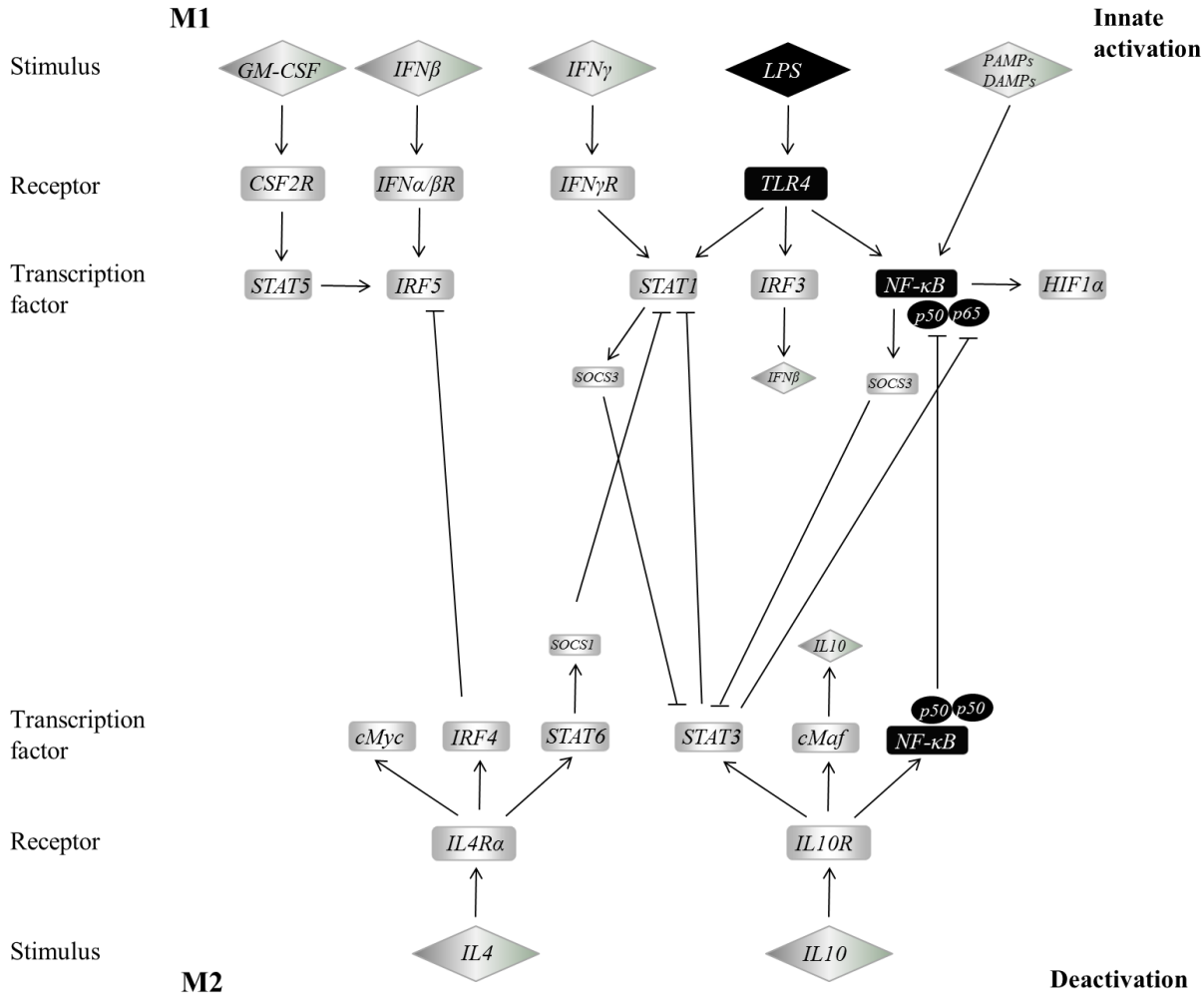

Figure 6.1: Mechanisms of macrophage activation.

The major regulatory pathways of macrophage polarization are shown in this figure. Macrophage polarization and activation status are tightly regulated by the balance of STAT1 and STAT3/6 levels. Predominant induction of activating NF-κB members and STAT1 induce an inflammatory phenotype, whereas predomination of STAT3, STAT6 and suppressive NF-κB members result in an anti-inflammatory phenotype. Downstream of STAT6, KLF4 suppresses NF-κB-dependent transcription. IL4 stimulation induces STAT6 and cMyc, which controls M2-associated genes together with IRF4 transcription, which inhibits IRF5 and thus reduces M1 polarization. IL10 stimulation promotes the M2 phenotype via induction of p50 NF-κB homodimers, cMaf, and STAT3. Modified after (Wang et al., 2014).

One of the best-known and best-characterized set is the Toll-like receptor (TLR) family. These extra- and intracellular receptors are activated by pathogen-associated molecular patterns (PAMPs) and are the subject of the next chapter.

6.1.3. The Toll-like receptor family

Macrophages are an essential part of the innate immune system and heavily rely on TLR signaling for their activation. The TLR/interleukin 1 receptor family consists of a conserved intracellular domain of roughly 200 amino acids (Toll/IL1R domain TIR) (Slack et al., 2000), a membrane-spanning domain and an immunoglobulin-like (IL1R) or a leucine-rich-repeat-motif (LRR) of 24-29 amino acids (Bell et al., 2003), classifying them as type I receptors. There are several different extra- and intracellular TLRs which are activated upon contact with different PAMPs. Some of the molecules recognized as PAMPs are lipopolysaccharide (LPS), bacterial flagellin, lipoteichoic acid, peptidoglycane and several foreign variations of nucleic acids, such as double-stranded RNA or unmethylated CpG-motifs (Kumar et al., 2011). Despite their highly conserved LRR, different TLR are capable of binding different substance classes as their ligands (Akira et al., 2001).

Table 6.1: TLR and their stimuli in humans
Modified after (Akira and Takeda, 2004).

Receptor	Ligands (excerpt)	Source of ligand	Production
TLR1	Triacyl lipopeptides	Bacteria, mycobacteria	IC
TLR2	Lipoprotein Lipoteichoic acid Viral capsid proteins	Various pathogens Gram-positive bacteria Viruses (e.g. influenza)	IC
TLR3	dsRNA	Viruses (e.g. HSV-1)	IC, IFN type I
TLR4	Lipopolysaccharide	Gram-negative bacteria	IC, IFN type I
TLR5	Flagellin	Bacteria	IC
TLR6	Lipoteichoic acid	Gram-positive bacteria	IC
TLR7	ssRNA	Viruses (e.g. HIV)	IC, IFN type I
TLR8	ssRNA	Viruses	IC, IFN type I
TLR9	CpG-containing DNA dsDNA	Bacteria and viruses Viruses (e.g. CMV)	IC, IFN type I

Some of these receptors, especially those recognizing nucleic acids (TLR3, TLR7, TLR8, TLR9) are expressed in the endosomes or lysosomes (Ahmad-Nejad et al., 2002, Latz et al., 2004). The other receptors can mostly be localized on the cell surface.

Multiple signaling pathways are activated after binding of PAMPs to TLRs, resulting in the activation of NF-κB and in turn mediating an inflammatory response. LPS, an endotoxin which can be found in bacterial cell membranes, is a classical PAMP and a potent activator of the Toll-like receptor 4, resulting in a robust induction of NF-κB.

In this project, macrophages were stimulated with LPS and infected with HIV, thus TLR4 and TLR7 are introduced in more detail.

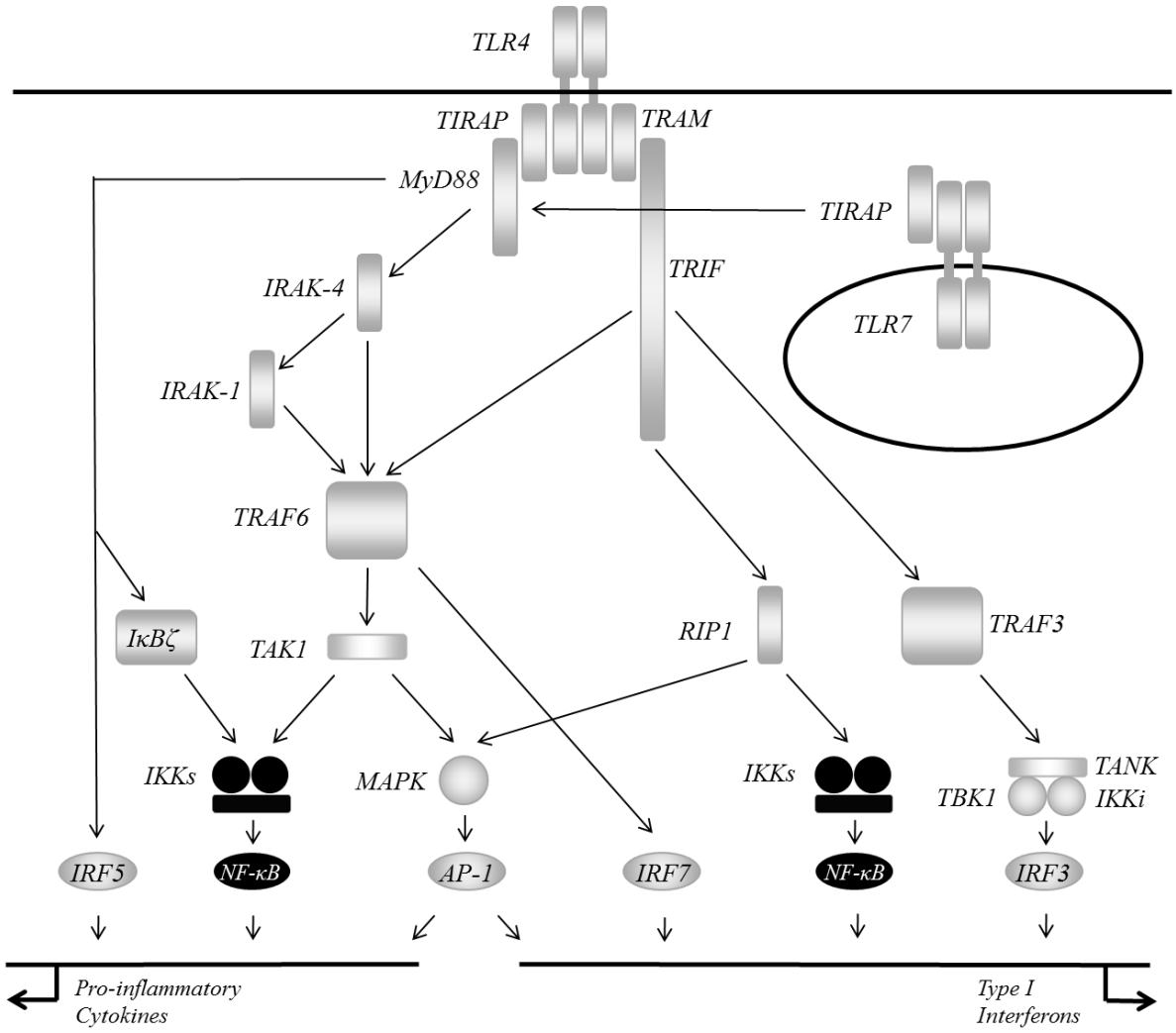

Figure 6.2: TLR4 and TLR7 signaling

TLR signaling can be divided in the MyD88 and the TRIF pathway. Both pathways converge in TRAF6 activation and subsequent NF-κB and AP-1-mediated expression of pro-inflammatory cytokines and AP-1 and STAT1-mediated expression of type I interferons. In addition, the TRIF dependent pathway mediates interferon type I expression by induction of NF-κB and IRF3, while the MyD88 dependent pathway induces cytokine expression mediated by IRF5. Modified after (Lu et al., 2008, Uematsu and Akira, 2007, Luu et al., 2014).

TLR4 is a cell surface receptor that is activated upon contact with LPS. It is the only TLR that is capable of recruiting all adaptor proteins. The signaling pathways induced by TLR4 are divided into MyD88-dependent and TRIF-dependent pathways. The MyD88-dependent pathway is described below for the TLR7 receptor.

Upon TLR4 stimulation, TIR-domain-containing adapter-inducing interferon-β (TRIF) is activated via the TRIF-related adaptor molecule (TRAM) and binds to tumor necrosis factor receptor-associated factor 3 (TRAF3), ultimately resulting in interferon-responsive factor 3 (IRF3) activation and expression of type I interferons. In addition, TRIF activates serine/threonine kinase receptor-interacting protein 1 (RIP1), which in turn phosphorylates

Inhibitor of kappa B-protein kinase IκK, releasing NF-κB proteins from their inhibitory IκB proteins and inducing type I interferon expression and pro-inflammatory cytokines. Another target of RIP1 is the MAP-kinase (MAPK), which phosphorylates activator protein I and thus induces the expression of type I interferons and of pro-inflammatory cytokines. Another target of TRIF is TNF receptor associated factor 6 (TRAF6) (Gohda et al., 2004, Lomaga et al., 1999), which is also part of the MyD88-dependent pathway and in turn activates NF-κB, MAPK and IRF7, thus inducing the expression of type I interferons and pro-inflammatory cytokines (Uematsu and Akira, 2007).

TLR7 is an endosomal receptor that is activated upon contact with single-stranded RNA (ssRNA). TLR7 can only recruit MyD88 via the Toll-interleukin 1 receptor (TIR) domain containing adaptor protein (TIRAP) and is thus restricted to the MyD88-dependent pathway. MyD88 activates IL1-receptor associated kinase 4 (IRAK4), which in turn phosphorylates IRAK1. Both activate TRAF6, thus converging with the TRIF-dependent pathway and inducing the expression of pro-inflammatory cytokines and type I interferons via NF-κB, MAPK and IRF7. MyD88 also activates IRF5 directly and upregulates IκBζ expression, subsequently again activating NF-κB (Uematsu and Akira, 2007).

NF-κB is a pivotal transcription factor in TLR signaling. In addition, $I\kappa B_{NS}$ is a protein strongly induced by NF-κB signaling. Thus, a more detailed introduction of NF-κB signaling is required here.

6.2. NF-κB, a crucial transcription factor

Gene expression is guided by general transcription factors, such as TATA binding protein. To respond to different external and internal stimuli, specific transcription factors, such as NF-κB, bind to their binding sequences to subsets of target genes, which thereby customize the cellular response to certain stimuli. A rapid and temporary adaption is often mediated by inducible transcription factors, such as the NF-κB protein family. NF-κB has been first discovered as a regulator of expression of the κ light chain gene in B-lymphocytes (Sen and Baltimore, 1986), where it plays a key role in the class switch during B-lymphocyte maturation. In the following years, NF-κB was discovered to be expressed in almost all animal cells and to be involved in many cellular responses to a large number of different stimuli, such as cellular stress, cytokines, irradiation, foreign antigens and growth signals (Hayden and Ghosh, 2012). These homo- or heterodimers regulate a wide range of genes responsible for cell proliferation and survival, which are essential for the proper function of the immune system via the regulation of cytokine production (Goudeau et al., 2003, Hayden and Ghosh, 2011, Samson et al., 2004).

The NF-κB protein family consists of five transcription factors: p50, p52, p65/RelA, RelB and c-Rel. These proteins share a nuclear localization sequence (NLS), enabling their transport from the cytosol to the nucleus, and a Rel-homology domain (RHD), enabling them to form homo- and heterodimers and to directly bind to certain binding motifs in the enhancer and promoter region of target genes. In addition, RelA, RelB and c-Rel contain a transactivation domain (TAD) which recruits proteins of the transcriptional machinery, such as Transcription factor IID and subsequently RNA polymerase II, which results in transcriptional activation of target genes after DNA binding (Dynlacht et al.). Consequently, NF-κB-DNA complexes containing a TAD trigger gene expression, while complexes lacking a TAD suppress the transcription probably by competitive inhibition.

NF-κB subunits are expressed constitutively and almost ubiquitously. In unstimulated cells, NF-κB dimers are inactive, as they form complexes with so called classical inhibitors of κB (IκB proteins) in the cytosol (Baeuerle and Baltimore, 1988, Beg and Baldwin, 1993). After activation, NF-κB activity is fine-tuned by posttranslational modifications of Rel-proteins such as sumoylations, phosphorylations, acetylations and ubiquitinylations and by expression of secondary response genes (Mankan et al., 2009, Chen and Greene, 2004).

NF-κB signaling can only work because of its rapid induction of gene expression. This is only possible due to the functional neutralization of NF-κB proteins by their inhibitors, the IκB proteins that are rapidly removed upon activation of certain receptors. Hence, NF-κB signaling and IκB proteins are heavily intertwined and require a more detailed introduction of IκB proteins.

6.2.1. IκB proteins

The IκB family consists of at least eight different proteins defined by their common ankyrin repeat sequence which allows protein-protein interactions.

The classical IκB proteins IκBα, IκBβ and IκBε are constitutively expressed and bind to NF-κB homo and heterodimers, thereby masking their NLS and inhibiting their nuclear translocation. Classical NF-κB activation, e.g. through TLR4 stimulation by lipopolysaccharide, triggers phosphorylation of IκBα or IκBβ that leads to a dissociation of the NF-κB-IκB complex, followed by polyubiquitylation and a rapid proteasomal degradation of the IκBα and nuclear translocation of NF-κB (Shirakawa and Mizel, 1989). Thereafter, NF-κB is shut off by NF-κB-dependent re-expression of IκBα, leading to new complex formation of NF-κB and IκB and nuclear export.

An alternative mode of NF-κB activation is mediated by p100 and p105. These proteins contain the ankyrin repeat domain and an additional RHD. Both proteins can act as NF-κB-inhibiting IκB proteins. However upon activation, p100 and p105 can also be cleaved into p50 and p52 monomers that relocalize to the nucleus (Meyer et al., 1991).

Besides the classical IκBs, atypical IκB proteins, called Bcl3, IκBζ, $IκB_{NS}$, IκBη and IκBL exist. These proteins contain the similar ankyrin repeat domains, but show some features distinct from classical IκBs. They are expressed at low levels in resting cells, but are rapidly induced after specific stimuli in an NF-κB dependent manner (Kitamura et al., 2000, Fiorini et al., 2002, Ohno et al., 1990). In addition, atypical IκBs are mainly located in the nucleus. Here, they modulate the expression of the secondary response genes in a NF-κB-dependent manner via various means, such as dimer exchange, recruitment of histone-modifying enzymes, stabilization of NF-κB dimers on the DNA and by forming nuclear complexes with NF-κB subunits. Atypical IκB proteins are capable of activating transcription of TAD-deficient NF-κB dimers via their own TAD. In addition, they can repress the formation of TAD-containing NF-κB dimers, such as p50/p65, thereby fine-tuning the NF-κB response (Chen and Greene, 2004, Mankan et al., 2009, Hayden and Ghosh, 2012).

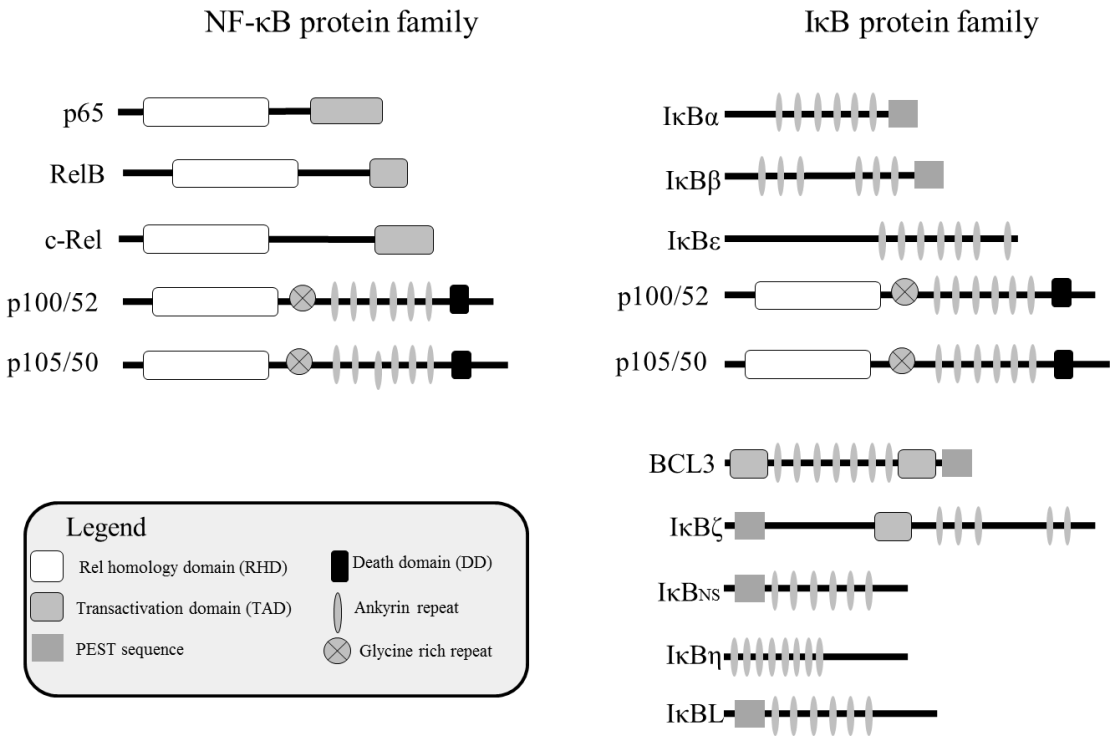

Figure 6.3: Structure of NF-κB and IκB proteins family.

The proteins shown above are the key proteins of the NF-κB pathway. Important protein structures are marked in the legend. NF-κB proteins are defined by their RHD that enable them to bind to certain DNA sequences, depending on post-translational modifications in that region. c-Rel, RelB and p65 also contain TADs. p100 and p105 can be cleaved in the glycine-rich repeat region, liberating the functional NF-κB protein p52 and p50, respectively. These NF-κB proteins do not contain a TAD. They can inhibit binding of TAD-containing NF-κB members and thus repress transcription. IκB proteins mainly consist of multiple ankyrin repeats mediating their interaction with NF-κB proteins. In addition, most IκBs contain a PEST sequence for proteasomal degradation. IκBζ and BCL3 contain TADs, enabling them to activate gene expression. As they lack a RHD, they are unable to bind to DNA alone, but are dependent on NF-κB dimers to initiate transcription of a target gene. Modified after (Hayden and Ghosh, 2012, Schuster et al., 2013).

Classical IκB proteins form a cytosolic complex with NF-κB proteins, thus inhibiting their action. Atypical IκB proteins, however, further fine-tune NF-κB signaling after their induction by NF-κB. One of these atypical IκBs, namely $IκB_{NS}$, is the main focus of this project, thus requiring a more detailed introduction.

6.2.2. NF-κB regulator $IκB_{NS}$

The atypical IκB protein $IκB_{NS}$ (encoded by *NFKBID*) was first described as an inducible IκB protein involved in the negative selection of T-cells (Fiorini et al., 2002). It consists of six ankyrin repeats, but lacks a TAD. Its mode of function is similar to the related IκBζ: It forms complexes with nuclear p50 homodimers, but not p50/p65 heterodimers, and destabilizes p50/RelA heterodimers (Yamazaki et al., 2001, Manavalan et al., 2010). Since it lacks a TAD, it may work as a repressor of transcription by competitive inhibition of binding of TAD containing atypical IκB proteins. After induction, $IκB_{NS}$ is rapidly degraded in a PEST-mediated manner (Park et al., 2014).

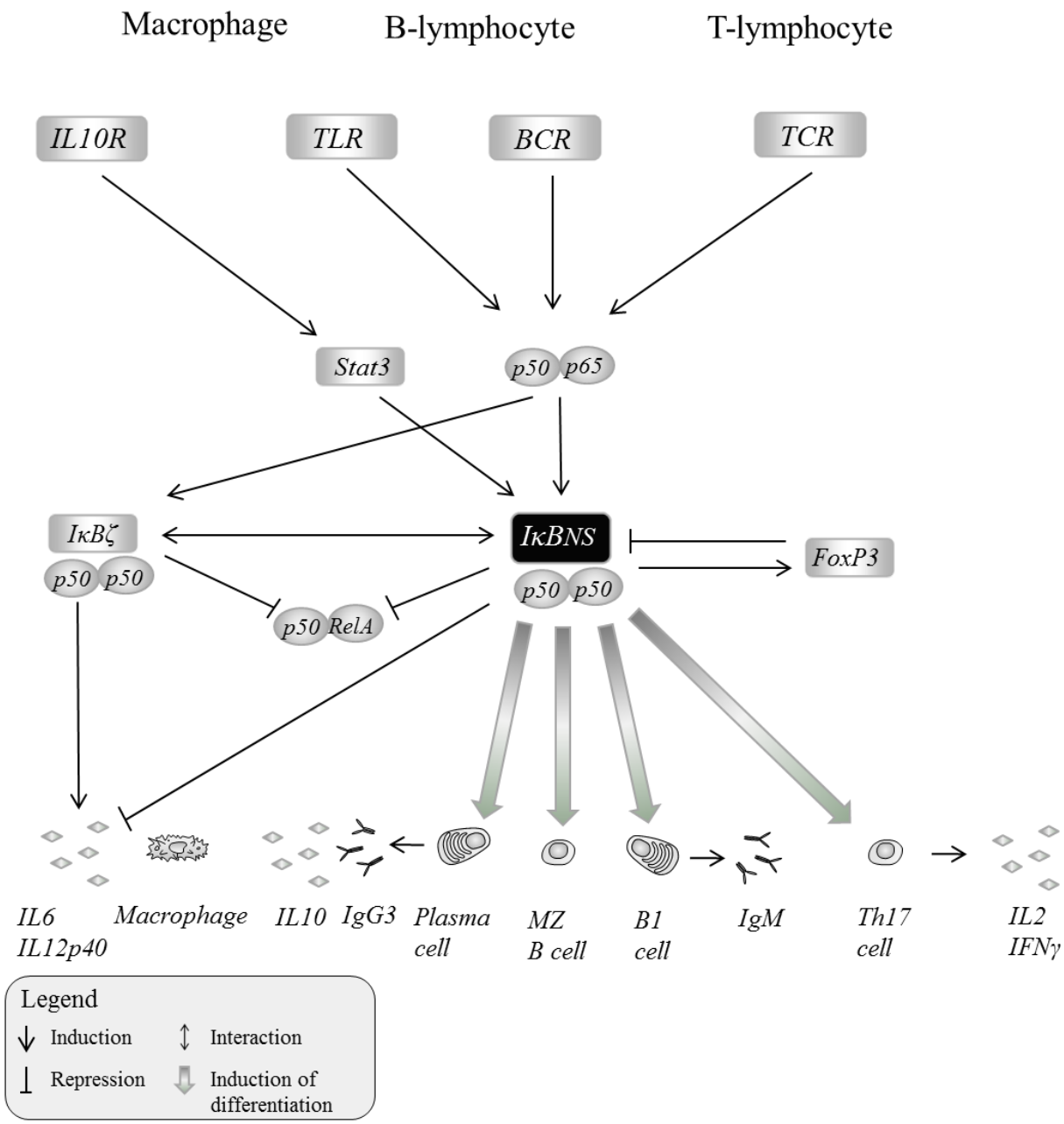

Figure 6.4: Effects of IκB$_{NS}$ on macrophages, B- and T-lymphocytes.

Stimulation of TLRs, B cell receptor (BCR) or T cell receptor (TCR) induces NF-κB activity, which leads to expression of IκB$_{NS}$ and IκBζ (Fiorini et al., 2002, Kitamura et al., 2000). STAT3-mediated IκB$_{NS}$ expression in macrophages can be triggered by IL10 (Hutchins et al., 2013). IκB$_{NS}$ and IκBζ destabilize p50/RelA heterodimers and stabilize and bind to p50 homodimers, regulating gene expression of NF-κB target genes (Yamazaki et al., 2001, Manavalan et al., 2010). IκB$_{NS}$ is indispensable for downregulation of IL6 levels after LPS stimulation of macrophages (Hirotani et al., 2005, Kuwata et al., 2006)

IκB$_{NS}$ is involved in B cell differentiation: Knockout of IκB$_{NS}$ results in the absence of B1 lymphocytes and IgM as well as marginal zone B cells (Pedersen et al., 2014, Arnold et al., 2012, Pedersen et al., 2016). Differentiation from plasmablasts to plasma cells and IgG levels are decreased (Touma et al., 2011). IκB$_{NS}$ up-regulates IL2 and IFNγ expression in T-lymphocytes during maturation, driving cell proliferation and Th17 differentiation (Schuster et al., 2012). It also upregulates FoxP3 expression, which downregulates IκB$_{NS}$ expression, resulting in a negative feedback loop (Marson et al., 2007, Schuster et al., 2012).

$I\kappa B_{NS}$ was first discovered because of its regulatory function in the negative selection of T-cells (Fiorini et al., 2002). However, subsequent studies revealed that it is dispensable for it, since $CD4^+$ and $CD8^+$ T-cell counts were identical between $I\kappa B_{NS}$-deficient and wild type mice (Touma et al., 2007). The reactivity against TCR-activating antigens was not impaired as well, although $I\kappa B_{NS}$ is induced by TCR stimulation in adult CD4 T-cells (Schuster et al., 2012). T-cell proliferation is slightly impaired due to reduced expression of IL2 and IFNγ after stimulation with anti-CD3 and anti-CD28 antibodies in $I\kappa B_{NS}$-deficient animals. This impairment can be overcome by PMA and ionomycin stimulation or by addition of exogenous IL2 (Kuwata et al., 2006, Touma et al., 2007). In addition, $I\kappa B_{NS}$ is involved in T-lymphocyte polarization: $I\kappa B_{NS}$ regulates the expression of FoxP3, a crucial factor for the development of regulatory T-lymphocytes (Treg). $I\kappa B_{NS}$-deficient mice have markedly decreased counts of Treg cells, but show no signs of autoimmune disease. This is due to the fact that $I\kappa B_{NS}$ is also crucial for Th17 differentiation, with strongly reduced levels of Th17 cells in $I\kappa B_{NS}$-deficient mice. However, Th1 helper cells are not affected by $I\kappa B_{NS}$ deficiency, resulting in severe inflammation in a DSS-induced colitis model (Annemann et al., 2015). Consequently, $I\kappa B_{NS}$-deficient mice are more resistant against Th17-mediated encephalomyelitis (Kobayashi et al., 2014)

In B cells, $I\kappa B_{NS}$ regulates B1a and B1b differentiation, as these subpopulations are missing in $I\kappa B_{NS}$-deficient mice (Pedersen et al., 2014). IgM levels are reduced, even in mice with a heterozygous mutation of $I\kappa B_{NS}$ (Pedersen et al., 2016). Moreover, the marginal zone B cells are decimated (Touma et al., 2011, Arnold et al., 2012). Similar to the impaired T-cell proliferation after TCR stimulation, the B cell proliferation and Ig class switch following LPS and anti-CD40 stimulation are reduced in $I\kappa B_{NS}$-deficient cells, as well as IL10 expression (Miura et al., 2016). The germinal center B cell population is reduced in young mice, but reaches wild type levels after 6 weeks. Additionally, the differentiation of plasma cells is impaired in $I\kappa B_{NS}$-deficient cells (Touma et al., 2011). Consistently, serum IgM and IgG3 levels are strongly decreased in $I\kappa B_{NS}$-deficient mice after influenza infection and the increase of antigen-specific IgG1 levels is delayed (Touma et al., 2011).

In macrophages, $I\kappa B_{NS}$ is induced by LPS and IL10 in a comparable manner (Hutchins et al., 2013, Kuwata et al., 2006). Loss of $I\kappa B_{NS}$ results in a prolonged and enhanced expression of IL6 and IL12p40 after LPS stimulation (Kuwata et al., 2006, Hirotani et al., 2005). However, IL2 expression is impaired in $I\kappa B_{NS}$-deficient thymocytes (Touma et al., 2007). This dual effect as an activator and as a repressor of the expression of different genes is a cardinal feature of the atypical IκB protein family. In addition, RelA/p50 dimers show a prolonged

binding to promoter sequences in IκB$_{NS}$-deficient macrophages, suggesting a quenching effect of IκB$_{NS}$ on NF-κB-mediated late response cytokine expression (Kuwata et al., 2006). In sum, IκB$_{NS}$ deficiency results in an increased susceptibility to LPS-induced endotoxin shock likely due to its function in inhibiting pro-inflammatory cytokine production. In line, IκB$_{NS}$ deficient mice are higher susceptible to DSS-induced colitis (Annemann et al., 2015). In addition, atherosclerosis is accelerated by prolonged IL6 secretion in LDL-receptor deficient mice (Akita et al., 2016). Thus, IκB$_{NS}$ constitutes an inhibitor of pro-inflammatory NF-κB gene expression in macrophages. On the other hand, IκB$_{NS}$ represents an important factor for the balance of pro- and anti-inflammatory T-lymphocyte subpopulations and a crucial factor for the differentiation of B-lymphocytes and B-lymphocyte subpopulations.

NF-κB signaling can be detected in almost every cell type. However, it has a greater significance and distinct functions only observable in some cell types. Thus, a more detailed introduction of NF-κB signaling in macrophages is needed for this project. Additionally, NF-κB signaling is not only important in the physiological setting, but also in disease. As HIV infection and diffuse large B cell lymphomas are also part of this project and NF-κB signaling has a central role in both pathological settings, a short introduction of the role of NF-κB in macrophages, HIV infection and diffuse large B cell lymphomas (DLBCL) is necessary.

6.2.3. NF-κB in macrophages

The NF-κB signaling pathway is pivotal for macrophage differentiation, activation and polarization. Common myeloid progenitor cells differentiate to granulocyte/macrophage progenitor cells following stimulation with GM-CSF and, subsequently, to monocytes following stimulation with M-CSF (Rosenbauer and Tenen, 2007). Both processes are regulated by NF-κB, as shown by an increase of colony-forming units of the myeloid hematopoietic line isolated from mice deficient for IκBα (Gerondakis et al., 1999). In addition, the GM-CSF receptor interacts with the IKK2 during ligand binding, resulting in its activation and subsequent NF-κB signaling (Ebner et al., 2003). GM-CSF also mediates the final differentiation step from circulating monocytes without detectable NF-κB activity to macrophages with high NF-κB activity. During these differentiation processes, NF-κB activation is essential due to its anti-apoptotic effect. This has also been shown by Gerondakis *et al.*, who found a high susceptibility of p65-deficient macrophages to apoptosis (Gerondakis et al., 1999).

After the differentiation process has been completed, resting macrophages again downregulate NF-κB activity. Upon exposure to PAMPs or cytokines, TLR or cytokine receptors are ligated, respectively. As described above, all TLR signaling pathways eventually converge on activation of NF-κB with subsequent expression of cytokines and secondary response molecules, resulting in a distinct polarization of the macrophage. However, depending on co-stimulation by more than one factor, the precise cytokine profile upregulated underlies great variation (Gerondakis et al., 1999).

6.3. NF-κB in disease

NF-κB is a master regulator of various cellular programs that are important for cell survival and growth, but in other circumstances also for cell death and inflammation. As these programs are fundamental for virus proliferation and spread as well as cancer development and progression, the NF-κB pathway is often hijacked as a driving force of these diseases (Hayden and Ghosh, 2012).

One pathogen successfully hijacking the NF-κB pathway is the human immunodeficiency virus HIV.

6.3.1. NF-κB in acute and chronic HIV infection

The NF-κB pathway is crucial to the response to viral infection as it activates transcription and secretion of antiviral factors, such as interferon beta, and thus initiates the antiviral response (Hiscott et al., 1989), and induces apoptosis. Some virus types use the apoptosis program to spread hidden from the humoral immune system within apoptotic bodies and to home towards and infect macrophages (Stewart et al., 2000). However, NF-κB activation can also render the cell less susceptible to infection- or immunity-induced apoptosis (Stewart et al., 2000), and promote cell cycle progression to the G1/S phase in some cell types directly or by induction of growth factors (Schuitemaker et al., 1994). Thus, it is not surprising that several viruses exploit this pathway to enhance their replication and the survival of their host cell.

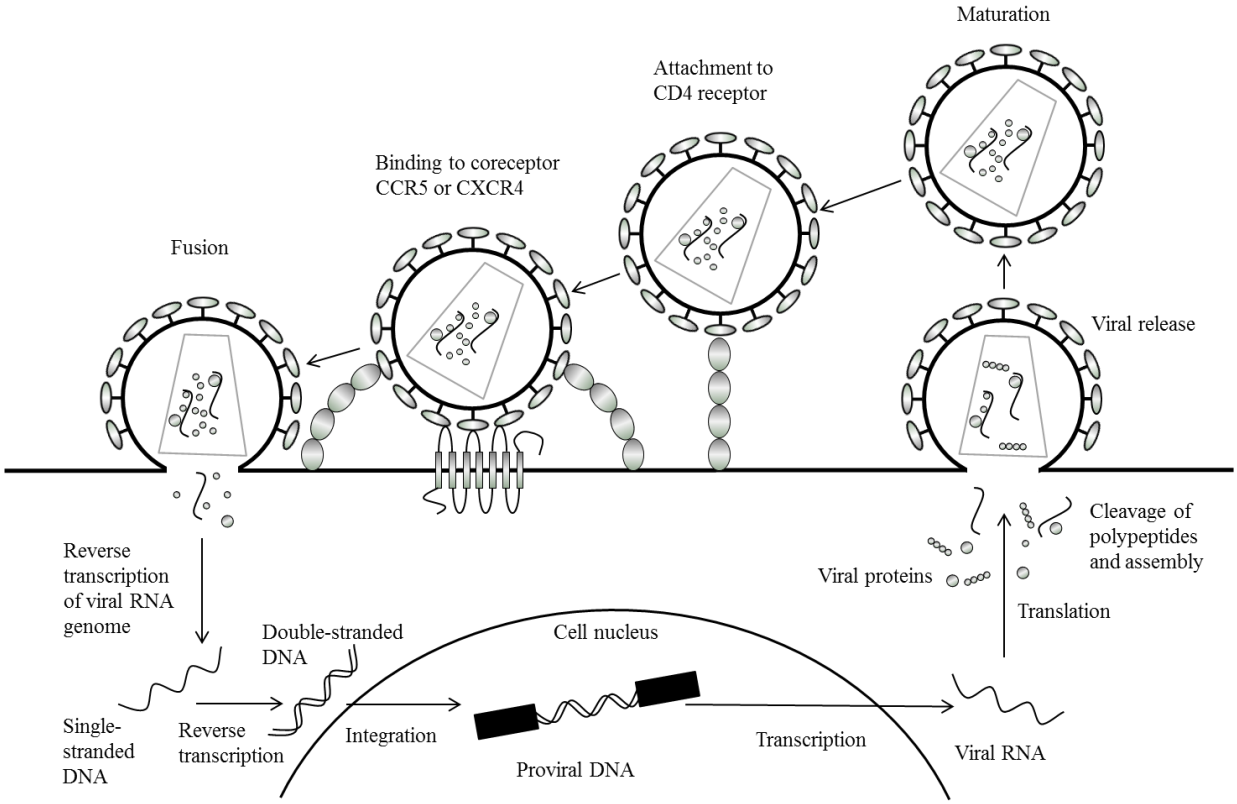

Figure 6.5: The life cycle of HIV

Simplified visualization of the different steps in the life cycle of HIV. Viral particles adhere to CD4 and a chemokine co-receptor. After attachment, the lipid bilayers of the host cell and the virus merge. As the virus penetrates the cell, the capsid and matrix proteins are degraded, releasing virus RNA and enzymes into the cytoplasm via endocytosis (Daecke et al., 2005). The error-prone viral enzyme reverse transcriptase converts the viral RNA into ssDNA and dsDNA. This dsDNA is joined by integrase and transferred into the nucleus, where it is spliced into the host's DNA (Engelman et al., 1991). The host's transcriptional machinery is used to produce viral RNA and mRNA for virus protein construction. The mRNA undergoes translation and the resulting multiprotein chains are transferred to the cell membrane. Here, the proteins form clusters for the production of new viral particles. The clusters form a bud in the cell membrane, within which the virus matures by cleavage of the multiprotein chains by the HIV protease to their proper size (Kohl et al., 1988). After detachment of the bud, the new viral particle is ready to infect another cell of the immune system (Moss, 2013). Modified after (Maartens et al., 2014).

One of these viruses is HIV. It inhibits myelocyte apoptosis by constitutive NF-κB activation (DeLuca et al., 1998). In addition, two NF-κB-binding sites are located in the promoter-proximal region of the HIV long terminal repeat (LTR), rendering the expression of HIV RNA highly NF-κB-dependent (Kwon et al., 1998).

HIV enters the cell by binding to CD4, a surface marker found on T lymphocytes, monocytes and macrophages. Although T lymphocytes are the main target of HIV and their depletion leads to the AIDS phenotype, macrophages are recognized as an important earlier target of HIV. In addition, infected macrophages survive and produce viral particles for longer periods than T lymphocytes (Sharova et al., 2005).

The NF-κB pathway is activated as soon as HIV binds to CD4, resulting in the fusion of the viral and cellular membranes. After integration of the viral DNA into the host genome, NF-κB is downregulated, stopping transcription of HIV RNA. However, activation of NF-κB in infected macrophages triggers HIV transcription and production of viral particles. After this initial step, several pathways that converge in NF-κB activation are continuously stimulated by HIV: Envelope protein gp120 engages the CD4 receptor pathway, stimulating NF-κB via Ras/Raf and PI-3K (Flory et al., 1998); the viral protein Tat phosphorylates IKK, leading to rapid induction of NF-κB via the canonical pathway (Manna and Aggarwal, 2000); TLR7 is stimulated by viral RNA; and via autocrine stimulation with IL1β and TNFα (Asin et al., 1999). While NF-κB activation is sufficient for expression of TNFα and pro-IL1β, the latter requires activation by cleavage by the inflammasome. The inflammasome is induced by the TLR7 stimulation of a productive HIV infection (Guo et al., 2014).

The constitutive activation of NF-κB and inflammasome causing constant inflammation is the main cause of the pathological processes leading to AIDS (Doitsh et al., 2010).

In summary, the progression of a chronic HIV infection to AIDS is NF-κB-dependent, making it an interesting target for future HIV treatments.

As mentioned before, viral infection is not the only setting in which the NF-κB pathway is activated and hijacked. Also several cancer entities, such as diffuse large B cell lymphomas, display constitutive activation of NF-κB signaling.

6.4. Diffuse large B cell lymphomas

NF-κB is a major mediator of inflammation. However, while acute inflammation results in an effective clearance of cancer cells, chronic inflammation promotes carcinogenesis (Karin, 2009). In addition, proliferation of immune cells is tightly regulated by NF-κB (Gerondakis and Siebenlist, 2010). Thus, NF-κB is actively involved in the progression of many neoplastic diseases, such as lymphomas.

6.4.1. Molecular subtypes

B lymphocytes pass through many differentiation steps during their life. During differentiation, several double-strand breaks and ligations occur to create antibody diversity. However, this also leads to a high incidence of malignant transformation, resulting in leukemia and lymphomas (Jung et al., 2006).

Thirty to forty percent of newly diagnosed lymphomas can be histologically classified as diffuse large B cell lymphomas (DLBCL). However, this group can be further divided into three different subtypes, namely germinal-center B cell-like (GCB), activated B cell-like (ABC), and primary mediastinal B cell-like (PMBL) DLBCL. They differ greatly in their gene expression profiles, suggesting different stages of differentiation in their cells of origin (Lenz and Staudt, 2010).

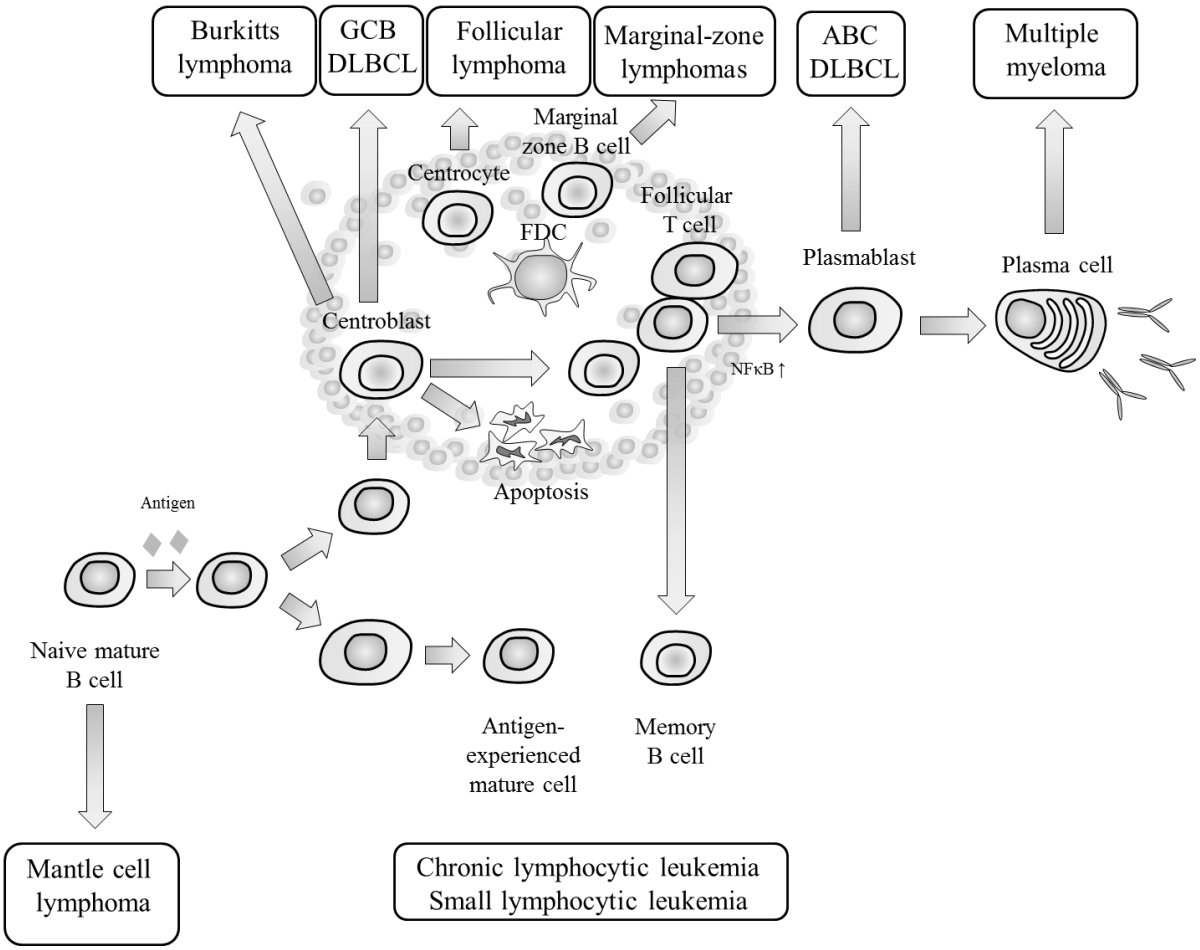

Figure 6.6: Different lymphomas and B cell development

Scheme of the different B cell lymphoma-subtypes and multiple myeloma in association with the B cell differentiation process. Lymphomas, although similar in appearance microscopically, show distinct gene expression patterns that resemble those of different stages of the B cell development. Malignancies derived from germinal center cells still carry the genetic signature of their physiological equivalent, with oncogenic mutations subverting the normal differentiation program. Thus, mantle cell lymphomas resemble naïve mature B cells, Burkitt's lymphomas and GCB DLBCL resemble centroblasts, follicular lymphomas resemble centrocytes, marginal-zone lymphomas resemble marginal zone B cells, ABC DLBCL resemble plasmablasts, and multiple myelomas resemble plasma cells on the transcriptional level. Lymphomas have acquired additional mutations circumventing apoptosis (e.g. BCL2 translocation), gaining independence of growth signals (NF-κB translocation) and disabling the differentiation program (interference with Blimp-1), thereby leading to uncontrollable growth (Alizadeh et al., 2000, Klein et al., 2006, Basso et al., 2004, Ci et al., 2009). Modified after (Lenz and Staudt, 2010)

GCB lymphomas show the expression signature of germinal center B cells. In addition, apoptosis is circumvented by several mutations. Common mutations are the t(14;18) translocation, p53 mutations and loss of the tumor suppressor PTEN (Saito et al., 2007, Rosenwald et al., 2002).

ABC lymphomas can be matched to B lymphocytes that have entered the plasma cell differentiation program. They constitutively express NF-κB due to constitutively active MyD88 or amplification of NF-κB and, consequently, also IRF4 (Care et al., 2014). However,

the final differentiation step is blocked due to interference with Blimp-1 expression, a transcription factor essential for plasma cell differentiation (Shaffer et al., 2002, Pasqualucci et al., 2006). NF-κB activation also upregulates IL6 and IL10 production, which in turn acts as an autocrine signal towards the cells upregulating STAT3 and JAK proteins (Ding et al., 2008, Lam et al., 2008). In addition, most ABC lymphomas overexpress BCL2, thereby suppressing apoptosis (Iqbal et al., 2006). The INK4-ARF locus is often deleted, leading to genomic instability and inability to enter the senescence program (Lenz et al., 2008). In concert, these factors lead to an increased resistance to chemotherapy, resulting in a poor clinical prognosis.

The third subtype, called PMBL, shows an expression pattern similar to the rare thymic B cell and a clinical presentation corresponding to Hodgkin's lymphomas. Key mutations are the amplification of JAK2 and the deletion of suppressors of JAK2, leading to an increased expression of STAT6 and repression of BCL6 (Ritz et al., 2013, Guiter et al., 2004). In addition, amplification of PDL1 and PDL2 suppress the T cell response, thus enabling the lymphoma to survive in the thymus (Green et al., 2010). However, in contrast to Hodgkin's lymphoma, it also expresses genes characteristic for mature B cells (Savage et al., 2003).

These subtypes vary a lot in the overall survival rates after chemotherapy and responsiveness to targeted therapy, showing the clinical value of this subgroup classification. GCB and PMBL are associated with a favorable outcome, whereas the prognosis of patients with ABC lymphomas are generally not very favorable (Wright et al., 2003, Rosenwald et al., 2002, Rosenwald et al., 2003, Lossos et al., 2004)

6.4.2. NF-κB in diffuse large B cell lymphomas

NF-κB is overexpressed in several lymphoma subtypes, namely the ABC subtype, PMBL, Hodgkin's lymphoma and marginal-zone lymphoma. Intriguingly, inhibition of NF-κB proved to be fatal to the tumor cells *in vitro*, showing an addiction to NF-κB signaling and downstream cytokine expression (Compagno et al., 2009, Hailfinger et al., 2009, Ferch et al., 2009). The expression of secondary response genes of NF-κB is also elevated, with constitutively high levels of the atypical IκBs proteins BCL3, IκBζ and $I\kappa B_{NS}$. Knockdown of BCL3 and IκBζ proved to be lethal for lymphoma cell lines with high NF-κB activity, but not for GCB DLBCL (Nogai et al., 2013, Ibrahim et al., 2011a). This addiction to atypical IκBs is not surprising, as they regulate gene expression of several cytokines that are crucial for DLBCL survival and growth, such as IL6 and IL10 (Yamamoto et al., 2004, Chang and Vancurova, 2014), and thus indirectly regulate levels of the JAK/STAT3 axis.

6.5. Research goals

NF-κB is a key transcription factor involved in the regulation of many different target genes and cellular fates. Therefore, understanding the molecular mechanism of how NF-κB functions in different cell types is crucial to manipulate this signaling pathway in autoimmune diseases, during infection or during tumor progression. One layer of NF-κB regulation involves the atypical IκBs that fine-tune NF-κB-mediated gene expression and ultimately cell fate. One of these cofactors constitutes $I\kappa B_{NS}$. $I\kappa B_{NS}$ as well as other family members, such as IκBζ and Bcl3, can regulate T- and B-lymphocyte differentiation and activation, but little is known about the role of $I\kappa B_{NS}$ in macrophages and tumor cells. Previous research hinted at an inhibitory role of $I\kappa B_{NS}$ on IL6 and IL12 expression, but a global transcriptome analysis of $I\kappa B_{NS}$ deregulated cells is still missing. Moreover, the functional role of $I\kappa B_{NS}$ in macrophages as well as cancer cell lines has not been sufficiently elucidated.

To define conserved $I\kappa B_{NS}$ target genes, target gene expression will be analyzed in the human macrophage like cell line THP-1 as well as in ABC DLBCLs. In ABC DLBCLs our lab revealed a remarkably constitutive overexpression of $I\kappa B_{NS}$. Moreover, we already elucidated the existence of two $I\kappa B_{NS}$ isoforms that might have specialized functions.

With this project we aim to elucidate the target genes of the $I\kappa B_{NS}$ isoform 1 and isoform 2 overexpression in human macrophages in response to the TLR4 stimulating agent LPS. Basis for the selection of putative target genes represents a transcriptome analysis of LPS-stimulated murine $I\kappa B_{NS}$ knockout macrophages. Similar target genes will be validated in $I\kappa B_{NS}$-overexpressing DLBCL cell lines.

7. Materials and methods

7.1. Materials

7.1.1. Technical devices

Table 7.1: Technical devices

Device	Company
Autoclave	Systec, Linden, Germany
Block heater	Kleinfeld Labortechnik, Gehrden, Germany
Blotting chamber	Biozym, Hessische Oldendorf, Germany
Cell counting chamber *Neubauer Improved*	Marienfeld, Lauda-Königshofen, Germany
Centrifuge *5417R*	Eppendorf, Hamburg, Germany
Centrifuge *Avanti J-30I*	Beckman Coulter, Brea, California, USA
Centrifuge *Multifuge 3 S-R*	Heraeus, Hanau, Germany
Electrophoresis system Mini Format 1D, for SDS-Page	Bio-Rad Laboratories, Hercules, CA, United States
Epgradient Mastercycler	Eppendorf, Hamburg, Germany
Freezer -20°C	Bosch, Gerlingen, Germany
Freezer -80°C	Thermo, Waltham, Massachusetts, USA
Fusion-FX7 SPECTRA	Vilber, Eberhardzell, Germany
Incubator Hera Cell 240	Heraeus, Hanau, Germany
Kryo chamber	Nalgene, Thermo, Waltham, Massachusetts, USA
Laminar flow cabinet *Hera Safe*	Heraeus, Hanau, Germany
Light Cycler 480 II	Roche, Mannheim, Germany
Liquid nitrogen tank *LS 4800*	Taylor-Wharton, Theodore, AL, USA
Magnetic stirrer *MR Hei-Standard*	Heidolph, Schwabach, Germany
NanoDrop 1000	Peqlab, Erlangen, Germany
pH-meter	Mettler Toledo, Columbus, Ohio, USA
Pipettes Eppendorf Research Series 2100 (0.1-2.5µl; 2-20µl; 20-200µl; 100-1000µl)	Eppendorf, Hamburg, Germany
Power Pac HC (SDS-PAGE + Western Blot)	Biorad, Vienna, Austria
QuBit 2.0 Fluorometer	Thermo, Waltham, Massachusetts, USA
Refrigerator 4°C	Bosch, Gerlingen, Germany
Roller mixer *SRT9*	Bibby scientific, Stone, Staffordshire, USA
Sonication device *Bioruptor OCD 200*	Diagenode, Liège, Belgium
Timer	Roth, Karlsruhe, Germany
Vacuum pump *Vacuubrand BVC21*	Vacuubrand, Wertheim, Germany
Vortex *Genie 2*	Heidolph, Schwabach, Germany
Waage *CP423S-0CE*	Sartorius, Göttingen, Germany
Water bath *Aqualine AL25*	Lauda, Lauda-Königshofen, Germany
Zeiss *Axiovert 135*	Zeiss, Jena, Germany
Zeiss Axiovert 40C	Zeiss, Jena, Germany
Zeiss *HXP 120 Fluorescence Illuminator*	Zeiss, Jena, Germany
Flow cytometer *BD LSR II*	BD, New Jersey, USA
Multiwell reader *Mithras LB 940*	Berthold Technologies, Bad Wildbad, Germany

7.1.2. Consumables

Table 7.2: Consumables

Product	Company
Bacteria culture dishes	Sarstedt, Mümbrecht, Germany
Bacteria culture vials (14ml)	BD, New Jersey, USA
Cell culture dishes (5 cm, 10 cm)	Greiner, Frickenhausen, Germany
Cell culture plates (6-well)	Greiner, Frickenhausen, Germany
Cryo tubes *Cryoline*	Thermo Scientific, Massachusetts, USA
Cell scraper (25 cm)	Sarstedt, Nümbrecht, Germany
Filter tips (10µl, 20µl, 200µl, 1,000µl)	StarLab, Ahrensburg, Germany
Sterile filter (0.2µm and 0.45µm)	Merck, Darmstadt, Germany
Syringe, 10ml, 50ml	Henke-Sass, Wolf, Tuttlingen, Germany
Parafilm	Brand, Frankfurt am Main, Germany
Whatman paper	Whatman, Dassel, Germany
Safe-lock reaction tube (1.5ml and 2.0ml)	Eppendorf, Hamburg, Germany
Falcon reaction tube (15ml, 50ml)	Greiner, Frickenhausen, Germany
Pipet tips (10µl, 200µl, 1,000µl)	Greiner, Frickenhausen, Germany
Protran nitrocellulose transfer membrane	GE Healthcare, Munich, Germany
Gloves	NitraTex, Staffordshire, United Kingdom
96-well plates for qPCR 384-well plates for qPCR	Roche, Mannheim, Germany
Transparent sealing foil for 96-well plate Transparent sealing foil for 384-well plate	Roche, Mannheim, Germany

7.1.3. Chemicals and reagents

Table 7.3: Chemicals and reagents

Substance	Article No.	Company
Ampicillin	K029.1	Roth
Acrylamide Rotiphorese (40%)	A515.1	Sigma
Ammonium persulfate (APS) p.a.	9502.2	Roth
Ammonium sulfate ($(NH_4)_2SO_4$) >99.5%, p.a.	A4418-1KG	Sigma
Bromophenol blue	A512.1	Roth
Calcium chloride dihydrate ($CaCl_2$ x $2H_2O$) >99%, p.a., ACS	C7902-500G	Sigma
Chloroform, Rotipuran p.a.	C2432-500ML	Sigma
Complete Protease Inhibitor EDTA free	04693116001	Roche
Dimethyl Sulfoxide (DMSO)	4380.0500	NeoLab Migge
Dithiotreitol (DTT)	6908.3	Roth
Deoxynucleotide triphosphates (dNTPs)	DNTP100-1KT	Sigma
Ethanol 99.9% p.a. (EtOH)	20821.330	VWR
Sodium Ethylene diamine tetraacetatic acid (Na-EDTA)	8043.2	Roth
Ethylene glycol tetraacetic acid (EGTA)	3054.2	Roth
Formaldehyde, 37% solution	A0823.1000	AppliChem
Glycerol, >99% p.a.	A1123.1000	AppliChem
Glycerophosphate (β-) disodium salt hydrate	G5422	Sigma
Glycine, >99%, p.a.	A1067.5000	AppliChem
HEPES Pufferan >99%, p.a.	A3724.0250	AppliChem
LB medium powder	L3522-1KG	Sigma
LB agar powder	L3147-1KG	Sigma
Hydrogen chloride (HCl)	4625.2	Roth

Agarose	2267.4	Roth
Nonidet P-40 substitute (NP-40)	74385	Fluka
Isopropanol 100%	20842.330	VWR
Magnesium chloride hexahydrate ($MgCl_2$ x $6H_2O$)	M2393-100G	Sigma
Methanol >99% (MetOH)	20847.307	VWR
Milk powder, blotting grade	A0830.1000	AppliChem
Phenol solution (pH 4.3) for RNA	P4682-100ML	Sigma
SPECTRA prestained protein ladder	26634	Thermo
6x DNA loading dye	R0611	Thermo
GeneRuler 1kb Plus DNA ladder	SM1331	Thermo
Phorbol 12-myristate 13-acetate (PMA)	P8139-1MG	Sigma
Puromycin	P9620	Sigma
Ionomycin	I0634-1MG	Sigma
G418	04727878001	Roche
Kanamycin	K1377-1G	Sigma
Random hexamer primer (0.2µg/µl)	SO142	Thermo
Sodium acetate (NaAc)	1.06267.1000	Merck
Sodium hydrogen carbonate ($NaHCO_3$), >99.5%, p.a., ACS, ISO	6885.1	Roth
Sodium chloride (NaCl)	27810.295	VWR
Sodium duodecyl sulfate (SDS)	CN30.3	Roth
Sodium hydrogenphosphate monohydrate ($NaHPO_4$ x H_2O), p.a.	1.06346.1000	Merck
Sodium (di-) hydrogenphosphate dihydrate (Na_2HPO4 x $2H_2O$) >99%, p.a.	T879.2	Roth
Sodium hydroxide (NaOH), pellets	6771.1	Roth
SYBR green	S9430-1ML	Sigma
Tetramethylethylenediamine (TEMED)	2367.3	Roth
Trisamine (Tris) Base, >99%, p.a.	T1503-1KG	Sigma
Trehalose dehydrate	22515	Usb corporation, Cleveland
Triton X-100, molecular biology grade	6683.1	Roth
Acetic Acid glacial (100%)	20104.298	VWR
Trizol QIAzol lysis reagent	79306	Qiagen
Tryptone	8952.2	Roth
Tween-20	8.22184.2500	Merck
Midori Green Advance	617004	Biozym
Urea	U5378-100G	Sigma

7.1.3.1. Buffers and solutions

Table 7.4: Buffers and solutions

Solution/buffer	Compounds and handling
WB running buffer	3 g/l Tris 18.5 g/l glycine 0.1% (w/v) SDS
WB transfer buffer	3 g/l Tris 18.5 g/l glycine 20 % (v/v) ethanol
WB blocking buffer	1x PBS 5% (w/v) milk powder
Cell lysis buffer	20 mM Tris-HCl pH 7.5 150 mM NaCl 1 mM Na_2EDTA 1 mM EGTA 1% Triton X-100 1 mM β-glycerophosphate 2 M Urea 1x Protease Inhibitor Cocktail (PIC)
5x SDS loading buffer (Laemmli-buffer)	0.35 M Tris pH 6.8 9.3 % Dithiotreitol 30 % Glycerin 10 % SDS 0.02 % Bromophenol blue
1x TAE	40 mM Tris base 20 mM acetic acid 1 mM EDTA
1x PBS-T	1x Dulbecco's PBS (Sigma) 1 ml/L Tween-20
PI	20 µg/ml PMA 1 mg/ml Ionomycin
HBS buffer	274 mM NaCl 10 mM KCl 1.4 mM $Na_2HPO_4*7H_2O$ 15 mM glucose 42 mM HEPES Adjust to pH 7.05 ± 0.05 with NaOH. Buffer was stored at 4°C.
Tris-HCl (1.5 M, pH 8.8)	1.5 M Tris base Adjust pH to 8.8 with hydrochloric acid
Tris-HCl (0.5 M, pH 6.8)	0.5 M Tris base adjust pH to 6.8 with hydrochloric acid
SDS 10 %	100g/L sodium dodecyl sulfate
LB agar/ampicillin	4% LB agar (Luria/Miller), autoclaved and cooled to 60°C 100 µg/ml ampicillin added, cast in petri dishes and stored at 4°C
LB medium/ampicillin	4% LB medium (Luria/Miller), autoclaved and cooled to 60°C 100 µg/ml ampicillin added and stored at 4°C

LB agar/kanamycin	4% LB agar (Luria/Miller), autoclaved and cooled to 60°C 50 µg/ml kanamycin added, cast in petri dishes and stored at 4°C
LB medium/kanamycin	4% LB medium (Luria/Miller), autoclaved and cooled to 60°C 50 µg/ml kanamycin added and stored at 4°C

7.1.3.2. Enzymes and kits

Table 7.5: Enzymes

Reagent	Company
DNase I (50U/µl)	Thermo Fisher Scientific
DNase I buffer	Thermo Fisher Scientific
RT Buffer, 5x	Thermo Fisher Scientific
Revert Aid Reverse Transcriptase (RT) 200 U/µl	Thermo Fisher Scientific
RiboLock RNase Inhibitor (40U/µl)	Thermo Fisher Scientific
RNase A (100mg/ml)	Qiagen
Taq polymerase	Primetech
pENTR/D-TOPO cloning kit	Thermo Fisher Scientific
FastDigest BsmBI	Fermentas
FastAP	Fermentas
T4 PNK	New England Biolabs
Green MasterMix (2x) - No Rox	Genaxxon

Table 7.6: Kits

Name	Company
QuBit Protein Assay Kit	Thermo Fisher Scientific
GeneJet plasmid miniprep kit	Thermo Fisher Scientific
GeneJet plasmid maxiprep kit	Thermo Fisher Scientific
Gateway cloning kit	Thermo Fisher Scientific
Pierce ECL Western Blotting Substrate	Thermo Fisher Scientific
SuperSignal West Femto Maximum Sensitivity Substrate	Thermo Fisher Scientific
Quick blunting kit	New England Biolabs
Quick Ligase kit	New England Biolabs
Dual luciferase reporter assay system	Promega

7.1.3.3. Antibodies

Table 7.7: Primary antibodies

Antibody target	Clone, ID	Source organism	Dilution for immunoblotting	Company
Actin (β-)	2920	Mouse	1/5000	Cell signaling
$I\kappa B_{NS}$	ab182633	Rabbit	1/500	abcam
IκBζ	9244	Rabbit	1/1000	Cell signaling
BCL3	sc-185	Rabbit	1/1000	Santa Cruz
NF-κB p65	8242	Rabbit	1/500	Cell signaling
NF-κB p65 phospho-Ser536	3033	Rabbit	1/500	Cell signaling
STAT1	9172	Rabbit	1/1000	Cell signaling
STAT1 phospho-Tyr701	9167	Rabbit	1/1000	Cell signaling
STAT3	9139	Mouse	1/1000	Cell signaling
STAT3 phospho-Tyr705	9131	Rabbit	1/1000	Cell signaling

Table 7.8: Secondary antibodies

Antibody	Cat. number	Dilution	Company
Donkey anti-goat IgG HRP	sc-2020	1:10 000	Santa Cruz
Goat anti-mouse IgG HRP	31430	1:10 000	Thermo Scientific
Goat anti-rabbit IgG HRP	65-6120	1:10 000	Thermo Scientific

Table 7.9: FACS antibodies

Antibody	Cat. number	Company
APC mouse anti-human CD81	561958	BD Pharmingen
APC anti-human CD11c	301613	BioLegend
PE anti-human CD14	367103	BioLegend
IgG2b control APC	22225036	ImmunoTools
IgG2b control PE	22225034	ImmunoTools

7.1.4. Eukaryotic cell culture

Table 7.10: Materials for eukaryotic cell culture

Reagent	Company
1x (RPMI)-1640	Sigma Aldrich
1x Dulbecco's Modified Eagle Medium (DMEM)	Sigma Aldrich
Penicillin 10 000 U/ml Streptomycin 10 mg/ml (Pen/Strep)	Sigma Aldrich
Trypsin/EDTA	Sigma Aldrich
Fetal Calf Serum (FCS)	Sigma Aldrich
1x Dulbecco's phosphate buffered saline (PBS)	Sigma Aldrich
Glutamine 200 mM	Sigma Aldrich

Table 7.11: Cell culture media

Medium	Compounds
Full RPMI	1x RPMI 10% (v/v) FCS 1% (v/v) Pen/Strep
ABC medium	1x RPMI 20% (v/v) FCS 1% (v/v) Pen/Strep
Full DMEM	1x DMEM 10% (v/v) FCS 1% (v/v) Pen/Strep

Table 7.12: Cell lines

Cell lines	Origin	Medium
BJAB	GCB DLBCL	Full RPMI
SuDHL-4	GCB DLBCL	Full RPMI
HBL-1	ABC DLBCL	ABC medium
OCI-Ly3	ABC DLBCL	ABC medium
THP-1	Acute monocytic leukemia	Full RPMI
HEK293FT	Human embryonic kidney cells, harbouring SV40 large T antigen	Full DMEM

7.1.5. Prokaryotic cell culture

Table 7.13: Bacteria strain

Strain	Description	Company
NEB 5α	Competent E.coli	New England Biolabs

Table 7.14: Bacteria medium and agar

Solution/buffer	Compounds and handling
LB Medium	20 g/l LB-Medium powder Antibiotic as needed
LB Agar	35 g/l LB agar powder Antibiotic as needed

7.1.6. Oligonucleotides and plasmids

7.1.6.1. Oligonucleotides

Table 7.15: qPCR primers

Primer	Sequence 5'-3'	Target gene
BCL3_forward	GCCTCAGCTCCAATGGTC	BCL3
BCL3_reverse	GAGGAGCCATGGGGAATC	BCL3
IκBζ_forward	GCATTTGGTTCCCGATGGC	IκBζ
IκBζ_reverse	TTCCCTTCAGGATACGTCGG	IκBζ
STAT1_forward	AGGTTAACGTTCGCACTCTG	STAT1
STAT1_reverse	GCTGCTGAAGTTCGTACCAC	STAT1
STAT3_forward	GACTCTCAATCCAAGGGGC	STAT3
STAT3_reverse	CCTCTGCCGGAGAAACAG	STAT3
DUSP1_forward	ACCACCACCGTGTTCAACTTC	DUSP1
DUSP1_reverse	TGGGAGAGGTCGTAATGGGG	DUSP1
DUSP2_forward	GACTCCAGGGCTCCTGTCTAC	DUSP2
DUSP2_reverse	GCAGGTCTGACGAGTGACTG	DUSP2
IRF4_forward	GCGGTGCGCTTTGAACAAG	IRF4
IRF4_reverse	ACACTTTGTACGGGTCTGAGA	IRF4
BCL2_forward	AGTACCTGAACCGGCACCT	BCL2
BCL2_reverse	GCCGTACAGTTCCACAAAGG	BCL2
IL1b_forward	ATGATGGCTTATTACAGTGGCAA	IL1β
IL1b_reverse	GTCGGAGATTCGTAGCTGGA	IL1β
IL8_forward	TTTTGCCAAGGAGTGCTAAAGA	IL8
IL8_reverse	AACCCTCTGCACCCAGTTTTC	IL8
IL1RA_forward	AAGGCAGTGGAAGACCTTGTG	IL1RA
IL1RA_reverse	AGCAATGAGCTGGTTGTTTCTC	IL1RA
CXCL1_forward	TCAATCCTGCATCCCCCATAG	CXCL1
CXCL1_reverse	CAGGAACAGCCACCAGTGAG	CXCL1
CXCL10_forward	TGCAAGCCAATTTTGTCCACG	CXCL10
CXCL10_reverse	CTGCATCGATTTTGCTCCCC	CXCL10
TNFa_forward	CAAGGACAGCAGAGGACCAG	TNFa
TNFa_reverse	CCGGATCATGCTTTCAGTGC	TNFa
SpiB_forward	CCAGCAGGAACTGGTACAGG	SpiB
SpiB_reverse	ACTTACCGTTGGACAGCCCT	SpiB
Fas_forward	GTGGACCCGCTCAGTACG	Fas
Fas_reverse	TCTAGCAACAGACGTAAGAACCA	Fas
CCL2_forward	ATAGCAGCCACCTTCATTCCC	CCL2
CCL2_reverse	AGATCTCCTTGGCCACAATGG	CCL2
CCL8_forward	TCACGTTAAAGCAGCAGGTG	CCL8
CCL8_reverse	GCCCTCCAAGATGAAGGTTT	CCL8
VEGFa_forward	TTCCAAGATGCCCAGGAGG	VEGFα
VEGFa_reverse	AGTGGTTTCAATGGTCTGAGGAC	VEGFα
bActin_forward	CGACAGGCTGCAGAAGGAG	β-Actin
bActin_reverse	GTACTTGCGCTCAAGAGGAG	β-Actin
RPL37a_forward	AGATGAAGAGACGAGCTGTGG	RPL37a
RPL37a_reverse	CTTTACCGTGACAGCGGAAG	RPL37a
MX1_forward	TGGCATAACCAGAGTGGCTG	MX1
MX1_reverse	GGCTGATTGTCTCCTGCCTC	MX1
CCL3_forward	AGTTCTCTGCATCACTTGCTG	CCL3
CCL3_reverse	CGGCTTCGCTTGGTTAGGAA	CCL3
CCL4_forward	CTGTGCTGATCCCAGTGAATC	CCL4
CCL4_reverse	TCAGTTCAGTTCCAGGTCATACA	CCL4

CCL5_forward	CCAGCAGTCGTCTTTGTCAC	CCL5
CCL5_reverse	CTCTGGGTTGGCACACACTT	CCL5
IFNb_forward	TCTCCTGTTGTGCTTCTCCAC	IFNβ
IFNb_reverse	GCAGTATTCAAGCCTCCCATTC	IFNβ

Table 7.16: CRISPR guide RNA oligos

Target	Source	Orientation	Sequence
$I\kappa B_{NS}$	Shalem *et al.*, 2013	Sense	caccgGCTCACGAATGTCAAGACGC
		Antisense	aaacGCGTCTTGACATTCGTGAGCc

7.1.6.2. Plasmids

Table 7.17: Plasmids

Plasmid	Source	Description
pInducer 20	Addgene plasmid #44012	Vector containing an open reading frame under the control of an UbC promoter encoding for rtTA3 and a neomycin resistance cassette for selection. Another open reading frame is surrounded by attR1 and attR2 sites for GATEWAY cloning. Here, the promoter consists of a minimal CMV promoter with a TetO sequence upstream. In the presence of doxycycline, the rtTA3 binds to the TetO sequence, leading to strong expression of the sequence in the ORF. Harbors an ampicillin resistance cassette for amplification in *E.coli*.
pMD2.G (VSV-G)	Trono Lab	Vector encoding for viral envelop protein under the control of a CMV promoter. Harbors an ampicillin resistance cassette for amplification in *E.coli*.
M420	AG Dietrich, GSH Frankfurt	Vector encoding for eGFP under the control of a CMV promoter. Contains a RNA packaging signal, LTR sequences for genomic insertion of the target sequence and a 3'SIN/LTR for generation of replication deficient lentivirus. Harbors an ampicillin resistance cassette for amplification in *E.coli*.
pCMVΔR 8.91 (8.91)	Trono Lab	Vector encoding for gag, pol and rev genes under the control of a CMV promoter. Harbors an ampicillin resistance cassette for amplification in *E.coli*.
pRDI_292	Trono Lab	Vector containing an open reading frame under the control of a CMV promoter with adjacent puromycin resistance cassette. Contains LTR sequences for genomic insertion of the target sequence, a RNA packaging signal and a 3'SIN/LTR for generation of replication deficient lentivirus. Harbors an ampicillin resistance cassette for amplification in *E.coli*.
pENTR	Thermo Fisher Scientific	Part of the pENTR/D-TOPO kit. Contains cDNA of genes surrounded by attL1 and attL2 sites for GATEWAY cloning without a promoter. Harbors a kanamycin resistance cassette for amplification in *E.coli*.
pX330	Zhang Lab	Vector containing an open reading frame under the control of an EFS promoter encoding for Cas9-IRES-puromycin resistance gene. Additionally, it contains an RNA expression cassette under the control of an U6 promoter with a 2 kb spacer between two different BsmBI cutting sites for oligonucleotide insertion to yield a guide RNA. Harbors an ampicillin resistance cassette for amplification in *E.coli*.

7.1.7. Software

Table 7.18: Software

Name	Company
Excel, Powerpoint, Word	Microsoft, Redmond, WA, United States
NanoDrop Software	PeqLab
Fusion CAPT	Vilmer
GraphPad Prism	Graphpad Software Inc.
ImageJ	NIH
LC480 II Software	Roche
FlowJo	FlowJo LLC
MicroWin2000	mikrotek

7.2. Methods

All methods were performed at room temperature, unless otherwise indicated.

7.2.1. Experimental methods in molecular biology

7.2.1.1. Polymerase chain reaction

Polymerase chain reaction was performed using the Platinum Pfx DNA Polymerase (Invitrogen) following the manufacturer's instructions, using 100 ng template DNA and adding 5 µl 10x PCR$_X$ enhancer solution to the reaction.

Table 7.19: Platinum Pfx thermocycler program

Temperature	Time	
94°C	5 min	
94°C	15 sec	35 cycles
55°C	30 sec	
68°C	2 min	
68°C	2 min	

7.2.1.2. Restriction digest of plasmids

Required restriction enzymes were obtained from Fermentas. The digests were performed following the manufacturer's instructions. 2 U of the restriction enzyme were added to 2 µg plasmid in 1x FastDigest buffer and incubated for 15 min at 37°C.

7.2.1.3. Plasmid dephosphorylation

To avoid self-ligation of the cut CRISPR/Cas9 plasmid, the sticky ends were dephosphorylated using the FastAP (Fermentas). As the plasmid was cut using FastDigest BsmBI, only 2 U FastAP had to added to the reaction mix of 6.2.1.2 prior to the restriction reaction.

7.2.1.4. Agarose gel electrophoresis of DNA

DNA fragments were separated by size using agarose gel electrophoresis. For that purpose, 1% GenAgarose LE (Roth) was dissolved in 1x TAE buffer using a microwave. Subsequently, 4 µl Midori Green Advance (Biozym Diagnostic), a nucleic acid stain, was added per 100 ml of agarose. The liquid agarose was transferred into a gel casting system (PerfectBlue Gelsystem Midi S, Peqlab) and cooled to RT for polymerization.

Next, an appropriate amount of 5x DNA loading dye was combined with the DNA samples and transferred into the gel pockets. For DNA size quantification one additional pocket was loaded with 5 µl of GeneRuler 1 kb Plus DNA Ladder (Fermentas). Hereafter, separation was performed in gel chambers filled with 1x TAE, applying a voltage of 4 V/cm until appropriate separation was achieved. Separated DNA fragments were visualized for analysis with FUSION FX and for subsequent use with UV light illuminator.

7.2.1.5. Extraction and ligation of DNA fragments

DNA bands were cut out under UV light visualization. The DNA fragments were extracted using the DNA Gel Extraction kit (Fermentas) and ligated using the Quick Ligase (NEB) following the respective manufacturer's instructions.

The DNA bands were cut out and transferred to a 2 ml Eppendorf cup. Binding buffer was added 1:1 (w/v). Next, the mix was incubated at 60°C for 10 min. The dissolved agarose was then transferred to the purification column, centrifuged for 1 min, 12000 rpm, RT. The flow-through was discarded. The column was washed once by adding 700 µl washing buffer and centrifuged as before. The flow-through was again discarded and the empty column centrifuged once more to remove residual ethanol. Next, the column was transferred into a 1.5 ml Eppendorf cup. 20 µl nuclease-free water was added and incubated for 2 min. The cup was again centrifuged for 2 min. DNA concentrations were measured using the NanoDrop 1000.

7.2.1.6. CRISPR-Cas9 mediated genomic knock-out

The most precise method to assess the function of a protein is to eliminate said protein from the cell and compare it to wild-type cells. A new method to remove a protein on the genomic level is the CRISPR-Cas9 (clustered regular interspaced palindromic repeats/CRISPR associated protein 9) mediated knock-out. This method is derived from the adaptive bacterial defense system against phages and foreign plasmids and consists of a endonuclease capable of binding RNA at certain repetitive sequences and cutting DNA (Cas9) as well as a short RNA sequence consisting of said repetitive sequence and a guide sequence targeting a certain part of the genome (guide RNA) (Jinek et al., 2012). During expression of both Cas9 and guide RNA in a cell, the genomic DNA is specifically cut at the binding site of the guide RNA, resulting in a non-sticky double strand break. The broken strand activates DNA repair mechanisms, namely the error-prone non-homologous end joining. The re-joined DNA fragments now contain indel-mutations, resulting in a frame shift mutation of the downstream gene and thus deleting the functional protein derived from the gene (Lieber, 2010).

In this project, the plasmid developed by the Zhang lab (Shalem et al., 2014) was used. Here, both the Cas9 and the guide RNA are expressed from one lentiviral vector, along with a puromycin resistance cassette. The specific targeting sequence targeting the first exon of $I\kappa B_{NS}$ was inserted using the restriction digest and ligation method and subsequently transduced into the cells using the lentiviral transfer.

7.2.1.7. Annealing and insertion of gRNA-oligonucleotides

Guide RNA sequences for IkB_{NS} knockout by CRISPR were obtained from (Shalem et al., 2014). Corresponding forward and reverse DNA oligonucleotides forming a double strand with a 5' CACC and a 5' AAAC overhang were ordered from Sigma Aldrich. The oligonucleotides were annealed and phosphorylated in single reactions composed as seen in table 6.20.

Table 7.20: Reaction mix for oligo annealing

1 µl	Oligo 1 (100 µM)
1 µl	Oligo 2 (100 µM)
5 µl	Quick Ligase Buffer (NEB)
2.5 µl	ddH_2O
0.5 µl	T4 PNK (NEB)
10 µl	total

Reactions were carried out in an Epgradient Mastercycler (Eppendorf) using the following two step protocol:

Table 7.21: Annealing and phosphorylation thermocycler program

Action	Temperature	Time
Phosphorylation	37°C	30 min
Annealing	95°C	5 min
	95°C-25°C at 5°C/min	15 min

The annealed, phosphorylated oligonucleotides were ligated into the cut, dephosphorylated plasmid backbone using the QuickLigase kit following manufacturer's instructions.

Table 7.22: Reaction mix for oligo insertion

X µl	BsmBI digested plasmid (50 ng)
1 µl	Diluted annealed oligo
5 µl	Quick Ligase Buffer (NEB)
To 10 µl	ddH_2O
1 µl	Quick Ligase (NEB)
11 µl	total

The mix was incubated for 15 min at RT and transformed into competent NEB5α.

7.2.1.8. TOPO-cloning

Amplified DNA fragments were purified using agarose gel electrophoresis. The extracted fragment was inserted into the pENTR/D-TOPO vector (Invitrogen) following the manufacturer's instructions.

The DNA sequence for the insertion was produced via PCR using primers with a 5' CACC overhang and added in a 1:1 molar ratio to the pENTR/D-TOPO vector.

Table 7.23: Reaction mix for pENTR/D-TOPO reaction

3 µl	PCR product
1 µl	Salt solution
1 µl	Sterile water
1 µl	TOPO vector
6 µl	total

The mix was incubated for 5 min at RT and transformed into competent NEB5α.

7.2.1.9. Gateway cloning

After confirmation of the insertion of the desired DNA sequence, the insert in the pENTR backbone was transferred to the pInd20 expression plasmid (Meerbrey et al., 2011) using the Gateway system (Invitrogen) following the manufacturer's instructions. The template plasmid contains a ccdB (suicide gene) in its open reading frame, stopping bacteria with untransformed plasmids from growth.

Table 7.24: Reaction mix for the Gateway reaction

5 µl	pENTR vector (300 ng)
2 µl	Destination vector (300 ng)
4 µl	5x LR clonase buffer
5 µl	TE buffer
4 µl	LR clonase mix
20 µl	total

The mix was briefly vortexed and incubated for 1 h at RT. The reaction was stopped by adding 2 µl proteinase K, and the mix was transformed into competent NEB5α.

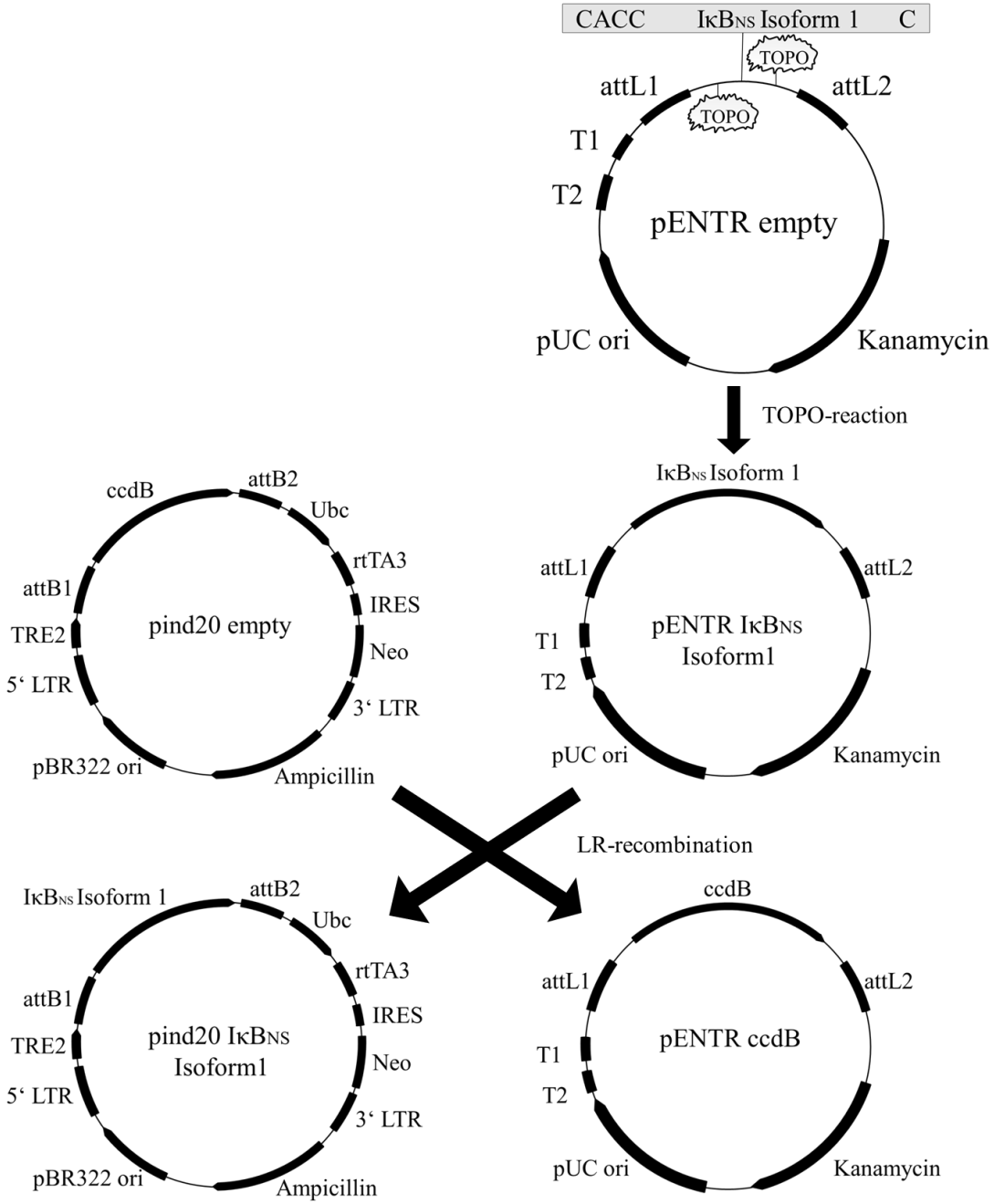

Figure 7.1: Workflow for pInd20 IκB$_{NS}$ expression vector generation.

IκB$_{NS}$ isoform 1 cDNA was amplified with PCR primers containing overhangs required for the TOPO reaction. The DNA was purified via agarose gel electrophoresis. The cDNA was inserted into the pENTR backbone using the TOPO reaction. Resulting plasmids were sequence analyzed. Plasmids containing the desired insert were used for the LR-recombination reaction to transfer the IκB$_{NS}$ isoform 1 cDNA into the pInd20 plasmid backbone. The plasmids derived from this reaction were sequence tested and expanded for further use.
T1/2: T1 and T2 transcriptional termination sites; attL1/2: Bacteriophage λ-derived recombination site for Gateway reaction; attR1/2: Bacteriophage λ-derived recombination site before Gateway reaction; attB1/2: Bacteriophage λ-derived recombination site after Gateway reaction;TRE2: Tet-responsible element for doxycycline-induced gene expression; Ubc: Ubc promoter for constant protein expression; rtTA3: reverse tetracycline transactivator protein of TetOn-system; IRES: Internal ribosomal entry site for expression of two genes in one open reading frame; ccdB: Bacterial suicide gene (gyrase-inhibitor); pBR322 ori: pBR322 origin of replication for plasmid replication; pUC ori: pUC origin of replication for plasmid replication. Modified after (Meerbrey et al., 2011)

The reaction products were transfected into NEB5α via heat-shock transformation and spread on agar plates containing kanamycin. Single clones were picked the next day, expanded in liquid culture and a mini prep was performed. The pENTR plasmids were then sent to Eurofins for sequencing. The sequencing results of the final plasmid are shown in the appendix 12.

7.2.1.10. Transformation of competent *E.coli* bacteria

The plasmids for the production of lentivirus particles were generated by transforming them into competent NEB5α bacteria (NEB) for amplification.

0.5 µg plasmid DNA was added to 50 µl competent NEB5α and incubated on ice for 15 min. Next, the cells were heated to 42°C for 30 sec for heat-shock transformation, followed by 2 min cooling on ice. 500 µl pre-warmed SOC medium (NEB) was added and the bacteria were incubated for another 30 min on a shaker at 37°C. Thereafter, the cells were spread on a LB plates containing 100 µg/ml ampicillin or 100 µg/ml kanamycin and incubated overnight.

7.2.1.11. Plasmid preparation

Three colonies were picked from each plate and transferred into 5 ml LB medium containing the selection antibiotic and incubated overnight. Plasmids were extracted from 4 ml bacteria suspension and purified using the MiniPrep Kit (Fermentas) following the manufacturer's instructions. The remaining 1 ml was stored at 4°C for further use. Nucleotide concentrations were measured photometrically using the NanoDrop 1000.

To verify the insertion and correct orientation of insert, 100 ng DNA in 15 µl ddH_2O were sent to Eurofins for sequencing.

For higher plasmid amounts, the 1 ml bacteria solution of colonies containing the desired plasmid are added to 200 ml antibiotic-containing LB medium and incubated overnight. The plasmids were extracted using the Maxi/Midiprep Kit (Fermentas) following the manufacturer's instructions. The DNA pellet was reconstituted with 200 µl nuclease-free water. Nucleotide concentrations were measured photometrically using the NanoDrop 1000, diluted to 1 µg/ml and stored at -20°C.

7.2.1.12. Isolation of total cellular RNA

Total RNA isolation from THP-1 and DLBCL cells was performed using phenol-chloroform-extraction method.

The cells were harvested by removing the medium completely and adding 1 ml TRIZOL reagent directly to the cells (adherent cells) or by pelleting the cells for 5 min, 1000 rpm at RT, removing the supernatant and resuspending the pellet in 1 ml TRIZOL reagent. The reagent was transferred to a 1.5 ml tube and either frozen at -80°C or used directly.

For extraction, 200 µl Chloroform was added and the samples were vortexed for 15 sec to degrade proteins and separate RNA from DNA. The sample was incubated for 2 min at RT and subsequently centrifuged for 5 min, 13000 rpm at 4°C. The upper, clear phase, containing the RNA, was added to 0.5 ml Isopropanol in a new 1.5 ml Eppendorf tube and vortexed.

Samples were incubated again for 10 min on ice to ensure sufficient RNA precipitation. Following that, the sample was centrifuged for 30 min, 13000 rpm at 4 °C. The supernatant was discarded and the pellet was washed once by adding 150 µl 70% ethanol, vortexing it and lastly pelleting it again by centrifugation for 1 min at 13000 rpm, 4°C. The supernatant was discarded and the RNA pellet was shortly air-dried. Finally, the pellet was dissolved in 100 µl nuclease-free water.

7.2.1.13. DNase I digest of RNA samples

To remove any residual genomic DNA, a DNase I digest of the RNA samples was performed before reverse transcription of the RNA into cDNA. 20 µl DNase I mix was added to the samples and incubated for 30 min at 37°C.

Table 7.25: Composition of DNase I mix per one reaction

12 µl	10x DNase I buffer
0.25 µl	DNase I, hc
1 µl	RNase I inhibitor
6.75 µl	Nuclease-free water
20 µl	total

After incubation, the enzyme mix was removed using phenol-chloroform extraction. For this purpose, 150 µL phenol-chloroform mix (5:1, pH 4.3) was added to the samples and vortexed. Subsequently, samples were centrifuged for 1 min at 13000 rpm at 4 °C. The clear, upper phase was mixed with 375 µl 96% ethanol and 17 µl NaAc in a new 1.5 ml Eppendorf cup. The samples were thoroughly vortexed and incubated for at least 1h at -80°C to ensure sufficient RNA precipitation. For final purification, the samples were centrifuged for 30 min, 13000 rpm at 4°C. The supernatant was discarded and the pellet washed once again by adding 150 µl 70% ethanol, short vortexing and centrifuging it for 1 min, 13000 rpm at 4°C. The RNA was shortly air-dried and dissolved in 10-30 µl nuclease-free water.

The RNA solution was stored at -80°C or used directly for cDNA synthesis.

7.2.1.14. Photometric detection of nucleic acid concentrations

Nucleic acid concentrations were quantified using the NanoDrop 1000 (PeqLab). 2 µl sample was measured at a wavelength of 260 nm. RNA was subsequently diluted to 400 ng RNA/µl, DNA was diluted to 1000 ng DNA/µl.

7.2.1.15. cDNA synthesis

The total cellular RNA was reverse transcribed by following the manual of the MMuIV reverse transcription kit (Thermo Fisher Scientific). First, 1 µg RNA was diluted to 10 µl and added to 2 µl random hexamer primers (Thermo Fisher Scientific). The mix was incubated for 5 min at 70°C. Next, the mix was spun down shortly and 8 µl of master mix was added. Reverse transcription was conducted by incubation of the sample for 1 h at 42°C. The enzyme was inactivated by heating the sample up to 65°C for 10 min.

After synthesis, the cDNA was diluted 1:20 with nuclease-free water and stored at -20°C.

Table 7.26: Master mix for cDNA synthesis

4 µl	5x RT buffer
1 µl	20 mM dNTPs
1 µl	RNase inhibitor (40 u/µl)
1 µl	MMuIV RT enzyme
1 µl	Nuclease free water
8 µl	total

7.2.1.16. Primer design

For qPCR primer design, the Primer blast program of the NCBI website was used (*www.ncbi.nlm.nih.gov/tools/primer-blast/).*

The criteria for primer design are listed below:

Template size: 50-200 bp, Primer size: 18-24, GC content: 40-60%, Melting temperature tm: 58.0-62.0°C, Max. Poly X: 5.00, Max. self-complimentary: 3.00, GC clamp: 1

The primers were designed to include at least one intron to reduce the likelihood of contaminating genomic DNA being amplified.

The calculated oligonucleotides were ordered at Sigma-Aldrich (www.sigmaaldrich.com) and Metabion (www.metabion.com). Upon arrival, the lyophilized oligonucleotides were reconstituted to 100 µM with nuclease-free water and stored at -20°C. For real-time PCR analysis, a working solution was prepared by mixing forward and reverse primer together at a concentration of 10 µM, which was stored at -20°C.

7.2.1.17. Quality control of primers

Before their use, the primers' efficiency and specificity had to be validated. Thus, a dilution series of cDNA (1:20, 1:40 and 1:80) was prepared as a test template and a test qPCR was performed for each newly designed primer pair. The compounds used in the qPCR samples are listed in table 6.27. For testing of the primers and analysis of the samples a 384-well plate was used. The PCR program is depicted below (table 6.28).

Table 7.27: Compounds of qPCR reaction mixes

6.25 µl	SYBR green mix
0.5 µl	Primer working solution
3.25 µl	Nuclease free water
2.5 µl	cDNA sample (1:20 diluted)
12.5 µl	total

Table 7.28: Standard thermocycler program for real-time PCR

Temperature	Time	
95°C	15 min	
95°C	15 sec	45 cycles
60°C	45 sec	
95 °C	1 min	
Melting curve 65.0 -95.0°C	0.5°C/10sec	

The primer specificity and efficiency were calculated from the Ct values resulting from the qPCR. In theory, the non-diluted sample should yield a Ct value of 1.00 lower than the 2-fold diluted and 2.00 lower than the 4-fold diluted test sample.

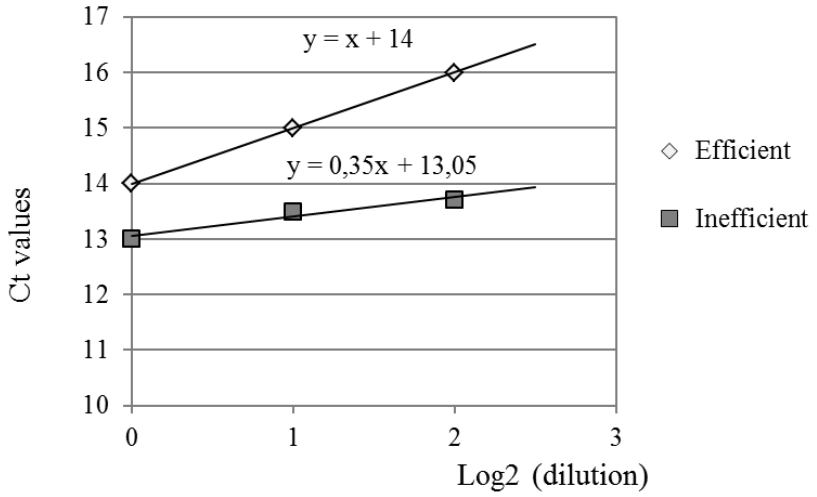

Figure 7.2: Ct values at different template dilutions

Shown above are theoretical Ct values from a primer validation using undiluted, 2-fold and 4-fold diluted template cDNA plotted against the Log2 of the respective dilution. The light grey graph shows an efficient primer with a slope of 1, while the dark grey graph shows an inefficient primer with a slope of 0.35.
Hence, primer efficiency was evaluated by generating a plot depicting the log2 of the cDNA input on the x-axis against the Ct-values on the y-axis. The plot of a good primer pair should show a linear correlation between Ct values and dilution factor which has a slope of 1.00 and a regression of higher that 0.95. As a high specificity means that only one sequence is amplified by the primer pair, the resulting product should have a distinct melting temperature. The melting temperature yielded by the product of specific primers results in a distinct peak in the melting curve, whereas multiple peaks or an astringent curve without peaks shows a lack of specificity of the primer pair. Non-specific or inefficient primers were re-designed and replaced.

7.2.1.18. Quantification of relative gene expression

Relative gene expression was assessed by qPCR analysis using the LightCycler 480 II (Roche). For each experiment, biological triplicates were generated by using three independently extracted RNA/cDNA samples. Reaction mixes were composed as shown in table 6.27. After pipetting of the samples and reaction mixes, the plates were sealed with optical foil, shortly vortexed and centrifuged (1 min, 1200 rpm, RT) to gather all fluid in the bottoms of the wells. Real-time PCR using the protocol shown in table 6.28 was always directly performed following the preparation of the plates.

Two independent reference genes (*beta actin* and *RPL37a*) were analyzed in parallel to normalize the samples to possible variations of the cDNA concentration.

For calculation of the relative mRNA levels the ΔΔCt method was applied. The Ct values of the reference genes were subtracted from the Ct values of the target gene for the first normalization step to generate the ΔCt value. Next, the ΔCt value from the control sample (untreated, transfected with the empty backbone) was subtracted from the ΔCt value of every other sample, yielding the ΔΔCt value. ΔΔCt value of control samples was therefore set to 0.

Each qPCR cycle resembles the doubling of the DNA template; thus, Ct values represent logarithmic values to the basis of 2. Consequently, the mean expression ratio was calculated using the following formula: $2^{(-\Delta\Delta Ct)}$. This results in a control or untreated cells set as 1, a mean expression ratio of >1 showing up-regulation and a mean expression ratio between 0 and 1 showing down-regulation of a gene.
Statistical significance was calculated using the paired student's t-test.

7.2.2. Immunobiological methods

7.2.2.1. Protein harvest

For protein analysis, total cell lysates were prepared. Thus, adherent cells were scraped with medium and suspension cells were shaken up. Cells and medium were transferred to a 15 ml Falcon tube (Eppendorf) and pelleted (5 min, 1200 rpm at RT). Subsequently, the pellet was resuspended in 1 ml PBS, centrifuged again (5 min, 1200 rpm at RT) and dissolved in an appropriate amount of cell lysis buffer. Cells from a 6-well were taken up in 150 µl lysis buffer and cells from a 10 cm cell culture dish in 400 µl lysis buffer. The cell lysates were put on ice for further processing. In addition to the chemical breakup, the cells were also disrupted physically by thorough pipetting, short vortexing and sonication to fracture bulky genomic DNA (10 min, 30 sec on/off, Bioruptor Diagenode). Protein concentration of the cell lysates was determined using the QuBit Protein assay kit.

7.2.2.2. Determination of the protein concentration (Qubit)

Protein concentrations were assessed using the Qubit assay kit (Thermo Fisher Scientific). Each sample was diluted 1:10 with water and 1 µl of the diluted sample was added to 199 µl Qubit working solution. After thorough vortexing, the relative protein concentrations were assessed using the Qubit 2.0 fluorometer (Thermo Fisher Scientific). For calculation of the protein concentration, standard solutions were measured in parallel. For subsequent SDS-PAGE and the following immunoblotting, protein samples were denatured by boiling them with ¼ Laemmli buffer for 5 min at 95°C. For the protein analysis, 40-100 µg protein was loaded on acrylamide gels and SDS-PAGE was performed.

7.2.2.3. SDS-PAGE

The proteins were separated according to their size using the SDS-PAGE method. SDS adds numerous negative charges to proteins, making the original charge irrelevant and resulting in a constant relation of charge and molecular weight. This leads to a separation of the proteins solely by their mass. SDS-PAGE is performed with a stacking gel that concentrates the samples and a subsequent running gel that separates the proteins according to their mass. The pre-cast gels were mounted in a tank containing 1x running buffer and samples were transferred into pre-formed gel pockets next to a pre-stained protein ladder. Next, a low voltage of 100 Volt was applied until the samples reached the intersection between the stacking and running gel. Finally, the higher power of 140 Volt was applied leading to the separation of the samples by migration of the proteins from the cathode to the anode.

Table 7.29: Composition of gels for SDS-PAGE

Compound	Stacking gel (5%)	Running gel (12%)
Water	14.24 ml	15 ml
Tris-HCl, pH 6.8 (0.5 M)	2.4 ml	-
Tris-HCl, pH 8.8 (1.5 M)	-	12 ml
SDS (10%)	300 µl	480 µl
APS (10%)	200 µl	225 µl
Glycerol	-	4.8 ml
TEMED	20 µl	20 µl
Acrylamide-bisacrylamide (40%)	1.9 ml	15 ml

7.2.2.4. Immunoblotting

Since proteins in polyacrylamide gels are inaccessible to antibodies, they were transferred to a nitrocellulose membrane before detection. Upon incubation with a primary antibody directed against the target, HRP-tagged secondary antibodies were used for signal amplification and subsequent chemoluminescence detection (Renart *et al.*, 1979; Towbin *et al*, 1979).

For protein transfer from gel to membrane, the gel and membrane were put between sponges and two layers of Whatman-papers forming a moist chamber around the gel and the membrane. This stack was fastened in a cassette that was now transferred into a tank containing blotting buffer. The anode was placed on the side of the membrane and the cathode on the side of the gel. Transfer of the proteins took place at a constant voltage (2 h 100 V or 25 V overnight). The electrical field works against a considerable resistance, resulting in a great amount of heat development during the blotting. To avoid the destruction of the protein samples, the tank containing the blots and transfer buffer was put on ice and transferred into the cold room for the duration of the transfer.

To avoid unspecific binding of the primary antibody, the membrane was blocked in 5 % milk/PBS for 1 h at RT before the primary antibody was administered. Next, the primary antibody diluted in 5% milk/PBS was added to the membrane and incubated overnight while rotating. The next day, the blot was washed thoroughly (3 times for 10 min with PBS-T) and the secondary antibody diluted in 5% milk/PBS was added. After 1 h of incubation at RT, rotating, the blots were again thoroughly washed 3 times for 10 min with PBS-T. ECL Western blotting substrate was prepared by mixing equal volumes of luminol reagent (Luminol Enhancer Solution, Promega) and the Oxidizing Reagent (Peroxide Solution, Promega) and was kept on ice. The membrane was placed between the covers of a propylene sheet protector. The ECL Western blotting substrate was added and air pockets were gently smoothed out. The insert plate was inserted into the Fusion FX7 Spectra and exposed for an appropriate time. To assay low protein expression levels, Femto staining solution was prepared by adding equal volumes of SuperSignal Western Femto Luminol Enhancer Solution (Thermo Fisher Scientific) and SuperSignal Western Femto Stable Peroxide Buffer (Thermo Fisher Scientific) and used instead of ECL Western blotting substrate.

7.2.2.5. Cytokine Array

Cytokines in the supernatant of cell cultures can be measured using the ELISA system. The proteome profiler assay is based on the same principles as an ELISA. Here, the antibodies are already bound to a membrane in double spots, allowing the testing of the supernatant for the concentrations of several cytokines at once.

The assay was performed following the manufacturer's protocol, using 500 µl supernatant from stimulated cells seeded at a density of 150 000 in 2 ml medium. The membranes were blocked for 1 h at RT to reduce unspecific binding of cytokines. During the blocking, the samples were adjusted in their volume according to the number of cells on the plate. The detection antibody cocktail was added directly to the samples and incubated for 1 h at RT. After the incubation, the samples were transferred to the membranes and incubated overnight.

The next day, the membranes were washed three times for 10 min at RT in washing buffer. The HRP-streptavidin was added and incubated for 30 min at RT. After another washing, the membranes were placed between the covers of a propylene sheet protector. ECL Western blotting substrate was prepared and added as described in 6.2.3.6and air pockets were gently smoothed out. The insert plate was inserted into the Fusion FX7 Spectra and exposed for an appropriate time. Data evaluation was performed using ImageJ.

7.2.2.6. Fluorescence-assisted cell sorting

Cell surface proteins are accessible to antibodies without lysis of the cells, allowing us to measure their expression on single cells. In the fluorescence-assisted cell sorting (FACS) method, these antibodies are coupled with fluorophores that are capable of emitting light of specific wavelength after excitation with a certain, different wavelength by a laser, allowing a specific readout of surface marker expression levels.

$2*10^5$ THP-1 cells were seeded per sample (2 Mio/ 20 ml) and treated as described in 7.2.3.8. The cells were scraped off in 10 ml PBS and pelleted for 5 min at 12000 rpm, RT. Next, 2 million cells were resuspended in 100 µl FACS buffer and incubated for 10 min at RT. 20 µl of that cell suspension were transferred to a fresh FACS tube containing 80 µl FACS buffer and the FACS antibodies in a final dilution of 1:50. For each fluorophore, an isotype control was created analogous to the regular stain. The solutions were incubated for 30 min at RT. After that, 900 µl FACS buffer were added, the tubes were flicked and centrifuged for 5 min at 12000 rpm, RT. The supernatant was discarded, the pellet was resuspended in 900 µl FACS buffer and centrifuged for 5 min at 12000 rpm, RT. The supernatant was discarded, and the pellet was resuspended in 400 µl FACS buffer for subsequent measurement. Data analysis was performed using FlowJo FACS data evaluation software.

7.2.3. Cell-biological methods

7.2.3.1. Determination of cell numbers

Cell numbers were determined using the Improved Neubauer Chamber slides (Hausser Scientific) as per manufacturer's instructions. 10 µl cell suspension were pipetted into the chamber and cells within the four 4x4 squares were counted under the Zeiss Axiovert 135 microscope. The resulting number was divided by 4 and multiplied with 10^4, yielding the number of cells per ml suspension.

7.2.3.2. Cell culture of suspension cells

Cells were cultured at a humidified atmosphere with 5% CO_2 at 37°C.

THP-1 and GCB DLBCL cells were cultured in full RPMI medium. ABC DLBCL cells were cultured in ABC medium. For stably transfected cell lines, full RPMI medium was freshly supplemented with 1 µg/ml puromycin.

Cells were regularly split for 2-3 times per week. Hence, the medium containing the cells was transferred into a 50 ml Falcon tube (Eppendorf) and centrifuged (5 min, 1000 rpm at RT). The supernatant was aspirated and the pellet was resuspended in 10 ml fresh medium. 1 ml cell suspension was transferred into a new 75 cm^2 cell culture flask containing 9 ml fresh cell culture medium.

7.2.3.3. Cell culture of adherent cells

Adherent cells were cultured in an incubator with a humidified atmosphere with 5% CO_2 at 37°C. HEK293FT cells were cultured in full DMEM. Cells were passaged when they were confluent in a cell culture flask. First, cells were incubated in Trypsin-EDTA (5 ml per 75 cm^2 flask, PAA) for 5 min at 37°C. Afterwards 5 ml culture medium were added and the cells were pelleted (5 min, 1000 rpm at RT). The supernatant was removed and cells were resuspended in 10 ml full DMEM. 1ml of the suspension was added to 15 ml culture medium in a new 75 cm^2 flask.

7.2.3.4. Freezing of cells

To maintain a low passage number of the cell lines cultured, cells were regularly frozen and stored in liquid nitrogen. The cells were trypsinized, if necessary, centrifuged (5 min, 1000 rpm at RT) and resuspended in an adequate amount of medium yielding a density of $2 \cdot 10^6$ cells/ml. 500 µl cell suspension were added to 500 µl freezing buffer and transferred into cryo vials. The cryo vials were first placed in freezing units containing isopropanol and placed at -80°C for 24 h. After one day, they were transferred to a tank containing liquid nitrogen for long time storage.

7.2.3.5. Thawing of cells

Frozen cells were rapidly thawed in a water bath at 37°C and immediately transferred into 10 ml of appropriate medium. This solution was centrifuged for 5 min, 1000 rpm at RT. The supernatant was aspirated to remove the toxic DMSO and the pellet was resuspended in 5-10 ml of cell line-specific medium for cultivation.

7.2.3.6. Transfection of HEK293FT via calcium-phosphate-precipitation

The transfection of HEK293FT cells for the production of lentivirus was performed using calcium phosphate (Graham and van der Eb, 1973). $1x10^6$ HEK293FT cells were seeded in a 10 cm dish and transfected with 2.5 µg overexpression construct, 1.6 µg 8.91 plasmid and 1 µg VSV-G plasmid 18 to 24 h after seeding (Naldini et al., 1996, Stewart et al., 2003). Plasmid DNA was mixed with 500 µl HeBS buffer and 440 µl sterile water. Subsequently, 60 µl 2 M $CaCl_2$ solution was quickly added to the mix, followed by thorough vortexing and incubation for 30 min at 37°C. Next, the transfection mix was added drop-wise to the cells and incubated with the cells overnight at 37°C. The following day, the medium of the transfected cells was exchanged and kept on the HEK293FT cells for 48 h for maximum virus concentration. As a control, a virus containing the empty backbone of the overexpression construct and a virus expressing eGFP were generated in parallel.

7.2.3.7. Viral transfection of THP-1 and DLBCL cells

Stable overexpression cell lines were generated using lentivirus-mediated transduction, since lentivirus are capable of stably integrating long DNA sequences with a high efficiency into host cells. The lentivirus was produced by transiently transfecting HEK293FT cells with the respective overexpression construct and the lentiviral packaging plasmids using the calcium-phosphate precipitation method. As a control, the empty backbone of the overexpression construct and a lentiviral plasmid containing an eGFP overexpression cassette were generated and transfected in parallel dishes. 48 h post transfection, the medium containing lentiviral particles was transferred from the HEK293FT cells to the target cells after passing it through a 0.45 µm filter. Polybrene (8 mg/ml) was added to the supernatant in a dilution of 1:1000. The virus and target cells were incubated for 24 h in the incubator at 37°C. Virus incubation was stopped by pelleting the cells, washing them three times with PBS and reconstituting them in full RPMI medium in a fresh cell culture flask. 48 h post-transduction, transfection efficiency was assessed by detecting the green fluorescence of GFP-expressing control cells using the Zeiss fluorescence microscope.

As the overexpression constructs contain an open reading frame with a puromycin or neomycin resistance gene sequence, stably transduced cells were selected by cultivation with a medium containing an appropriate concentration of puromycin or G418. After the selection, dead cells were removed by centrifugation at 500 rpm for 5 min. The surviving cells were subsequently cultured in medium containing puromycin or G418 to maintain the overexpression.

Since lentiviruses are categorized as safety class 2 (S2) organisms, all work described here was performed under S2 safety rules.

7.2.3.8. Differentiation and stimulation of THP-1 cells

Originally, THP-1 cells were derived from a 1 year-old boy suffering from acute monocytic leukemia (Tsuchiya et al., 1980). Cells stably display the phenotype of blood monocytes while at the same time sustain their ability to divide. After treatment with phorbol 12-myristate 13-acetate (PMA), however, they stop dividing and differentiate into macrophages, thus being an excellent tool to examine human macrophages *in vitro* (Auwerx, 1991).

For the experiments, THP-1 cells were differentiated to macrophages and activated by LPS. For this purpose, cells from the sustained culture were centrifuged (5 min, 1200 rpm at RT), reconstituted in complete RPMI medium and counted using a Neubauer counting chamber.

Depending on the planned experiment, cells were seeded into 6-well plates ($1.5x10^5$ cells in 2 ml full RPMI), 10-cm culture dishes ($5x10^5$ cells in 10 ml full RPMI) or 20-cm culture dishes ($1x10^6$ cells in 20 ml full RPMI). 10 mg/ml PMA was added 1:10 000 and the cells were incubated for 3 days. Next, the medium was aspirated and replaced with fresh medium. The cells were left to rest for 4 days. 1 mg/ml LPS was added 1:1000 for another 1 h and 2 h (RNA extraction) or 4 h (protein extraction) or 8 h (FACS), with an equal amount of carrier solution added to the controls.

7.2.3.9. Stimulation of DLBCL pInd20 IκB$_{NS}$ isoform 1

The DLBCL cell lines used are derived from cells extracted from samples from different patients suffering from DLBCL. The cells were transfected with a lentivirus containing a doxycycline-inducible IκB$_{NS}$ isoform 1 expression cassette. Prior to experiments, IκB$_{NS}$ isoform 1 expression had to be induced by adding 1 µg/ml Doxycycline for 24 h (protein extraction and RNA extraction). The late time point for RNA extraction was chosen since the effects were mediated by the overexpressed protein on the transcriptional level (secondary response). Thus, enough time for the cells to produce IκB$_{NS}$ isoform 1 and generate the RNA response to it was needed.

Depending on the planned experiment, cells were seeded into 6-well plates ($5x10^5$ cells in 2 ml full RPMI) or 10-cm culture dishes ($2x10^6$ cells in 10 ml full RPMI).

8. Results

8.1. Identification of IκB$_{NS}$ target genes

Since IκB$_{NS}$ belongs to the protein family of atypical inhibitors of kappa B proteins, it should have comparable functions like the other family members such as BCL3 or IκBζ. The main feature of these inhibitor proteins is the regulation of so-called "secondary response genes" that are induced by NF-κB activation. This leads to an arranged expression of cytokines and other transcription factors, which finally ends in activation of a negative feedback loop.

8.1.1. Overexpression and genomic knockout of IκB$_{NS}$ in THP-1

The stable acute monoblastic leukemia cell line THP-1 can be differentiated *in vitro* to cells that closely resemble macrophages. To examine the effect of IκB$_{NS}$ in macrophages, a knock-out system was established. In addition, the two most highly expressed isoforms of IκB$_{NS}$ were overexpressed to assess differences in their regulatory function on macrophage biology.

For that purpose, THP-1 cells were lentivirally transduced with silencing and overexpression constructs for the specific human IκB$_{NS}$ sequences. Also a lentiviral overexpression GFP-harboring cell line was generated as a control for infection efficiency. After expansion of transduced THP-1 cells with a positive visible eGFP, cells were selected by puromycin treatment. After one week of selection, the surviving cells were tested for depletion and overexpression of the target protein.

To examine the effect of IκB$_{NS}$ in macrophages, THP-1 cells needed to be differentiated to macrophages. As IκB$_{NS}$ expression is strictly NF-κB-dependent, NF-κB activity had to be induced to properly examine the effect of IκB$_{NS}$ overexpression in macrophages in a state when it is expressed physiologically.

Before any further experiments were performed, the presence of IκB$_{NS}$ overexpression was confirmed via immunoblotting.

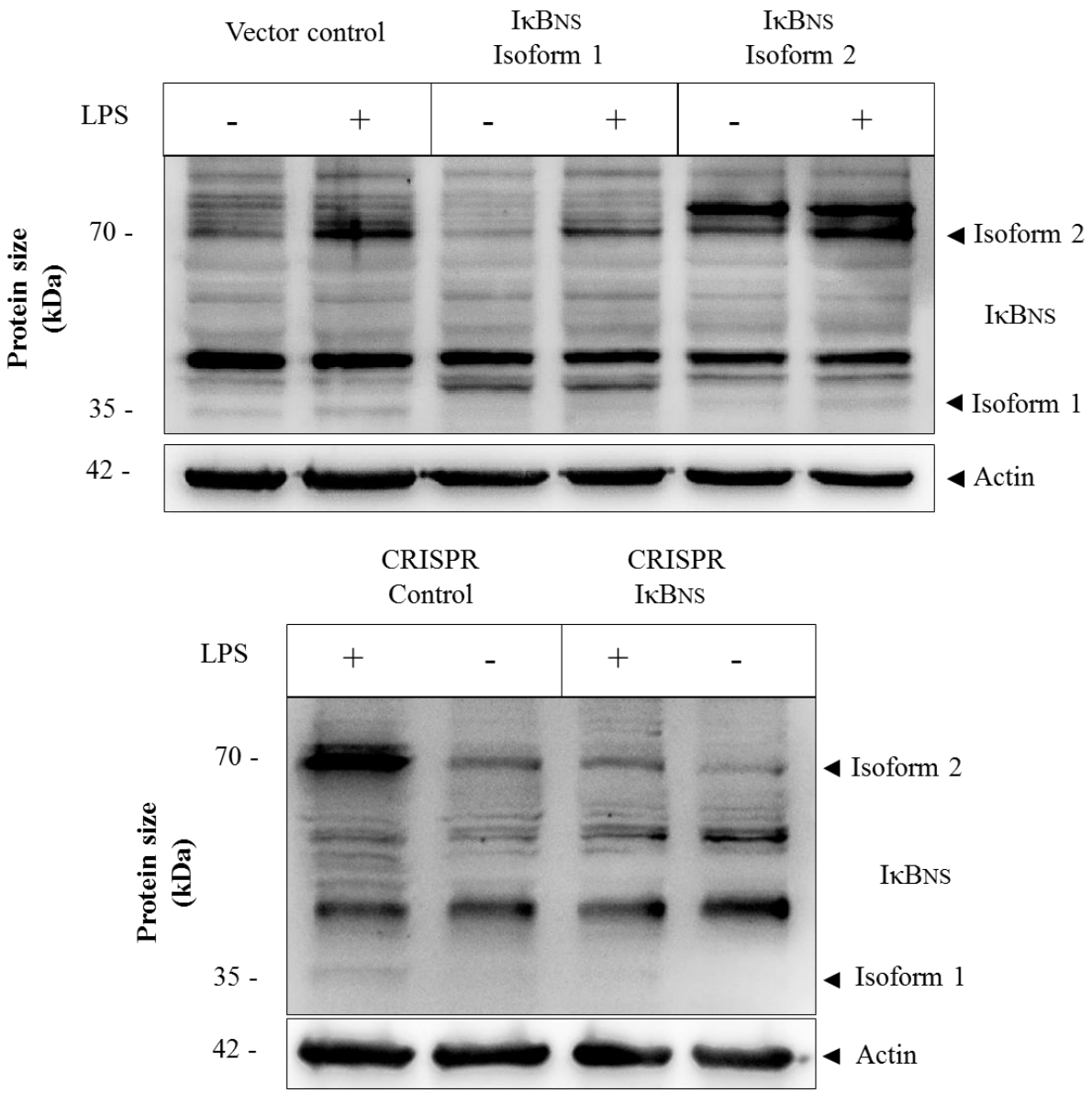

Figure 8.1: Overexpression of $I\kappa B_{NS}$ isoforms 1 and 2 and knock-out of $I\kappa B_{NS}$ in THP-1 cells.

Cells were transduced with overexpression constructs containing $I\kappa B_{NS}$ isoform 1 and 2 and the empty vector as control for the overexpression (upper blots) as well as with the CRISPR/Cas9 lacking a guide RNA as a control and the CRISPR/Cas9 targeted against $I\kappa B_{NS}$ for the knockout (lower blots). Subsequently, they were differentiated to macrophages using 1 µg/ml PMA for 3 days, followed by 4 days of further incubation in fresh medium. The cells were then stimulated with 1 µg/ml LPS for 4 hours (+LPS) or an equal volume of carrier solution was added as control (-LPS). Following stimulation, the cells were harvested for protein extraction and immunoblot analysis using antibodies targeting $I\kappa B_{NS}$ isoforms 1 and 2 and an antibody targeting β-actin as a loading control. In each lane, 40 µg of protein lysate was loaded.

The analysis showed an LPS-induced expression of IκB$_{NS}$ isoform 1 and 2 in all cells containing the overexpression constructs. In the cells overexpressing isoform 1 and 2, additional bands slightly larger than the respective overexpressed IκB$_{NS}$ isoform appeared, possibly due to posttranslational modifications of the proteins.

Bands representing IκB$_{NS}$ isoform 1 and 2 were detectable in the CRISPR control after LPS stimulation. In the cells with CRISPR targeting IκB$_{NS}$, no induction of IκB$_{NS}$ was visible after LPS stimulation.

In conclusion, the generated cell lines appeared suitable for the analysis of the effect of IκB$_{NS}$ overexpression and depletion in macrophages.

8.1.2. IκB$_{NS}$ is involved in the regulation of NF-κB proteins

Preliminary data from our lab have shown a reciprocal between atypical inhibitors of kappa B proteins in murine macrophages (unpublished data). Hence, the effects of IκB$_{NS}$ isoforms on BCL3 and IκBζ mRNA and protein levels were examined in a human macrophage cell system.

As IκB$_{NS}$ mRNA expression is directly regulated by the NF-κB unit p65, protein levels of p65 were examined. NFκB activity is mainly regulated via post-translational modifications, thus we also examined the levels of phosphorylated p65.

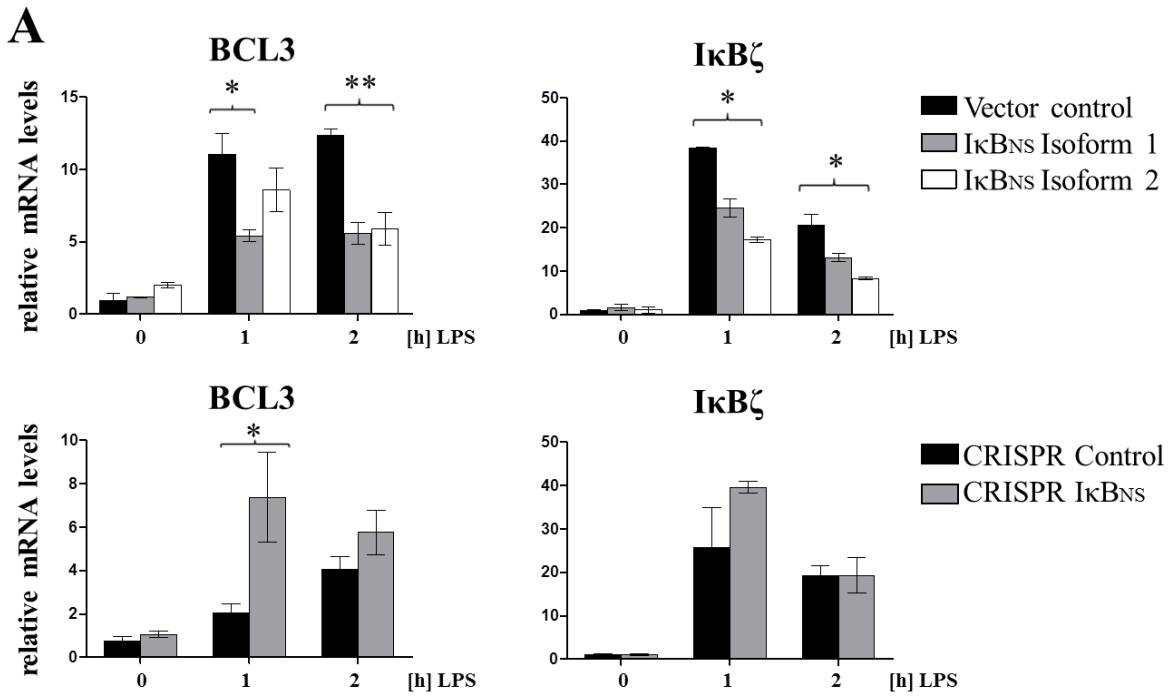

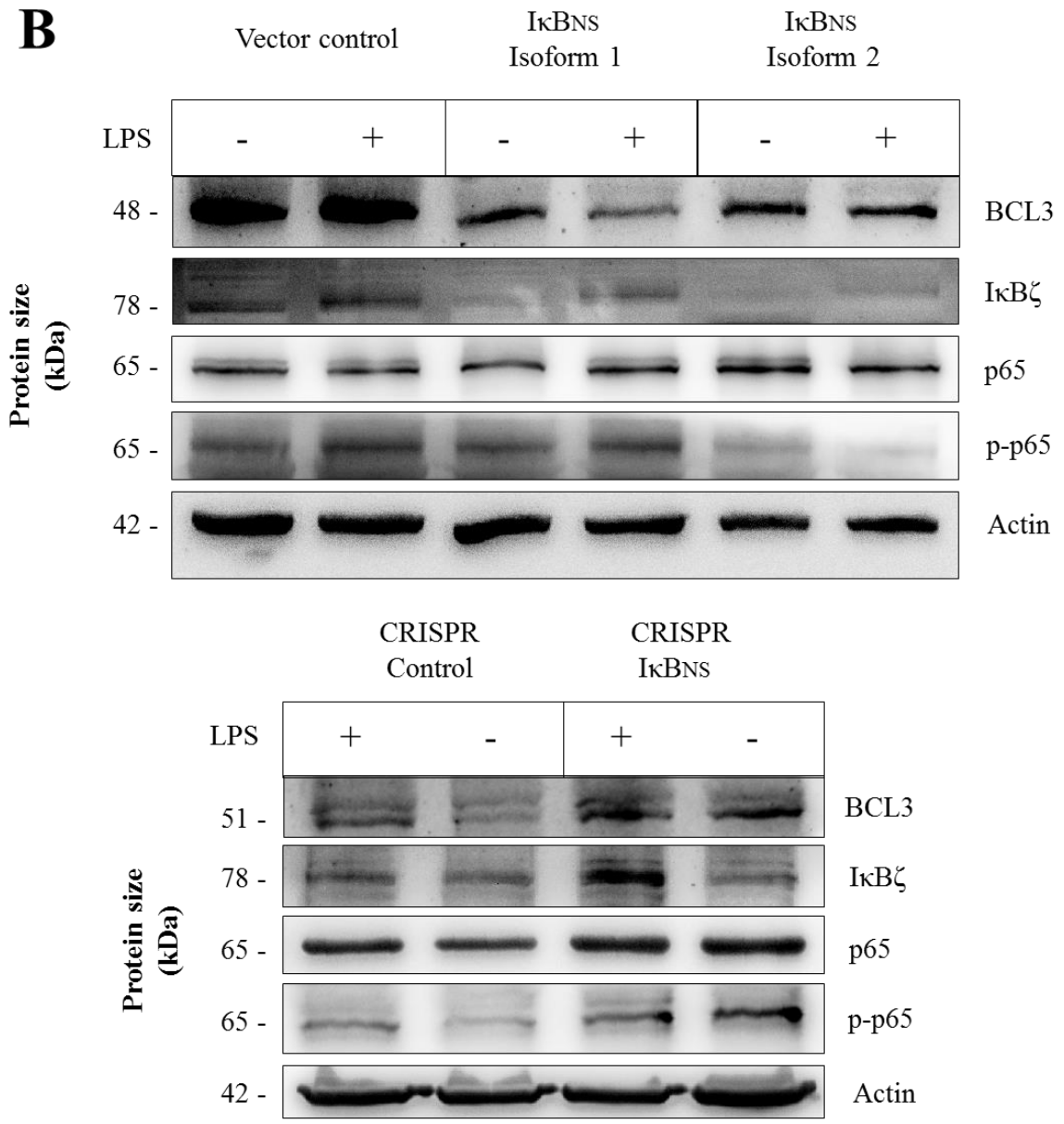

Figure 8.2: Altered BCL3 and IκBζ protein levels and p65 phosphorylation in THP-1 overexpressing $I\kappa B_{NS}$ isoforms 1 and 2 and with $I\kappa B_{NS}$ knocked out.

A. *BCL3 and IκBζ RNA levels were downregulated in THP-1 cells overexpressing $I\kappa B_{NS}$ isoform 1 and 2. Knock-out of $I\kappa B_{NS}$ resulted in enhanced expression of BCL3 and IκBζ mRNA after 1 h stimulation, while RNA levels converged after 2 h. THP-1 cells were treated as described in Figure 8.1. Following stimulation for 1 h and 2 h, the cells were harvested for subsequent RNA extraction and qPCR using primer pairs targeting BCL3 or IκBζ cDNA for analysis and a primer pair targeting β-actin cDNA as a house keeper for normalization. Standard deviations derive from biological triplicates and two experiments. Asterisks show statistical significance calculated using the student's t-test. * $p \leq 0.05$ and ** $p \leq 0.005$.*

B. *$I\kappa B_{NS}$ overexpression resulted in reduced expression of BCL3 and IκBζ as well as lower levels of phosphorylated p65. Knock-out of $I\kappa B_{NS}$ resulted in increased levels of phosphorylated p65 and IκBζ and BCL3 proteins after LPS stimulation. THP-1 cells were treated as described in Figure 8.1. Following stimulation, the cells were harvested for protein extraction and analysis via the immunoblotting method, using antibodies targeting BCL3, IκBζ, p65 and phospho-p65 (p-p65) for analysis, respectively, and an antibody targeting β-actin as a loading control. In each lane, 40 µg of protein lysate was loaded.*

IκB$_{NS}$ isoform 1 overexpression suppressed BCL3 and IκBζ expression on the transcriptional level while not interfering with post-translational p65 activation, while IκB$_{NS}$ isoform 2 affected BCL3 and IκBζ gene expression as well as post-translational p65 activation. Conversely, knock out of IκB$_{NS}$ resulted in enhanced expression of BCL3 and IκBζ as well as an enhanced activation of p65, confirming the results of the analysis of IκB$_{NS}$ overexpression.

8.1.3. Effect of IκB$_{NS}$ on STAT signaling

As described above, atypical inhibitors of kappa protein family members BCL3 and IκBζ have already been shown to regulate expression and activation of proteins of the inflammasome, namely STAT1 and STAT3. Consequently, the effect of IκB$_{NS}$ overexpression and knockout on the transcription and posttranslational activation by phosphorylation of these factors was examined.

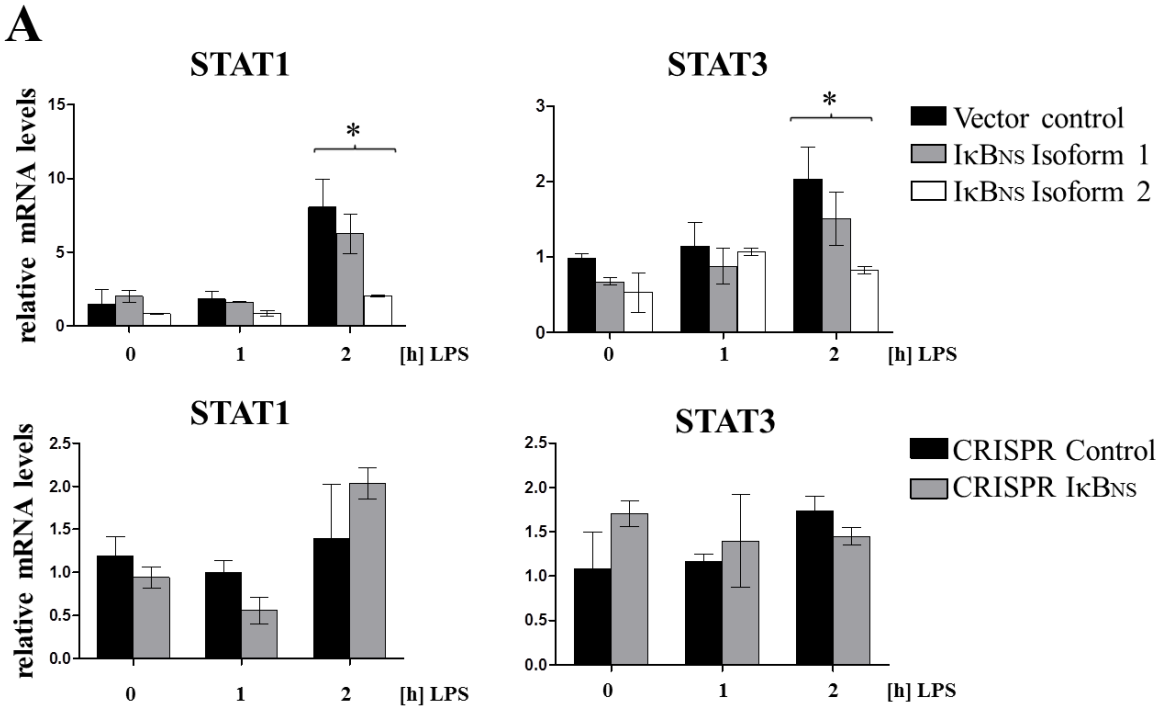

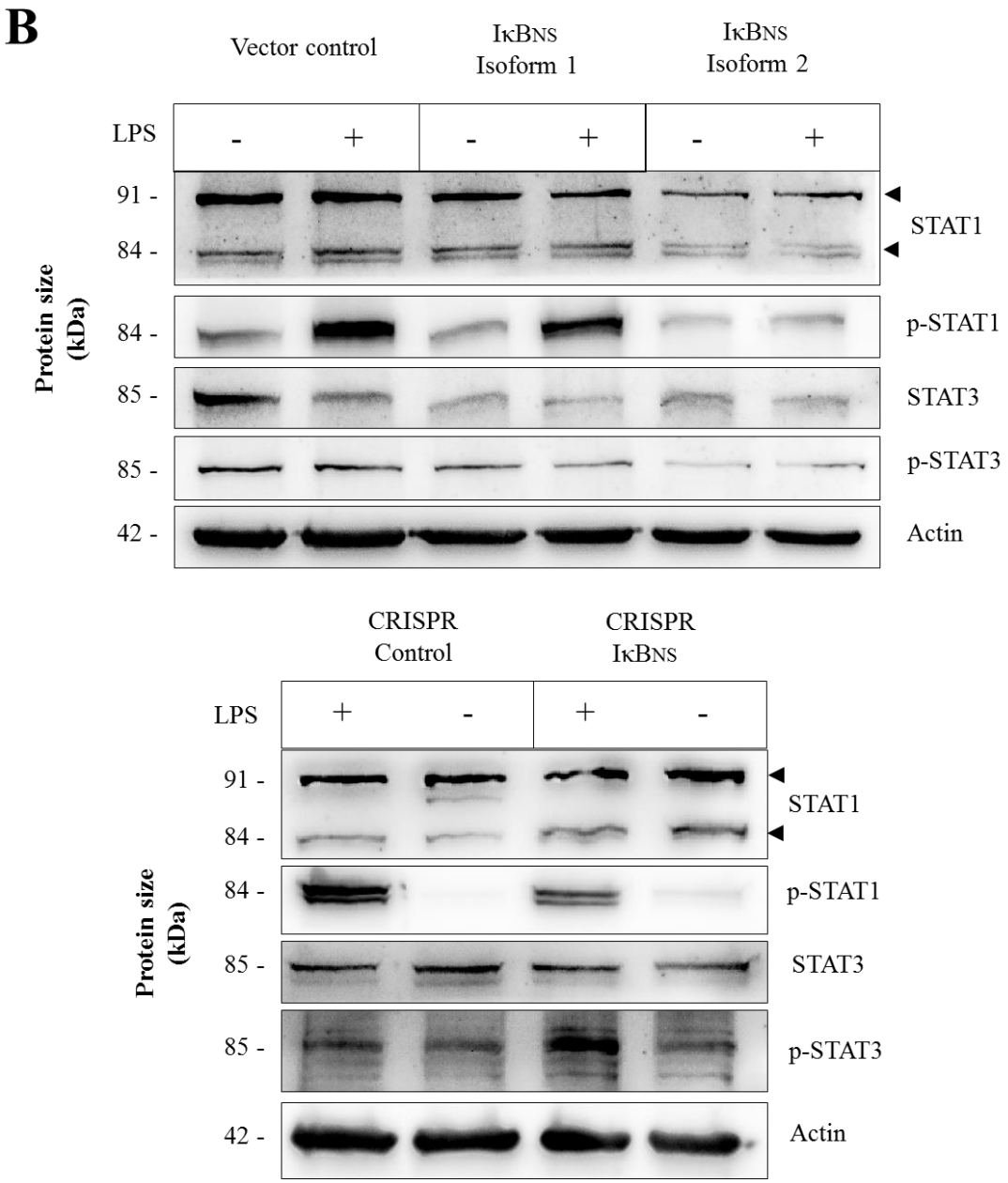

Figure 8.3: Effect of IκB$_{NS}$ overexpression and knock-out on STAT signaling

A. *STAT1 and STAT3 mRNA levels were decreased in cells overexpressing IκB$_{NS}$ isoform 2, while overexpression of isoform 1 had no significant effect on STAT1 and STAT3 mRNA levels. STAT1 and STAT3 mRNA levels were unchanged by the knockout of IκB$_{NS}$. THP-1 cells were treated as described in Figure 8.1. Following stimulation for 1 h and 2 h, the cells were harvested for subsequent RNA extraction and qPCR using primer pairs targeting STAT1 or STAT3 cDNA for analysis and a primer pair targeting β-actin cDNA as a house keeper for normalization. Standard deviations derive from biological triplicates and two experiments. Asterisks show statistical significance calculated using the student's t-test. * $p \leq 0.05$.*

B. *STAT1 and STAT3 protein levels were diminished in cells overexpressing IκB$_{NS}$ isoform 2. Consequently, p-STAT1 was depleted during IκB$_{NS}$ isoform 2 overexpression. STAT1 and STAT3 protein levels were unchanged by the knockout of IκB$_{NS}$. p-STAT1 levels were slightly decreased, while p-STAT3 levels were highly elevated. THP-1 cells were treated as described in Figure 8.1. Following stimulation, the cells were harvested for protein extraction and analysis via the immunoblotting method, using antibodies targeting STAT1, phospho-STAT1 (p-STAT1), STAT3 and phospho-STAT3 (p-STAT3) for analysis, respectively, and an antibody targeting β-actin as a loading control. In each lane, 40 µg of protein lysate was loaded.*

$I\kappa B_{NS}$ overexpression or knock-out had little effect on STAT1 and STAT3 gene expression. Since STAT signaling is mainly regulated on the post-translational level, the phosphorylation level of STAT1 and STAT3 proteins were also analyzed. $I\kappa B_{NS}$ isoform 1 overexpression showed little effect on the STAT protein phosphorylation, cells overexpressing $I\kappa B_{NS}$ isoform 2 showed reduced levels of phosphorylated STAT1 proteins. Conversely, cells with both $I\kappa B_{NS}$ isoforms knocked out showed reduced levels of phosphorylated STAT1 and strongly increased levels of phosphorylated STAT3 protein.

8.1.4. Regulation of secreted factors in activated macrophages by $I\kappa B_{NS}$

Upon activation macrophages start secreting large quantities of different cytokines, chemokines and acute phase proteins to attract and stimulate T-cells, B cells and other immune cells. Since NF-κB has already been shown to strongly regulate the expression of inflammatory cytokines, it is suggestive that $I\kappa B_{NS}$ may be involved in the fine-regulation of these processes.

To examine this regulation, mRNA levels of several secreted factors of macrophages were analyzed after 1 h and 2 h of LPS stimulation.

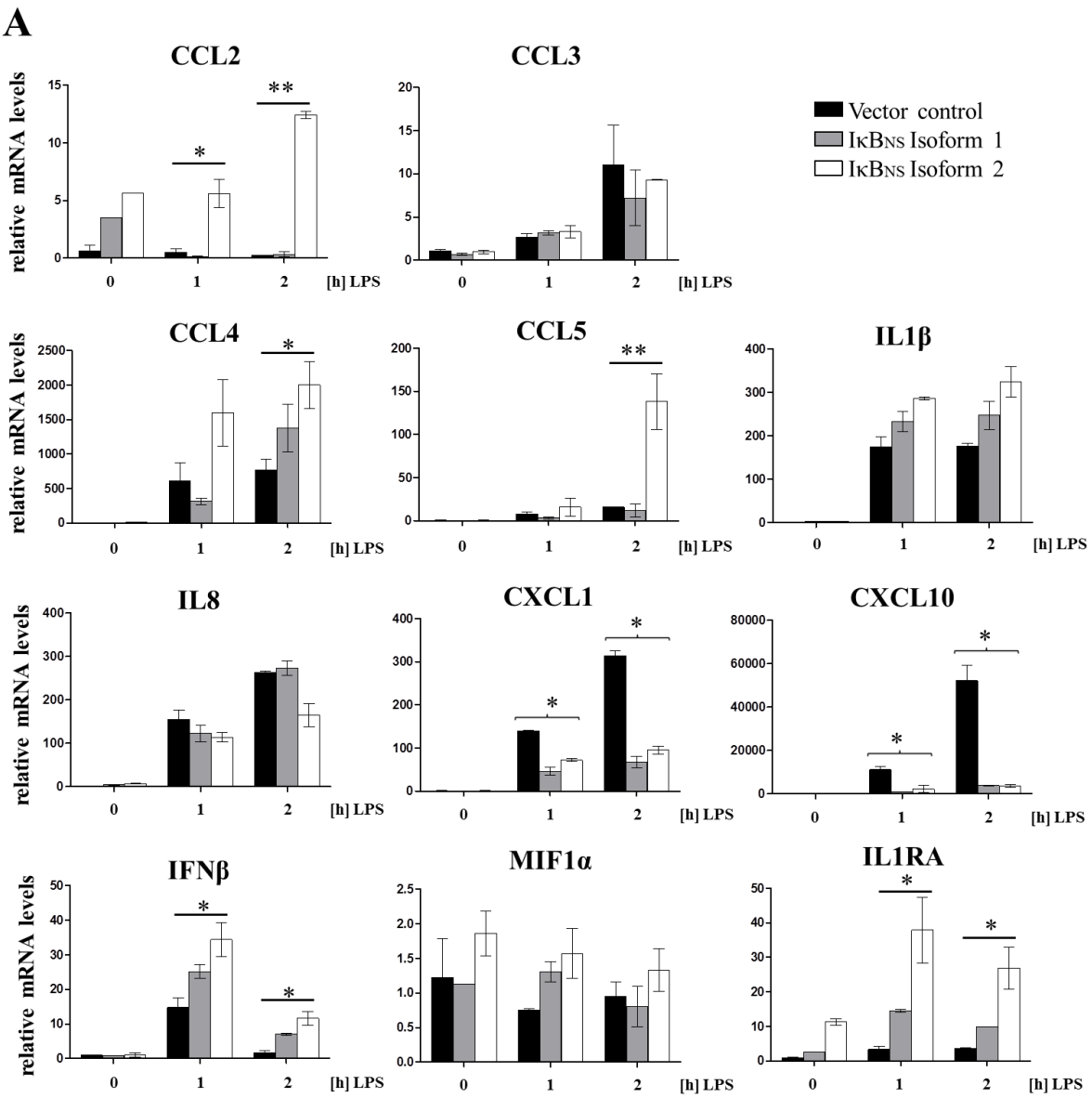
A
CCL2
CCL3
CCL4
CCL5
IL1β
IL8
CXCL1
CXCL10
IFNβ
MIF1α
IL1RA
relative mRNA levels
[h] LPS
Vector control
IκBNS Isoform 1
IκBNS Isoform 2

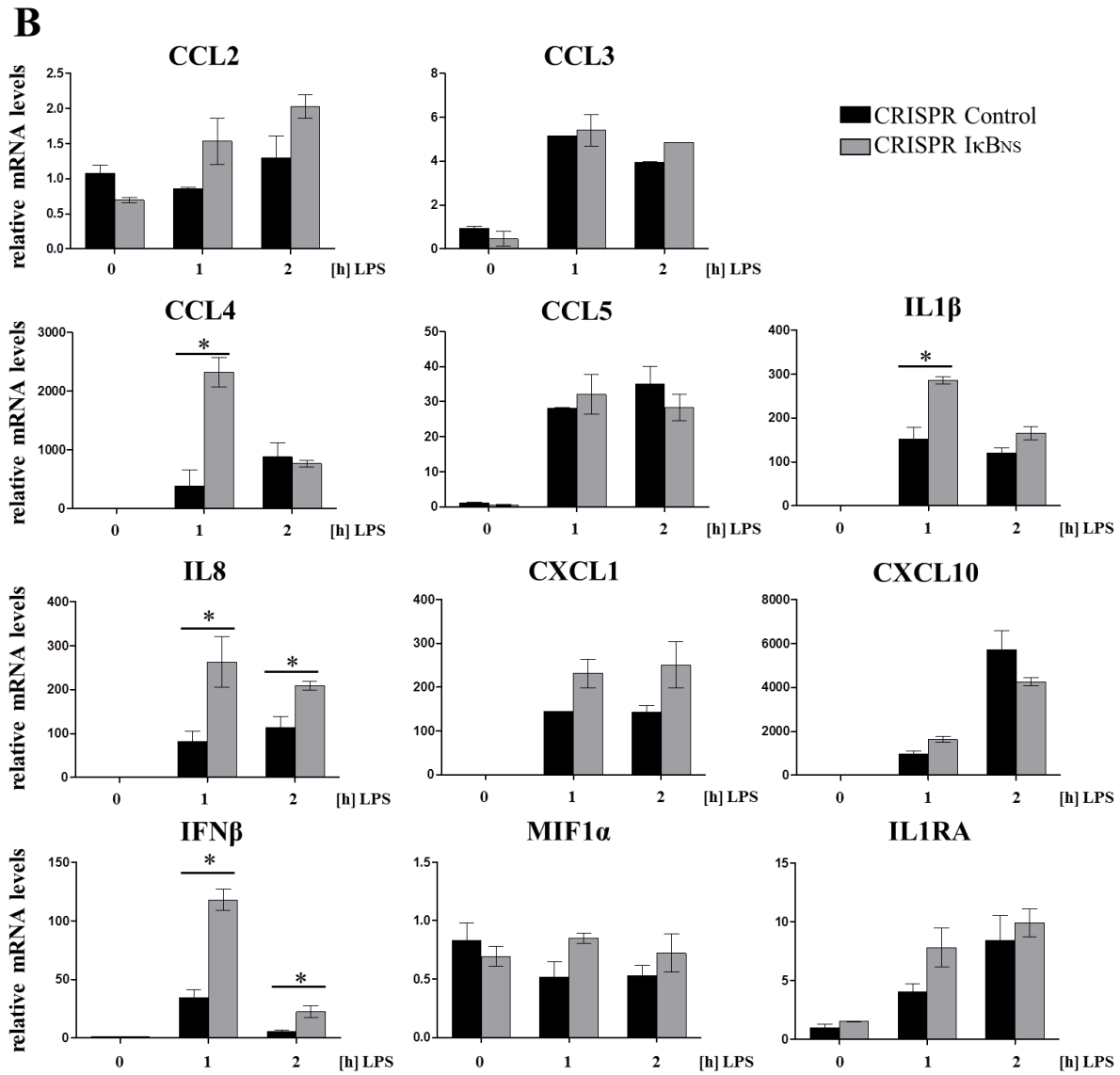

Figure 8.4: Overexpression (A) and knockout (B) of IκB$_{NS}$ resulted in differing expression levels of cytokines and chemokines.

*THP-1 cells were differentiated to macrophages using 1 µg/ml PMA for 3 days, followed by 4 days rest in fresh medium. The cells were then stimulated with 1 µg/ml LPS for 1 hour and 2 hours or an equal volume of carrier solution was added as control. Following stimulation, the cells were harvested for subsequent RNA extraction and qPCR using primer pairs targeting CCL2, CCL3, CCL4, CCL5, IL1β, IL8, CXCL1, CXCL10, interferon-β (IFNβ), MIF1α or interleukin 1 receptor-antagonist (IL1RA) cDNA for analysis and a primer pair targeting β-actin cDNA as a house keeper for normalization. This was performed with cells transduced with the empty vector as a control and with the cells transduced with the overexpression constructs containing IκB$_{NS}$ isoform 1 and 2 for the overexpression (A) as well as with cells transfected with the CRISPR/Cas9 lacking a guide RNA as a control and the CRISPR targeted against IκB$_{NS}$ for the knockout (B), respectively. Standard deviations derive from biological triplicates. Asterisks show statistical significance calculated using the student's t-test. * $p \leq 0.05$ and ** $p \leq 0.005$.*

Overexpression of IκB$_{NS}$ isoform 1 resulted in upregulation of IL1RA and downregulation of CXCL1 and CXCL10 mRNA levels, while overexpression of IκB$_{NS}$ isoform 2 resulted in upregulation of CCL2, CCL4, CCL5, IFNβ and IL1RA and downregulation of CXCL1 and CXCL10 mRNA levels. Cells with IκB$_{NS}$ knocked out showed an upregulation of IFNβ, CCL4, IL1β and IL8.

As the physiological effect of cytokines is mediated by proteins and protein levels are not only regulated at the transcriptional level, the levels of secreted cytokines in the culture medium were also directly assayed. To this means, THP-1 were differentiated to macrophages and stimulated with LPS for 24 h, thus giving the cells time to express, synthesize and secrete cytokines to the culture medium. Following this stimulation, the supernatant was harvested, normalized to the cell number and directly analyzed by means of the Human cytokine array panel A (R&D). As differences in the transcriptional activity were only sustained in the cells overexpressing IκB$_{NS}$ isoform 1 and 2, only the supernatants of the cells containing the overexpression constructs were examined.

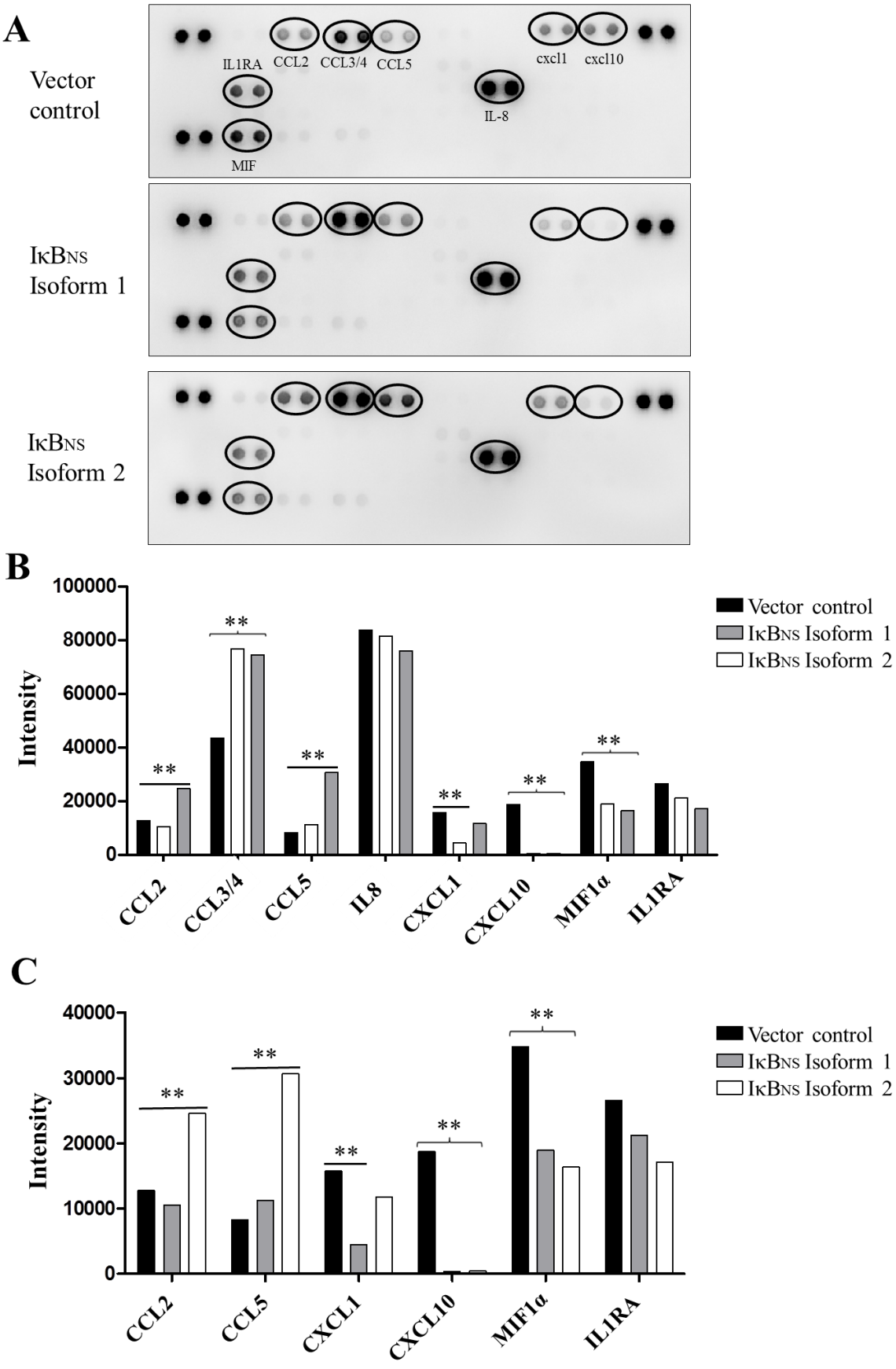
A
Vector control
IκBNS Isoform 1
IκBNS Isoform 2
IL1RA
CCL2
CCL3/4
CCL5
cxcl1
cxcl10
IL-8
MIF
B
Intensity
100000
80000
60000
40000
20000
0
**
CCL2
CCL3/4
CCL5
IL8
CXCL1
CXCL10
MIF1α
IL1RA
Vector control
IκBNS Isoform 1
IκBNS Isoform 2
C
Intensity
40000
30000
20000
10000
0
**
CCL2
CCL5
CXCL1
CXCL10
MIF1α
IL1RA
Vector control
IκBNS Isoform 1
IκBNS Isoform 2

Figure 8.5: Secretion of cytokines and chemokines by LPS-treated macrophages is altered during overexpression of IκB$_{NS}$ isoforms 1 and 2.

*THP-1 cells were treated as described in Figure 8.1 and stimulated for 24 h with LPS. Following stimulation, the supernatant was harvested for subsequent protein analysis using the Human cytokine array panel A (R&D). The adherent cells were scraped off in 5 ml PBS and counted for adequate normalization of the cell density. This was performed with cells transduced with the empty vector as a control and with the cells transduced with the overexpression constructs containing IκB$_{NS}$ isoform 1 and 2 for the overexpression, respectively. The duplicate dots shown in (A) represent the amount of cytokines in the supernatant and were quantified using the program ImageJ. The results of the quantification were averaged and are shown in (B) (all) and (C) (low intensity, for better visualization). Asterisks show statistical significance calculated using the student's t-test. * $p \leq 0.05$ and ** $p \leq 0.005$.*

Overexpression of IκB$_{NS}$ isoform 1 resulted in a downregulation of CXCL1 and CXCL10 protein secretion on the transcriptional level and an upregulation of IL1RA mRNA expression that was not reproducible on the protein level. Conversely, CCL3/4 levels were elevated and MIF1α levels were decreased on the protein level while there were no changes of mRNA levels.

Cells overexpressing IκB$_{NS}$ isoform 2 showed an upregulation of CCL2, CCL3/4 and CCL5 protein secretion and a downregulation of CXCL10 protein secretion on the transcriptional level. CXCL1 was downregulated and IL1RA was upregulated on the mRNA level while not being deregulated on the protein level. IFNβ was upregulated on the mRNA level. As it was not part of the cytokine array, no protein data of it are available. Conversely, MIF1α was downregulated on the protein level while not being deregulated on the mRNA level.

Cells with IκB$_{NS}$ knocked out only showed an upregulation of CCL4, IFNβ and IL8 on the mRNA level.

8.1.5. Effect of IκB$_{NS}$ on monocyte differentiation

NF-κB and STAT signaling play a pivotal role in the differentiation process of monocytes and in the determination of the cell type they differentiate to. As IκB$_{NS}$ overexpression and knock-out showed a marked effect on NF-κB and STAT signaling, it is highly suggestive that IκB$_{NS}$ has an impact on the fate of monocytes triggered to differentiate. Thus, following differentiation and stimulation of THP-1 cells, surface markers determining the differentiation path the monocytic cell has chosen were analyzed using fluorescence-assisted cell sorting (FACS).

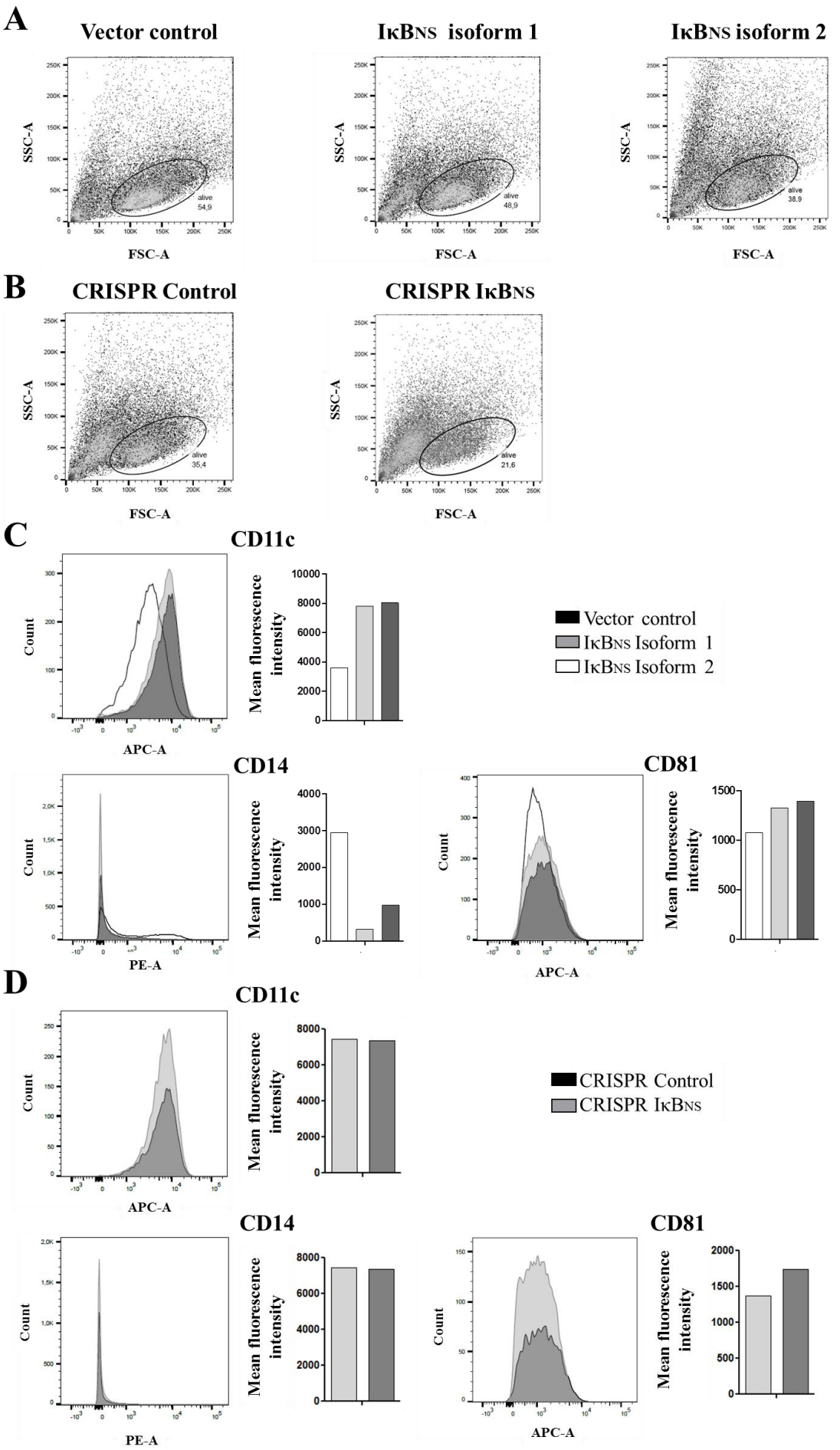
A
Vector control
IκBNS isoform 1
IκBNS isoform 2
SSC-A
FSC-A
alive
54,9
alive
48,9
alive
38,9
B
CRISPR Control
CRISPR IκBNS
alive
35,4
alive
21,6
C
CD11c
Count
APC-A
Mean fluorescence intensity
Vector control
IκBNS Isoform 1
IκBNS Isoform 2
CD14
PE-A
CD81
D
CD11c
CRISPR Control
CRISPR IκBNS
CD14
CD81

Figure 8.6: Effect of IκB$_{NS}$ overexpression and knock-out on macrophage- and dendritic cell-specific surface markers on THP-1 cells.

THP-1 cells were differentiated to macrophages using 1 µg/ml PMA for 3 days, followed by 4 days rest in fresh medium. The cells were then stimulated with 1 µg/ml LPS for 8 hours (+LPS) or an equal volume of carrier solution was added as control (-LPS). Following stimulation, the cells were harvested for FACS staining and analysis using fluorescent protein-coupled antibodies targeting CD11c, CD14 and CD81. Single cells were analyzed to a count of 10,000 cells was reached. This was performed with cells transduced with the empty vector as a control and with the cells transduced with the overexpression constructs containing IκB$_{NS}$ isoform 1 and 2 for the overexpression (sections A and C) as well as with cells transfected with the CRISPR/Cas9 lacking a guide RNA as a control and the CRISPR targeted against IκB$_{NS}$ for the knockout (sections B and D), respectively.

Overexpression of IκB$_{NS}$ isoforms 1 and 2 result in a shift in the balance from macrophages to dendritic cells in the differentiation process of THP-1, shown by a shift from CD14 high cells in the control to CD11c high cells during overexpression of IκB$_{NS}$, while not significantly influencing the activation of the cells after LPS stimulation. Knock-out of IκB$_{NS}$ did not show any effect on the balance between macrophages and dendritic cells or cell activation after LPS stimulation. Overexpression or knock-out of IκB$_{NS}$ did not show a significant effect on cell viability characterized by the respective population in the FSC/SSC plot.

8.1.6. IκB$_{NS}$ in HIV infection

The life cycle of HIV heavily relies on NF-κB signaling in both T lymphocytes as well as in macrophages (DeLuca et al., 1998), which form a major virus reservoir. In addition, STAT signaling is essential for host defense against viral infection (Chaudhuri et al., 2008) and appears to be regulated by IκB$_{NS}$. Thus, overexpression of IκB$_{NS}$ isoforms is highly likely to have an effect on the expression of pro-inflammatory cytokines after contact to viable viral particles. The part of the experiments requiring a biosafety level 3 laboratory were performed by Ramona Businger in the laboratory of Prof. Dr. Michael Schindler, following the protocol described by (Koppensteiner et al., 2012).

The viral particles were produced using HEK293FT cells. The virus concentration was determined using an ELISA targeting p24. The virus-containing supernatant was then transferred to the differentiated THP-1 with a concentration of 50 pg p24 per 200,000 cells. The cells were harvested 48 h later for RNA isolation and qPCR.

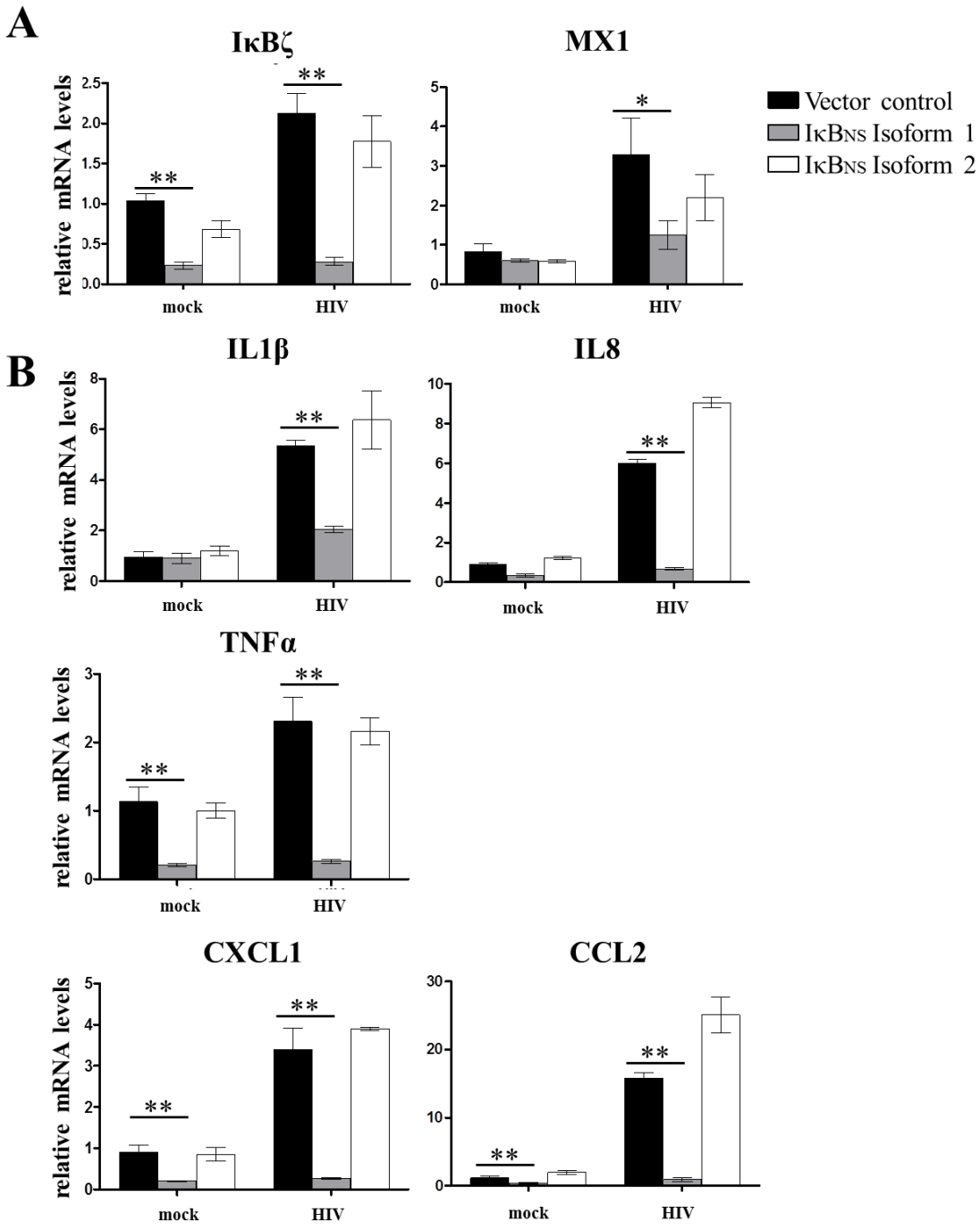

Figure 8.7: Effect of overexpression of IκB$_{NS}$ isoform 1 and 2 on the expression of intracellular (A) and secreted (B) factors after infection with HIV.

*THP-1 cells were differentiated to macrophages using 1 µg/ml PMA for 3 days, followed by 4 days rest in fresh medium. The cells were then exposed to viral particles generated in HEK293FT cells for 48 hours and subsequently harvested for RNA extraction and qPCR using primer pairs targeting IκBζ, MX1, IL1β, IL8, TNFα, CXCL1 and CCL2 cDNA for analysis and a primer pair targeting β-actin cDNA as a house keeper for normalization. This was performed with cells transduced with the empty vector as a control and with the cells transduced with the overexpression constructs for IκB$_{NS}$ isoform 1 and 2, respectively. Standard deviations derive from biological triplicates. Asterisks show statistical significance. * $p \leq 0.05$ and ** $p \leq 0.005$.*

Overexpression of IκB$_{NS}$ isoform 1 resulted in generally lower mRNA levels of all examined genes, namely IκBζ, MX1, IL1β, IL8, TNFα, CXCL1 and CCL2, after contact with HIV. However, this deregulation was partially visible in cells with mock treatment. Overexpression of IκB$_{NS}$ isoform 2 overexpression had no significant effects on the expression levels of the targets evaluated here.

8.2. Regulation of gene expression by IκB$_{NS}$ in DLBCL

8.2.1. Effect of IκB$_{NS}$ isoform 1 overexpression in DLBCL

The NF-κB pathway is highly active in many types of lymphoma and appears to be a key element of the survival and proliferation of lymphoma cells (Davis et al., 2001), making it an essential part of tumor progression *in vivo.* Hence, the analysis of downstream elements of the NF-κB pathway is crucial for a proper understanding of the disease and, subsequently, may be helpful in the development of new treatment options. As the other members of the atypical IκB protein family BCL3 and IκBζ have already been shown to be indispensable for DLBCL survival and pathogenesis, IκB$_{NS}$ may also be involved in these processes (Nogai et al., 2013, Ibrahim et al., 2011b). Here, the effect of IκB$_{NS}$ isoform 1 overexpression was examined in two of the most common diffuse large B cell lymphoma (DLBCL) subtypes, the germinal cell B cell-like (GCB) and the activated B cell-like (ABC) DLBCL, respectively.

In order to analyze the effect of IκB$_{NS}$ on gene expression in these cell lines, two GCB and two ABC DLBCL cell lines were generated with doxycycline-inducible overexpression of IκB$_{NS}$ isoform 1, using the pInd20 toolkit (Meerbrey et al., 2011).

After expansion, the inducibility of IκB$_{NS}$ isoform 1 had to be confirmed and a permanent overexpression had to be ruled out.

Hence, 1 µg/ml doxycycline was added to the culture medium for 24 h. Subsequently, the IκB$_{NS}$ expression was confirmed via the immunoblotting method. Figure 8.8 shows the control for effective induction of IκB$_{NS}$ isoform 1 overexpression in the DLBCL cell lines.

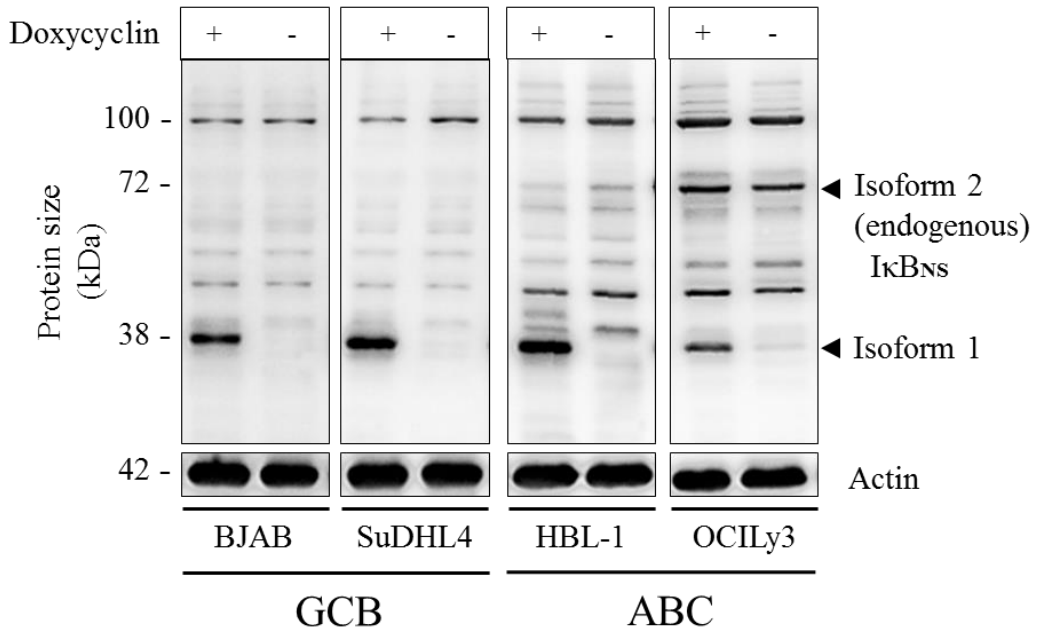

Figure 8.8: $I\kappa B_{NS}$ isoform 1 overexpression in DLBCL after 24 h of doxycycline stimulation.

DLBCL cells were transduced and selected for 7 days with 1 µg/ml G418. The cells were then treated with 1 µg/ml doxycycline or carrier solution. Following stimulation, the cells were harvested for protein extraction and analysis via the immunoblotting method, using an antibody targeting $I\kappa B_{NS}$ isoforms 1 and 2 for analysis and an antibody targeting β-actin as a loading control. In each lane, 40 µg of protein lysate was loaded. This was performed with BJAB and SuDHL-4 cells representing GCB DLBCL and HBL-1 and OCILy3 representing ABC DLBCL. Of each transfected cell line, unstimulated cells were used as a control and doxycycline-treated cells were used for the overexpression of $I\kappa B_{NS}$ isoform 1, respectively.

The analysis showed a new strong band with a size of 38 kDa after 24 h of doxycycline treatment, matching to an inducibly overexpressed $I\kappa B_{NS}$ isoform 1, which was only faintly visible in untreated HBL-1 and OCILy3. As ABC-DLBCL cells constitutively overexpress NF-κB, and $I\kappa B_{NS}$ represents a primary response NF-κB target gene, it was not surprising that the cells contained detectable amounts of $I\kappa B_{NS}$ isoform 1 even without additional stimulation and showed a constitutive expression of $I\kappa B_{NS}$ isoform 2.

In conclusion, these cell lines appeared suitable for the analysis of the effect of $I\kappa B_{NS}$ isoform 1 overexpression on DLBCL.

8.2.2. Expression of atypical IκB proteins is altered in DLBCL cells overexpressing $IκB_{NS}$ isoform 1

As mentioned above, preliminary data from our lab have already shown a reciprocal regulation of atypical inhibitors of kappa B proteins in murine macrophages, and BCL3 and IκBζ appeared to be deregulated due to overexpression of $IκB_{NS}$ isoform 1 in THP-1 cells as well. Since BCL3 and IκBζ have been shown to be essential for ABC DLBCL (Massoumi et al., 2006, Nogai et al., 2013), an effect of $IκB_{NS}$ isoform 1 on DLBCL survival may be mediated by these proteins.

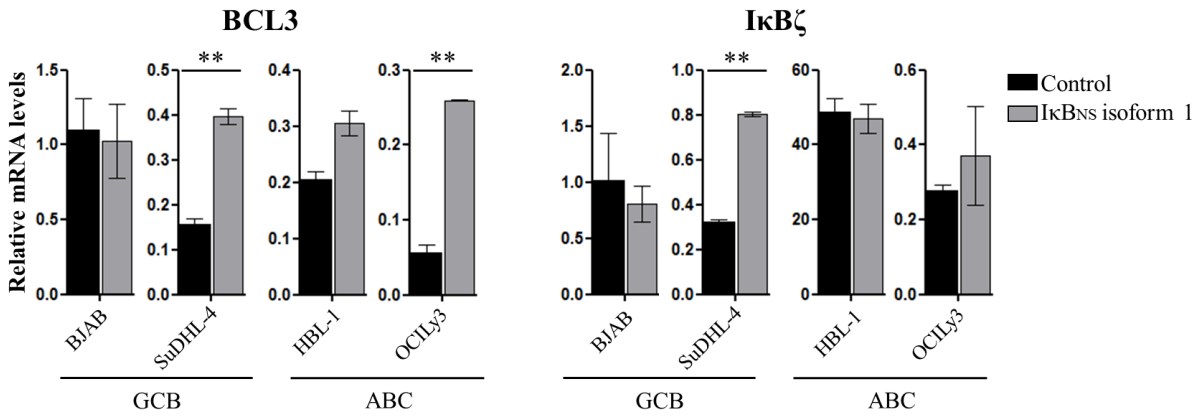

Figure 8.9: BCL3 and IκBζ RNA levels during $IκB_{NS}$ isoform 1 overexpression.

*DLBCL cells were treated with 1 µg/ml doxycycline or carrier solution for 24 h. Following stimulation, the cells were harvested for subsequent RNA extraction and qPCR using primer pairs targeting BCL3 or IκBζ cDNA for analysis and a primer pair targeting β-actin cDNA as a house keeper. This was performed with BJAB and SuDHL-4 cells representing GCB DLBCL and HBL-1 and OCILy3 representing ABC DLBCL. Of each transfected cell line, unstimulated cells were used as a control and doxycycline-treated cells were used for the overexpression of $IκB_{NS}$ isoform 1, respectively. The relative expressions were normalized onto the mRNA levels in BJAB. Standard deviations derive from biological triplicates and two experiments. Asterisks show statistical significance. * $p \leq 0.05$ and ** $p \leq 0.005$.*

BCL3 mRNA expression was elevated in SuDHL-4 and in both ABC cell lines during overexpression of $IκB_{NS}$ isoform 1. IκBζ mRNA levels, on the other hand, were only upregulated in SuDHL-4.

8.2.3. IκB$_{NS}$ isoform 1 and suppressors of MAPK Dusp1 and Dusp2

The MAPK/ERK pathway directly regulates cellular growth and, consequently, is involved in formation of hematological malignancies. The MAPK/ERK pathway in turn is regulated by dual specific protein phosphatase 1 and 2 (DUSP1 and DUSP2), thus making them interesting targets in DLBCL (Jeffrey et al., 2006, Koivula et al., 2011).

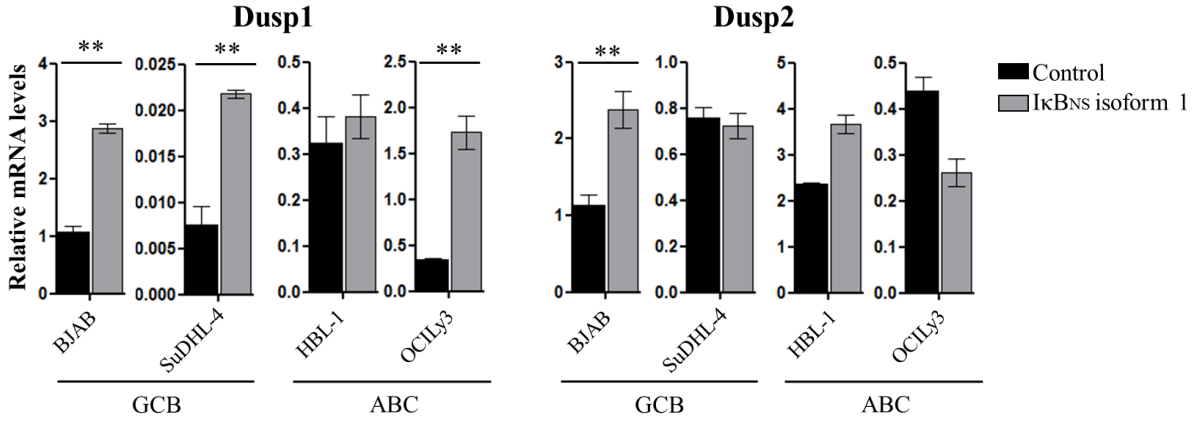

Figure 8.10: DUSP1 and DUSP2 mRNA levels in DLBCL cells upon IκB$_{NS}$ isoform 1 overexpression.

*DLBCL cells were treated as described in Figure 8.9. Dusp1 and Dusp2 mRNA levels were analyzed using qPCR. Standard deviations derive from biological triplicates and two experiments. Asterisks show statistical significance. * $p \leq 0.05$ and ** $p \leq 0.005$.*

DUSP1 mRNA levels were upregulated during overexpression of IκB$_{NS}$ isoform 1 in BJAB, SuDHL-4 and in OCILy3. DUSP2 mRNA levels were only upregulated in BJAB.

8.2.4. IκB$_{NS}$ overexpression leads to changes in the expression levels of the transcription factors IRF4 and SpiB

High expression levels of interferon regulatory factor 4 (IRF4) in combination with its essential cofactor SpiB are hallmarks of activated B cell-like (ABC) DLBCL and is secondary due to high NF-κB activity. IRF4 in concert with SpiB directly upregulates NF-κB protein expression and directly suppresses Interferon beta production. Consequently, a knockdown of IRF4 results in a suppression of NF-κB activity and augmented interferon-β expression, effectively inducing apoptosis (Yang et al., 2012, Care et al., 2014).

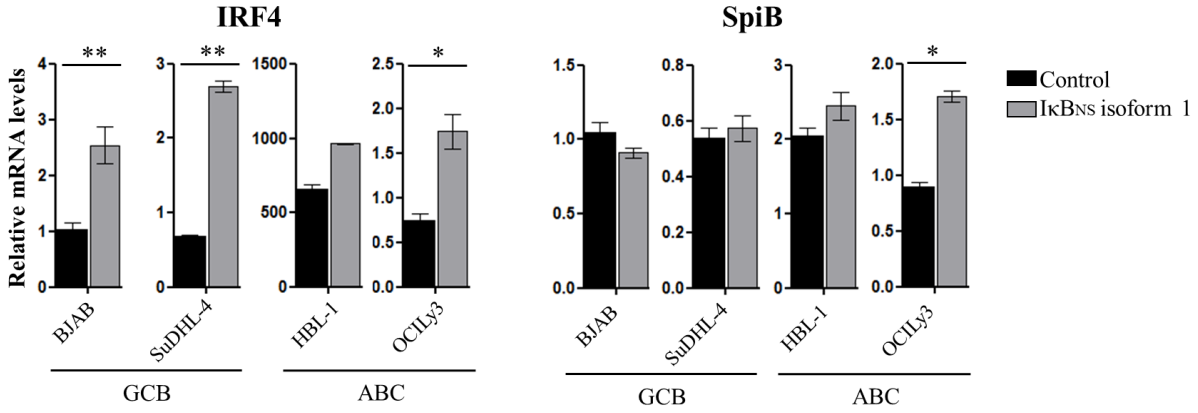

Figure 8.11: Deregulation of IRF4 and SpiB RNA levels due to IκB$_{NS}$ isoform 1 overexpression.

*DLBCL cells were treated as described in Figure 8.9. IRF4 and SpiB mRNA levels were analyzed using qPCR. Standard deviations derive from biological triplicates and two experiments. Asterisks show statistical significance. * $p \leq 0.05$ and ** $p \leq 0.005$.*

IRF4 mRNA levels were upregulated during overexpression of IκB$_{NS}$ isoform 1 in BJAB, SuDHL-4 and in OCILy3. SpiB mRNA levels were only upregulated in OCILy3.

8.2.5. IκB$_{NS}$ isoform 1 influences the expression of anti- and pro-apoptotic factors

Although many cells acquire potentially oncogenic mutations, only few tumors manage to grow and become clinically visible. This happens due to oncogene-induced apoptosis, which neutralizes the transformed cells before any damage can be done. However, this mechanism can be avoided by an elevated expression of anti-apoptotic factors such as BCL2.

On the other hand, Fas is a receptor whose activation induces apoptosis quite efficiently via the Fas-associated death-domain (FADD) signaling pathway, thus improving the prognosis of the disease (Hu et al., 2013, Kojima et al., 2006, Scandurra et al., 2010).

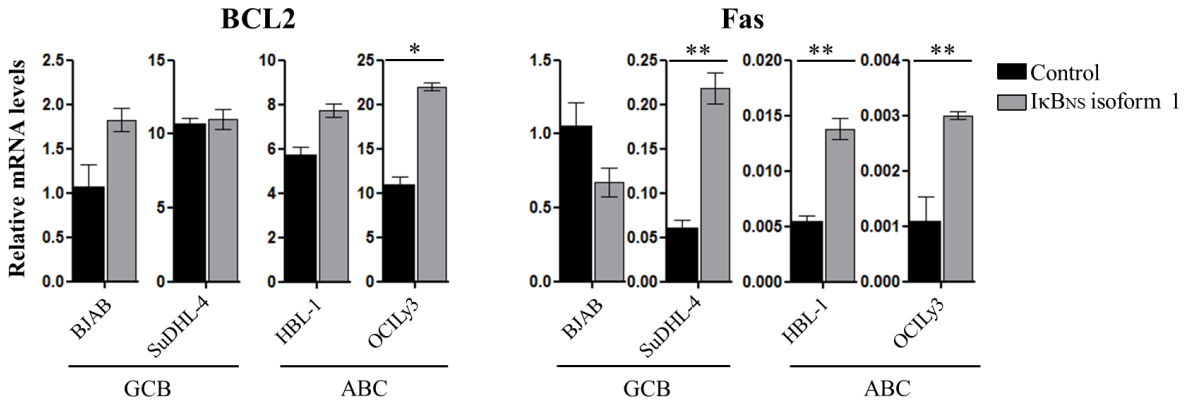

Figure 8.12: BCL2 and Fas were deregulated during IκB$_{NS}$ isoform 1 overexpression.

*DLBCL cells were treated as described in Figure 8.9. BCL2 and Fas mRNA levels were analyzed using qPCR. Standard deviations derive from biological triplicates and two experiments. Asterisks show statistical significance. * $p \leq 0.05$ and ** $p \leq 0.005$.*

BCL2 mRNA levels were not significantly deregulated during overexpression of IκB$_{NS}$ isoform 1. Fas mRNA levels were upregulated during overexpression of IκB$_{NS}$ isoform 1 in SuDHL-4, HBL-1 and in OCILy3.

8.2.6. IκB$_{NS}$ isoform 1 overexpression regulates cytokine and chemokine secretion in DLBCL cells

Several lymphomas secrete CCL2 and CCL8, thus recruiting monocytes that differentiate into a tumor-promoting M2 macrophages (Guilloton et al., 2012). As the prevalence of tumor-associated macrophages constitutes a negative prognostic marker for DLBCL, especially for the ABC subtype, it may be interesting to examine the effect of IκB$_{NS}$ isoform 1 overexpression on the expression levels of said chemokines. Furthermore, tumor vascularization is a crucial step in tumorigenesis, making VEGFα another interesting target (Kim et al., 2011).

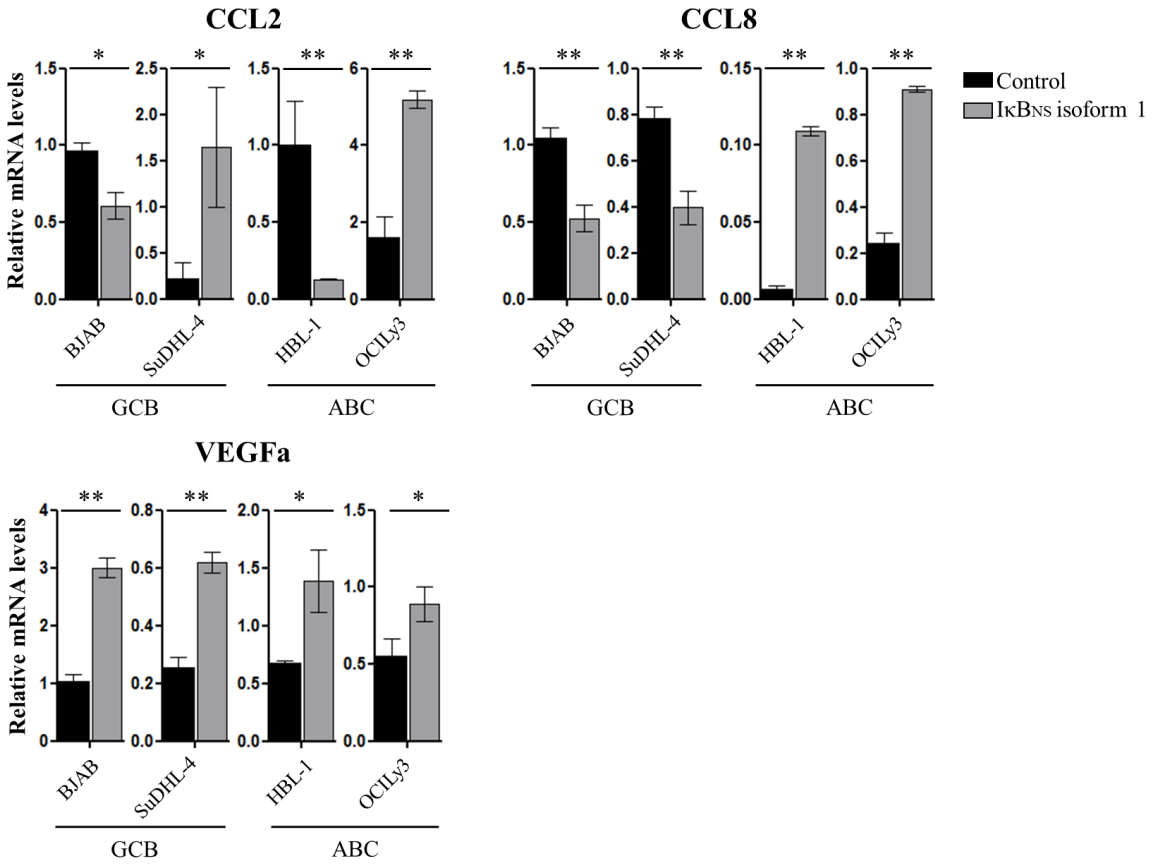

Figure 8.13: CCL2, CCL8 and VEGFα were deregulated during IκB$_{NS}$ isoform 1 overexpression in DLBCL.

*DLBCL cells were treated as described in Figure 8.9. CCL2, CCL8 and VEGFα mRNA levels were analyzed using qPCR. Standard deviations derive from biological triplicates and two experiments. Asterisks show statistical significance. * $p \leq 0.05$ and ** $p \leq 0.005$.*

CCL2 mRNA levels were upregulated during overexpression of IκB$_{NS}$ isoform 1 in SuDHL-4 and OCILy3, while being downregulated in HBL-1. CCL8 mRNA levels were downregulated in the GCB DLBCL cell lines BJAB and SuDHL-4, while being upregulated in the ABC DLBCL cell lines HBL-1 and OCILy3. VEGFα levels were upregulated in BJAB, SuDHL-4 and HBL-1.

9. Discussion

This project aimed to elucidate the role of the atypical inhibitor of NF-κB protein $I\kappa B_{NS}$ in macrophages and lymphomas. As NF-κB is a pivotal signaling pathway and involved in many biological processes, such as immune responses or carcinogenesis, a larger knowledge about its regulation processes of NF-κB is crucial for a better understanding of these processes and the ability to predict or treat them.

NF-κB signaling can be activated by more than 200 different stimuli and induces the expression and activation of more than 200 target genes involved e. g. in inflammation, cell proliferation, cell survival and tumor progression. Thus, NF-κB activity needs to be tightly regulated to provide an adequately selective and specific response to certain stimuli without causing auto-inflammatory diseases, such as CIAS1-related auto-inflammatory syndrome (CAPS) or Sjögren syndrome. A more detailed understanding of the fine-regulation in NF-κB signaling may help to understand human diseases and to develop specific treatments for them.

A pivotal role in NF-κB regulation is assigned to the inhibitor of NF-κB (IκB) protein family. In resting cells, classical IκB proteins bind to NF-κB protein dimers and mask their nuclear localization sequence (NLS), thus retaining them in the cytoplasm of the cell. Following an adequate stimulus, the IκB proteins are phosphorylated, ubiquitinylated and degraded in the proteasome, unleash the NF-κB dimers which proceed into the nucleus and initiate the expression of target genes.

In contrast to classical IκB proteins, which are constitutively expressed in the cytoplasm, atypical IκB proteins are only inducible produced in the nucleus of activated cells. Currently, this protein family consists of five proteins: BCL3, IκBζ, $I\kappa B_{NS}$, IκBη and IκBL. Despite their name, these proteins do not only inhibit NF-κB activity, but exert a regulatory function on NF-κB signaling by fine-regulating the transcriptional activity of NF-κB. BCL3, the best-characterized member of this protein family, mainly regulated the transcriptional activity of inhibitory p50 and p52 NF-κB homo- and heterodimers: It is capable of forming stable inhibitory complexes with p50 homodimers on the DNA, removing inhibitory p50/p52 heterodimers from the DNA or forming transcriptionally active complexes with them. Thus, BCL3 up- and downregulates the transcriptional activity of NF-κB target genes by interacting with coactivators, with corepressors or by direct regulation (Chiba et al., 2013, Schuster et al., 2013). Another member of the atypical IκB protein family, IκBζ also regulates the transcriptional activity of NF-κB target genes. IκBζ is capable of binding to p50 homodimers and activating transcription of downstream genes directly and by chromatin remodeling (Trinh et al., 2008). The third member of the atypical IκB protein family, namely $I\kappa B_{NS}$, is

only poorly characterized in human macrophages, lymphoid malignancies and its general role in NF-κB signaling. In addition, the existing data mainly describe a short isoform of IκB$_{NS}$ (IκB$_{NS}$ isoform 1), however, another isoform (IκB$_{NS}$ isoform 2) with 152 additional amino-acids at its N-terminus has been described (Mao et al., 2004). This project aims to define the effects of this second isoform and to compare it to the first isoform.

To this means, macrophages derived from the human monocytic leukemia cell line THP-1 were used. For the role of IκB$_{NS}$ in lymphoid malignancies, germinal B cell-like (GCB) diffuse large B cell lymphoma (DLBCL) cell lines BJAB and SuDHL-4 and activated B cell-like (ABC) DLBCL cell lines HBL-1 and OciLy3 were used. Transcriptional targets of IκB$_{NS}$ in macrophages were derived from the RNASeq microarray performed by Sebastian Lorscheid in our lab using LPS-stimulated peritoneal macrophages derived from IκB$_{NS}$ wild-type and IκB$_{NS}$ knock-out mice, respectively. For overexpression of IκB$_{NS}$ isoforms 1 and 2, THP-1 cells were lentivirally transduced with overexpression constructs containing IκB$_{NS}$ isoform 1 and isoform 2 cDNA in their expression cassettes, respectively. For the knock-out, THP-1 cells were transduced with the lentiviral CRISPR/Cas9 toolkit with a guide RNA targeting the first exon of genomic IκB$_{NS}$ (Shalem et al., 2014).

9.1. IκB$_{NS}$ in macrophages after TLR4 stimulation

After generation of THP-1 cell lines stably overexpressing IκB$_{NS}$ or with IκB$_{NS}$ knocked out, the cells were differentiated to macrophages using PMA using the method first described by Auwerx (Auwerx, 1991). Cells were subsequently treated with LPS, a conserved component of bacterial cell walls, thus simulating bacterial infection. LPS stimulation results in a strong activation of by stimulation of NF-κB-signaling via the pattern recognition receptor TLR4 (Kumar et al., 2011). Among other activators of NF-κB-signaling via pattern recognition receptors, LPS was chosen for our experiments, as it activates NF-κB signaling via two distinct pathways, resulting in strong and robust activation of NF-κB (Akira et al., 2001) and, subsequently, expression of the secondary response gene IκB$_{NS}$. To distinguish transcriptional and translational regulation of NF-κB targets by IκB$_{NS}$, gene expression was analyzed on the RNA level using qPCR and on the protein level using immunoblotting or a cytokine array.

The effect of knock-out of IκB$_{NS}$ on NF-κB target gene expression in murine macrophages after LPS stimulation has been previously analyzed by (Kuwata et al., 2006). This project therefore specifically explored the role of IκB$_{NS}$ isoform 1 and 2 in human macrophages after LPS stimulation. Expression of both endogenous IκB$_{NS}$ isoforms was strongly induced following LPS stimulation on the protein level, while it was not detectable on the protein level

in the cells CRISPR/Cas9 constructs targeting IκB$_{NS}$ in its first exon (Jinek et al., 2012). The macrophages with lentivirally induced overexpression of IκB$_{NS}$ isoform 1 and isoform 2 showed a strong expression of the respective protein, which was not significantly changed during LPS stimulation. Thus, we progressed to the examination of defined targets of IκB$_{NS}$ in human macrophages. As not all of the target genes identified by (Kuwata et al., 2006) were expressed in differentiated THP-1 cells, other relevant NF-κB target genes were analyzed, resulting in a distinct target panel.

Unfortunately, the most highly deregulated genes found by (Kuwata et al., 2006), namely IL6, IL10, IL12p40 and IL18, were not expressed by the differentiated THP-1 cells after 1, 2 or 4 h of LPS stimulation. However, THP-1-derived macrophages were used as model cell system, as they have a reasonably high resemblance to primary macrophages and can be derived from a stable cell line, which was essential for this project.

The analysis of other NF-κB target genes examined by their group showed a similar regulation pattern during knock-out of IκB$_{NS}$ for IκBζ, CCL2, CCL5, CXCL10 and MIF1α, as no significant deregulation was detectable. In contrast, IL1β showed a slight but significant upregulation in the cells with IκB$_{NS}$ knocked out. With no significant effect on the transcription of target genes after knock-out of a gene encoding one signaling protein, no transcriptional deregulation of these target genes should be expected during overexpression of said protein. However, genomic IκB$_{NS}$ encodes two distinct isoforms that may have distinct effects on NF-κB signaling, making a more detailed analysis necessary. The analysis of IκBζ and CXCL10 showed a downregulation of these targets by overexpression of IκB$_{NS}$ isoforms 1 and 2. CCL2 and CCL5 were upregulated during overexpression of IκB$_{NS}$ isoform 2, while showing no deregulation during overexpression of IκB$_{NS}$ isoform 1. IL1β and MIF1α were not deregulated during IκB$_{NS}$ overexpression.

Following these examinations, more pro-inflammatory and anti-inflammatory NF-κB target genes identified in murine macrophages in our lab by Sebastian Lorscheid (unpublished data) and suggested by scientific literature were analyzed. As data from our lab suggest a reciprocal regulation of atypical IκB protein family members and data showed a deregulation of IκBζ during overexpression of IκB$_{NS,}$ the effect of IκB$_{NS}$ on BCL3 was analyzed. In addition, since IκB$_{NS}$ sequesters NF-κB proteins in the cytosol (Tao et al., 2014), the effect of IκB$_{NS}$ on p65 phosphorylation and activation was analyzed. These analyses showed a suppressive effect of IκB$_{NS}$ isoform 1 and 2 overexpression on BCL3 expression and a suppressive effect of IκB$_{NS}$ isoform 2 overexpression on p65 phosphorylation, while knock-out of IκB$_{NS}$ resulted in elevated levels of BCL3 and phosphorylated p65, suggesting a suppressive effect of IκB$_{NS}$ on

NF-κB signaling. The overall levels of p65 were not deregulated, which is consistent with the fact that NF-κB activity is mainly regulated by post-translational modifications and not transcriptional or translational changes.

$I\kappa B_{NS}$ and IκBζ have been suggested to have reciprocal effects on some NF-κB targets, thus working as antagonists in NF-κB signaling (Hirotani et al., 2005, Yamamoto et al., 2004). Hence, target genes of IκBζ were added to the panel. The pro-inflammatory factors CXCL1 (Kayama et al., 2008) and IL8 (Goransson et al., 2009) are targets of IκBζ, making them likely targets of $I\kappa B_{NS}$. Knock-out of $I\kappa B_{NS}$ showed no effect on CXCL1 expression but enhanced expression of IL8. Overexpression of $I\kappa B_{NS}$ isoforms 1 and 2 led to repressed CXCL1 activity in parallel to CXCL10. This regulation is reciprocal to the effect of IκBζ, in line with the model of $I\kappa B_{NS}$ acting as antagonist to IκBζ.

Atypical IκB proteins do not only influence NF-κB proteins, but also directly interact with other important signaling pathways involved in inflammation, such as the JAK/STAT signaling (Squarize et al., 2006). Overexpression of $I\kappa B_{NS}$ isoform 1 as well as knock-out of $I\kappa B_{NS}$ showed no effect on STAT1 or STAT3 mRNA levels, while overexpression of $I\kappa B_{NS}$ isoform 2 resulted in reduced STAT1 and STAT3 expression. However, since STAT-activation is mainly regulated by post-translational modifications, levels of phosphorylated STAT1 and STAT3 were examined. Here, our analyses showed reduced levels of p-STAT1 during overexpression and knock-out of $I\kappa B_{NS}$ and no effect of overexpression of $I\kappa B_{NS}$ isoform 1 or 2 on p-STAT3 levels, while knock-out of $I\kappa B_{NS}$ resulted in high levels of p-STAT3. This shows a shift from STAT1 to STAT3 activity during knock-out of $I\kappa B_{NS}$. However, (Wu et al., 2009) have shown that IκBζ suppresses STAT3 activity. This suggests a similar effect of $I\kappa B_{NS}$ and IκBζ and opposes the idea of $I\kappa B_{NS}$ and IκBζ as antagonists. Pro-inflammatory CCL3 and 4 (Widmer et al., 1993), IFNβ (Hiscott et al., 1989) and anti-inflammatory IL1RA (Smith et al., 1994) are NF-κB target genes. Here, overexpression of $I\kappa B_{NS}$ isoform 1 showed no effect on the expression levels, while overexpression of $I\kappa B_{NS}$ isoform 2 led to higher expression levels of CCL4, IFNβ and IL1RA. Knock-out of $I\kappa B_{NS}$ resulted in enhanced expression of CCL4 and IFNβ.

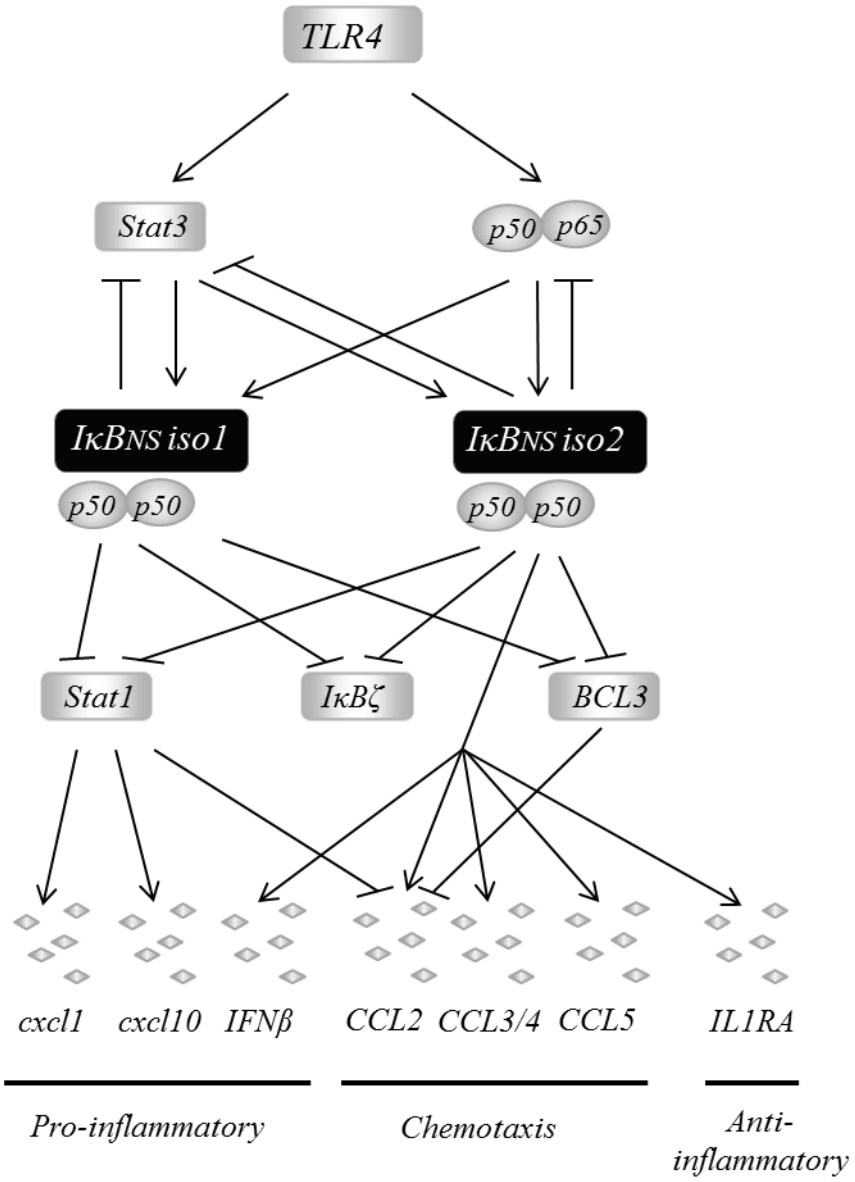

Figure 9.1: Simplified representation of the effect of $I\kappa B_{NS}$ overexpression in macrophages after LPS stimulation.

Following TLR4 activation, several intracellular signaling cascades are initiated, shown here by STAT3 and p50/p65 representing the NF-κB family. These proteins initiate the expression of $I\kappa B_{NS}$ isoforms 1 and 2, which in turn inhibit the activity of the former proteins. $I\kappa B_{NS}$ isoforms 1 and 2 inhibit the expression of the other members of the atypical IκB family, IκBζ and BCL3, and inhibit the activation of STAT1. This, in turn, results in suppression of the pro-inflammatory factors CXCL1 and CXCL10 and the activation of chemotactic CCL2 by both isoforms of $I\kappa B_{NS}$, while $I\kappa B_{NS}$ isoform 2 appears to activate pro-inflammatory IFNβ, chemotactic CCL3/4 and CCL5 and anti-inflammatory IL1RA, either directly or via another intermediate factor not examined here.

In summary, $I\kappa B_{NS}$ isoform 1 overexpression shows an indifferent or repressing effect on NF-κB target gene expression, consistent with (Schuster et al., 2013)'s review. Overexpression of $I\kappa B_{NS}$ isoform 2 showed a marked deregulation of most of the examined target genes and proteins, resulting in downregulation or upregulation of several transcription factors and pro-inflammatory secreted factors. This shows once again that $I\kappa B_{NS}$ as a member of the atypical

IκB protein family is not only an inhibitor, but a modulator of NF-κB signaling. The effect of the knock-out of $I\kappa B_{NS}$ was not always reciprocal to the effects of the overexpression of $I\kappa B_{NS}$ isoforms 1 and 2, suggesting an additive effect of these isoforms in the physiological context or another isoform accountable for these deregulations. Another possible cause may be an off-target effect of the CRISPR-Cas9 despite careful selection of the guide RNA and no microscopic change of phenotype of the THP-1. These questions can be elucidated by a full genome sequencing of the THP-1 with $I\kappa B_{NS}$ knocked out to rule out off-target effects, by generating THP-1 with only $I\kappa B_{NS}$ isoform 2 knocked out and by generating THP-1 cells overexpressing both $I\kappa B_{NS}$ isoform 1 and 2 in parallel.

Most analyses of the effect of $I\kappa B_{NS}$ on NF-κB signaling in macrophages have so far been performed in knock-out cells. Here, the data derived from murine knock-out cells (Kuwata et al., 2006) could be reproduced and expanded, suggesting a conserved effect of $I\kappa B_{NS}$ on NF-κB signaling. Overexpression of $I\kappa B_{NS}$, however, yielded data that could not be derived from the knock-out analysis. This shows the importance of a combined analysis of knock-out and overexpression to elucidate the effects of a signaling protein. However, the overexpression of proteins creates an unnatural state in the cell by flooding it with one protein, making the data derived from overexpression studies artificial. For a sound analysis of the effect of $I\kappa B_{NS}$ isoform 2, an isolated knock-out or knock-down of isoform 2 needs to be performed. $I\kappa B_{NS}$ isoform 1 cannot be knocked out without eliminating isoform 2, as only isoform 2 has a sequence that is not shared by the other isoform.

Finally, it is important to remember that THP-1 derived macrophages closely resemble primary macrophages, but have been developed from a cell line derived from an acute myeloid leukemia. Thus, they may not resemble human macrophages in every detail. Since the generation of $I\kappa B_{NS}$ knock-out macrophages from primary human monocytes using the CRISPR-Cas9 system is intricate and expensive and yields only few cells to perform the experiments with, THP-1 is an acceptable approximation.

9.2. Effect of IκB$_{NS}$ on macrophage differentiation

As NF-κB is also involved in the differentiation process of myeloid cells, IκB$_{NS}$ may have an effect on the differentiation process on THP-1. Thus, the precise cell type derived from THP-1 by PMA-driven differentiation has to be determined. Since the differentiation and activation status can be assayed via cell surface markers, a FACS analysis of differentiated and activated THP-1 was performed. CD11c was chosen as a marker for DC differentiation, CD14 as a marker for macrophage differentiation and CD81 as marker for activation (Murray and Wynn, 2011). Overexpression of IκB$_{NS}$ isoform 1 showed no significant effect on cell size and granularity, most importantly no new subpopulation in the plot. Cells overexpressing IκB$_{NS}$ isoform 2 showed a reduced population of viable cells. This suggests that overexpression of IκB$_{NS}$ isoform 1 does not impact cell viability, while IκB$_{NS}$ isoform 2 overexpression may cause minor cytotoxicity.

The population of viable cells in differentiated THP-1 expressing the CRISPR/Cas9 with guide RNA targeting IκB$_{NS}$ was greatly reduced in comparison with the cells expressing CRISPR/Cas9 alone. Overexpression of the Cas9 has already been shown to have cytotoxic effects (Jinek et al., 2012, Gasiunas et al., 2012), as it has a minor unspecific endonuclease activity. However, the marked greater toxicity of CRISPR/Cas9 with guide RNA targeting IκB$_{NS}$ suggests a cytoprotective role of IκB$_{NS}$, consistent with its suggested role as suppressor of inflammation (Kuwata et al., 2006), or off-target effects of the guide RNA. Analysis of the cellular surface markers revealed a marked increase of CD11c in cells overexpressing IκB$_{NS}$ isoform 1 and 2, while knock-out of IκB$_{NS}$ showed no effect. Consistently, overexpression of IκB$_{NS}$ isoform 1 and 2 resulted in a reduced intensity of CD14 on differentiated THP-1, while knock-out of IκB$_{NS}$ showed no effect again. CD81 levels remained unchanged in cells overexpressing IκB$_{NS}$ isoform 1 and 2 as well as in cells with IκB$_{NS}$ knocked out.

In summary, this suggests a shift from activated macrophages (CD11c low CD14 high CD81 high) to activated dendritic cells (CD11c high CD14 low CD81 high) in differentiated THP-1 cells overexpressing IκB$_{NS}$ isoform 1 and 2, while knock-out of IκB$_{NS}$ showed no effect on cell differentiation. However, since the differentiation state of a cell cannot be determined by using only 2 surface markers, more experiments will be necessary to validate these results.

9.3. IκB$_{NS}$ in macrophages during HIV infection

NF-κB signaling is pivotal for the infection and replication of HIV and commonly activated in infected cells via TLR7/8 stimulation (Chang and Altfeld, 2009). However, the effect of the atypical IκB protein family on HIV infection and progression has not been addressed at all. Since NF-κB is a central factor for the antiviral response (Mogensen and Paludan, 2001), but on the other hand is utilized by HIV for its replication (Hiscott et al., 2001), a delicate balance has to be found and maintained for viral activity. Atypical IκBs have already been shown to regulate the expression of antiviral genes, thus the effect of IκB$_{NS}$ isoform 1 and 2 overexpression on the expression of antiviral genes in macrophages infected with HIV were analyzed. Hence, macrophages were differentiated as described above and infected with HIV by Ramona Businger in the laboratory of Prof. Dr. Michael Schindler.

We have already shown an effect of IκB$_{NS}$ overexpression on IκBζ expression after TLR4 stimulation. Another important antiviral factor is interferon-induced GTP-binding protein MX1, which is also regulated by NF-κB (Gérardin et al., 2004). Here, our analyses showed a marked reduction of IκBζ and MX1 expression during overexpression of IκB$_{NS}$ isoform 1, while overexpression of IκB$_{NS}$ isoform 2 showed no effect.

Since the antiviral response is highly dependent on inflammatory cytokines and chemokines, the expression levels of several secreted factors were analyzed after HIV infection. Important factors in the antiviral response are IL1β, IL8, TNFα, CXCL1 and CCL2, most of which have been discussed in chapter 9.1. TNFα has been shown to be positively regulated by IκBζ (Kayama et al., 2008), suggesting a regulation of IκB$_{NS}$. Here, overexpression of IκB$_{NS}$ isoform 1 resulted in downregulation of expression of all five target genes, while overexpression of IκB$_{NS}$ isoform 2 showed no significant effect. This differs from the data collected from the cells stimulated with LPS: There, IκBζ and CXCL1 levels were reduced during overexpression of both isoforms of IκB$_{NS}$, while in viral infection mRNA levels were unchanged during overexpression of IκB$_{NS}$ isoform 2. IL1β and IL8 levels differ from the levels during LPS stimulation: There, they showed no deregulation, while overexpression of IκB$_{NS}$ isoform 1 during HIV infection resulted in decreased expression levels. CCL2 levels also differed: While the levels were unchanged during overexpression of IκB$_{NS}$ isoform 1 and elevated during overexpression of IκB$_{NS}$ isoform 2 in the LPS-stimulated cells, while here, IκB$_{NS}$ isoform 1 overexpression resulted in reduction of CCL2 mRNA levels and overexpression of IκB$_{NS}$ isoform 2 resulted in unchanged levels. TNFα expression levels were reduced during overexpression of IκB$_{NS}$ isoform 1, showing an antagonistic effect of IκB$_{NS}$ to IκBζ once again.

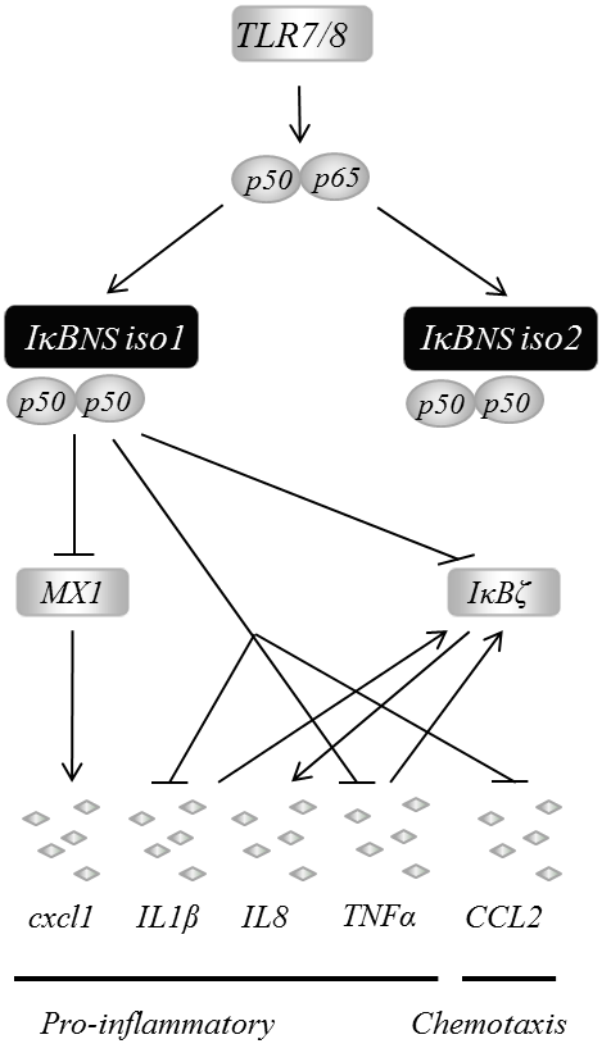

Figure 9.2: Simplified representation of the effect of $I\kappa B_{NS}$ overexpression in macrophages after HIV infection.

Following TLR7 and TLR8 activation, several intracellular signaling cascades are initiated, which culminate in the activation of NF-κB, represented by the p50/p65 dimer here. These proteins initiate the expression of $I\kappa B_{NS}$ isoforms 1 and 2. $I\kappa B_{NS}$ isoform 1 shows a repressing effect on MX1 and, subsequently, the pro-inflammatory CXCL1. $I\kappa B_{NS}$ isoform 1 appears to suppress the expression of chemotactic CCL2 and pro-inflammatory IL1β and TNFα either directly or via an intermediate factor not examined here. This results in a reduced induction of IκBζ and, subsequently, reduced pro-inflammatory IL8.

In summary, the analysis showed a marked suppressive effect of $I\kappa B_{NS}$ isoform 1 on the expression of antiviral response genes, while overexpression of $I\kappa B_{NS}$ isoform 2 showed no significant effect, differing from the data derived from the THP-1 stimulated with LPS. This may result in a greater production of viral particles in cells overexpressing $I\kappa B_{NS}$ isoform 1. These data greatly differ from the expression data from the TLR4 stimulation, which is not surprising as bacterial infection simulated by TLR4 stimulation and viral infection require highly different immune responses. This difference may be explained by the activation of different signaling pathways following TLR stimulation, as TLR4 activates both the MyD88

and TRIF-dependent pathways, while TLR7/8 only activate the MyD88-dependent pathway. HIV also modulates the cellular response not only by TLR7/8 stimulation, but also expression of signaling proteins. In addition, the mRNA data from the THP-1 cells stimulated with LPS were collected after 4 hours of stimulation, while the THP-1 cells were incubated with viral particles for 48 hours. This is due to the fact that LPS stimulates an extracellular receptor, alas induces a reaction much faster than a virus stimulating an intracellular receptor. In addition, HIV stimulates the receptors not only upon entering the cell, but also after it has stably integrated into the cellular genome (Chang et al., 2012). After integration, however, HIV induces a relatively stable TLR stimulation (Chang and Altfeld, 2009). Hence, to acquire quality data that can be reliably correlated with the data from the experiments with LPS stimulation, a kinetic after HIV infection has to be performed.

However, since the deregulation shows an equal trend in all targets analyzed, there exists the possibility of these results being an artifact. This is highly unlikely, as each data set is the average of the results of three independent experiments, but it still has to be ruled out by addition of a negative control and by further experiments to show whether overexpression of $I\kappa B_{NS}$ isoform 1 has indeed an effect on HIV infection efficiency and production of viral particles.

9.4. $I\kappa B_{NS}$ in diffuse large B cell lymphomas

As mentioned before, NF-κB signaling is not only important in macrophages, but among others also in lymphocytes and in lymphocyte-derived malignancies. Most importantly, IκBζ as another member of the atypical IκB protein family, has already been shown to be essential for survival and growth of the ABC subtype of DLBCL (Nogai et al., 2013). Unfortunately, no ABC DLBCL cells with a CRISPR/Cas9 and a guide RNA targeting $I\kappa B_{NS}$ could be generated, while cells could be transfected and expanded with a vector containing the CRISPR/Cas9 alone. GCB DLBCL cells could easily be transfected and expanded with the CRISPR/Cas9 alone and with a guide RNA targeting $I\kappa B_{NS}$. However, the latter was not surprising, as GCB DLBCL do not express $I\kappa B_{NS}$ without external stimulation.

The target genes examined were chosen from the data from (Nogai et al., 2013), who showed a critical role of IκBζ in ABC DLBCL. Here, the other atypical IκB protein BCL3 was upregulated in GCB and ABC cell lines. In contrast, IκBζ levels remained unchanged in ABC, but were upregulated in one GCB cell line. This highly differs from the data from LPS-stimulated macrophages, which may be explained by the different cell types macrophage and lymphoma and by the fact that high NF-κB levels in ABC DLBCL derive from aberrant B cell

receptor signaling, alas alternative activation of NF-κB, while TLR4 signaling in macrophages induces the classical NF-κB pathway. The chemoattractant CCL2 was not deregulated, also differing from the data from macrophage experiments. DUSP1 and IRF4 expression were upregulated during $I\kappa B_{NS}$ overexpression in GCB and ABC, while DUSP2 was not deregulated. As SpiB signaling is closely entangled with IRF4 in activated B cells and ABC DLBCL, SpiB expression levels were analyzed during $I\kappa B_{NS}$ overexpression, but only showed an upregulation in ABC cell line. In concert, this suggests a role for $I\kappa B_{NS}$ in DLBCL proliferation, as DUSP1 and IRF4 are potent activators of B cell proliferation. Anti-apoptotic and pro-apoptotic gene expressions were examined using the surrogate markers BCL2 and Fas. Here, overexpression of $I\kappa B_{NS}$ showed no effect on BCL2 expression levels, but increased Fas expression in all cell lines except for BJAB. However, since relative mRNA levels were still far below BJAB levels after upregulation, the physiological effect of this upregulation is a matter for discussion. In concert, overexpression of $I\kappa B_{NS}$ resulted in no upregulation of anti-apoptotic genes, but on the contrary in upregulation of a pro-apoptotic receptor, although probably not in a physiologically relevant manner. CCL8 and VEGFα were examined, as lymphomas heavily rely on the infiltration of monocytes and vessel growth. Here, analysis of the expression levels showed a downregulation of CCL8 levels in GCB and an upregulation ABC DLBCL during $I\kappa B_{NS}$ overexpression. This is consistent with data suggesting CCL8 expression as a negative prognostic marker for DLBCL, as it shows a shift from the GCB to the ABC subtype (Rosenwald et al., 2002). VEGFα levels were increased in all cell lines during overexpression of $I\kappa B_{NS}$, suggesting a conserved role for $I\kappa B_{NS}$ in vascularization.

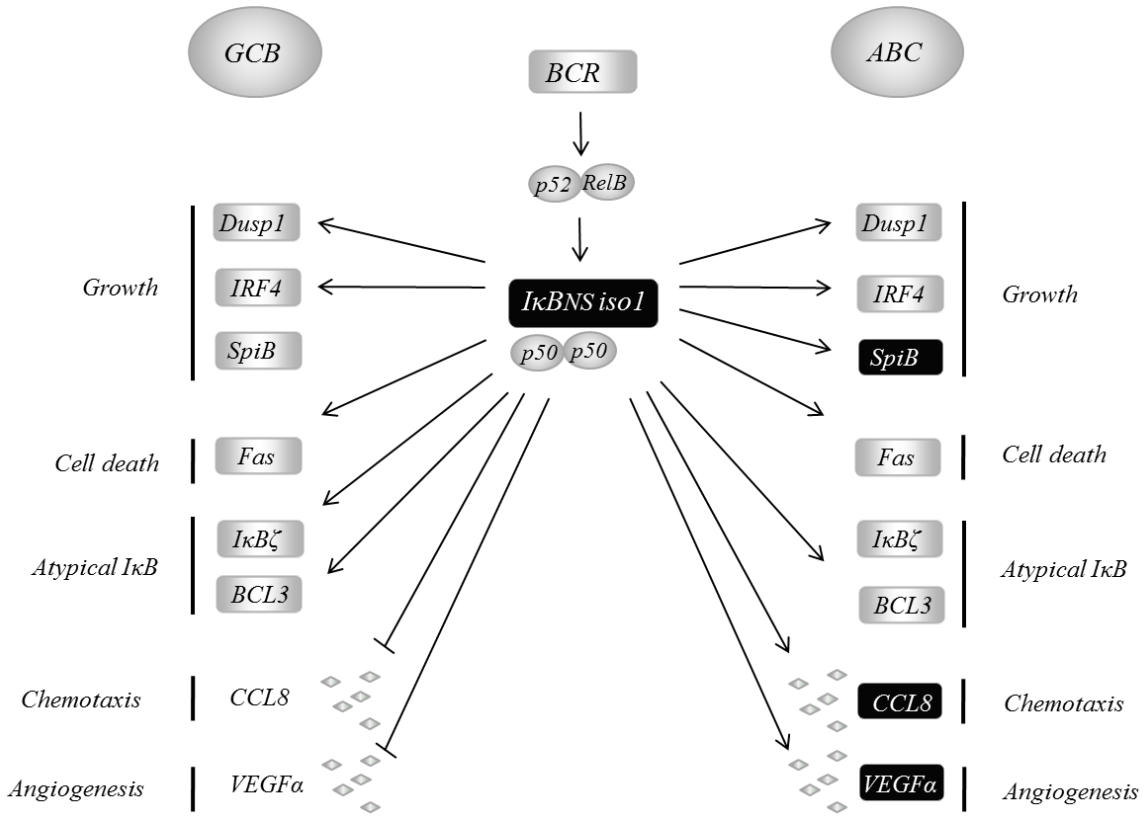

Figure 9.3: Simplified representation of the effect of $I\kappa B_{NS}$ isoform 1 overexpression in GCB and ABC DLBCL.

In ABC DLBCL, a mutation of the B cell receptor BCR or a downstream signaling protein results in constitutive activation of the alternative NF-κB pathway, represented by the p52/RelB heterodimer. In turn, this heterodimer induces expression of $I\kappa B_{NS}$. $I\kappa B_{NS}$ isoform 1 induces the expression of growth promoting DUSP1 and IRF4 in both GCB and ABC, while also inducing SpiB, an important factor for IRF4 function, in ABC only. The death receptor Fas is induced in both GCB and ABC. The atypical IκB protein BCL3 is induced in both GCB and ABC, while IκBζ is only induced in GCB. Finally, secreted factors CCL8 and VEGFα, which induce leukocyte infiltration and angiogenesis, are induced by $I\kappa B_{NS}$ in ABC, but are suppressed in GCB DLBCL. In total, $I\kappa B_{NS}$ isoform 1 appears to have a greater growth-promoting effect as well as an effect on the negative prognostic markers, angiogenesis and leukocyte infiltration, in ABC than in GCB.

In summary, $I\kappa B_{NS}$ appears to be involved in the regulation of the other members of the atypical IκB protein family, of cellular growth and of some secreted factors. Its effects appear to be conserved, as they do not differ greatly between GCB and ABC DLBCL, except for its effect on CCL8. However, the data discussed here was obtained from $I\kappa B_{NS}$ overexpression in a cell system that does not naturally express $I\kappa B_{NS}$ at all (GCB) or by additional overexpression in a system which already overexpresses $I\kappa B_{NS}$, adding a protein that was available in abundance in the first place. Thus, a reliable statement concerning the effect of $I\kappa B_{NS}$ in ABC DLBCL can only be made after generation of a knock-out cell line.

The data discussed here suggests a lack of growth signals after knock-out of $I\kappa B_{NS}$. This limitation may be avoided by using an inducible knock-down or knock-out system, allowing gene expression analysis directly subsequent to the removal of $I\kappa B_{NS}$ from the cells.

10. Outlook

This project provides a first insight into target genes of $I\kappa B_{NS}$ in human macrophages, showing a high level of conservation between its effects in the murine and the human cell system concerning immunomodulatory cytokines, other atypical IκB proteins and a small selection of intracellular transcription factors. $I\kappa B_{NS}$ isoform 1 and isoform 2 showed different effects on the analyzed target genes. However, the effects of overexpression of $I\kappa B_{NS}$ isoform 1 and isoform 2 were not reciprocal to the effects of knock-out of $I\kappa B_{NS}$, suggesting additional relevant isoforms of $I\kappa B_{NS}$ that have not been subject to analysis yet.

In this project, mRNA and protein levels have been analyzed in macrophages. However, the exact mode of regulation by $I\kappa B_{NS}$ is still to be examined. As it appears to be on the transcriptional level, this may be addressed using promoter studies, CHIP analysis and CoIPs.

Another mode of activation is the autocrine stimulation with cytokines, leading to the activation of STAT signaling. As the most prominent activator of STAT signaling was not expressed in THP-1 derived macrophages, there appears to be another activator of STAT signaling involved. The analysis of the effect of $I\kappa B_{NS}$ on macrophage differentiation showed great promise, however the experiments performed here were only preliminary. Additional surface proteins will be needed for a sufficient statement concerning the effect of $I\kappa B_{NS}$ on macrophage differentiation. Overexpression of $I\kappa B_{NS}$ showed a marked effect on target gene expression after infection of THP-1 cells with HIV. Here, analysis of additional targets needs to be performed and to be confirmed on the protein level. Further experiments will also address the infection efficiency of HIV during overexpression and knock-out of $I\kappa B_{NS}$ as well as the viral load produced by the infected cells to quantify the functional effect of $I\kappa B_{NS}$ on HIV infection and spread. The experiments performed in DLBCL suggested an important role for $I\kappa B_{NS}$ in ABC DLBCL, as no viable knock-out cell line could be generated and overexpression analysis of isoform 1 showed an effect of $I\kappa B_{NS}$ on growth factors in DLBCL. An inducible knock-out system may enable the analysis of ABC directly subsequent to removal of $I\kappa B_{NS}$. In addition, the effect of $I\kappa B_{NS}$ isoform 2 needs to be addressed, as well as whether the regulation of targets shown to be deregulated in macrophages is conserved in lymphoma cells as well.

In summary, this project showed a marked effect of $I\kappa B_{NS}$ on inflammation, cell differentiation, antiviral defense and lymphoma growth and survival. Thus, targeting $I\kappa B_{NS}$ may prove valuable in treatments of chronic inflammatory diseases, infectious diseases and cancer.

11. References

AHMAD-NEJAD, P., HÄCKER, H., RUTZ, M., BAUER, S., VABULAS, R. M. & WAGNER, H. 2002. Bacterial CpG-DNA and lipopolysaccharides activate Toll-like receptors at distinct cellular compartments. *European Journal of Immunology,* 32**,** 1958-1968.

AKIRA, S. & TAKEDA, K. 2004. Toll-like receptor signalling. *Nat Rev Immunol,* 4**,** 499-511.

AKIRA, S., TAKEDA, K. & KAISHO, T. 2001. Toll-like receptors: critical proteins linking innate and acquired immunity. *Nat Immunol,* 2**,** 675-80.

AKITA, K., ISODA, K., OKABAYASI, Y., SHIMADA, K. & DAIDA, H. 2016. Lack of IkappaBNS accelerates atherosclerosis in LDL receptor-deficient mice via increased interleukin-6 production. *Int J Cardiol,* 211**,** 61-3.

ALIZADEH, A. A., EISEN, M. B., DAVIS, R. E., MA, C., LOSSOS, I. S., ROSENWALD, A., BOLDRICK, J. C., SABET, H., TRAN, T., YU, X., POWELL, J. I., YANG, L., MARTI, G. E., MOORE, T., HUDSON, J., JR., LU, L., LEWIS, D. B., TIBSHIRANI, R., SHERLOCK, G., CHAN, W. C., GREINER, T. C., WEISENBURGER, D. D., ARMITAGE, J. O., WARNKE, R., LEVY, R., WILSON, W., GREVER, M. R., BYRD, J. C., BOTSTEIN, D., BROWN, P. O. & STAUDT, L. M. 2000. Distinct types of diffuse large B cell lymphoma identified by gene expression profiling. *Nature,* 403**,** 503-11.

ANNEMANN, M., WANG, Z., PLAZA-SIRVENT, C., GLAUBEN, R., SCHUSTER, M., EWALD SANDER, F., MAMARELI, P., KUHL, A. A., SIEGMUND, B., LOCHNER, M. & SCHMITZ, I. 2015. IkappaBNS regulates murine Th17 differentiation during gut inflammation and infection. *J Immunol,* 194**,** 2888-98.

ARMSTRONG, J. A. & HART, D. A. 1971. Response of cultured macrophages to mycobacterium tuberculosis, with observations on fusion of lysosomes with phagosomes. *The Journal of Experimental Medicine,* 134**,** 713-740.

ARNOLD, C. N., PIRIE, E., DOSENOVIC, P., MCINERNEY, G. M., XIA, Y., WANG, N., LI, X., SIGGS, O. M., KARLSSON HEDESTAM, G. B. & BEUTLER, B. 2012. A forward genetic screen reveals roles for Nfkbid, Zeb1, and Ruvbl2 in humoral immunity. *Proc Natl Acad Sci U S A,* 109**,** 12286-93.

ASIN, S., TAYLOR, J. A., TRUSHIN, S., BREN, G. & PAYA, C. V. 1999. Ikk Mediates NF-kB Activation in Human Immunodeficiency Virus-Infected Cells. *Journal of Virology,* 73**,** 3893-3903.

AUFFRAY, C., FOGG, D., GARFA, M., ELAIN, G., JOIN-LAMBERT, O., KAYAL, S., SARNACKI, S., CUMANO, A., LAUVAU, G. & GEISSMANN, F. 2007. Monitoring of blood vessels and tissues by a population of monocytes with patrolling behavior. *Science,* 317**,** 666-70.

AUWERX, J. 1991. The human leukemia cell line, THP-1: A multifacetted model for the study of monocyte-macrophage differentiation. *Experientia,* 47**,** 22-31.

BAEUERLE, P. & BALTIMORE, D. 1988. I kappa B: a specific inhibitor of the NF-kappa B transcription factor. *Science,* 242**,** 540-546.

BASSO, K., KLEIN, U., NIU, H., STOLOVITZKY, G. A., TU, Y., CALIFANO, A., CATTORETTI, G. & DALLA-FAVERA, R. 2004. Tracking CD40 signaling during germinal center development. *Blood,* 104**,** 4088-96.

BEG, A. A. & BALDWIN, A. S. 1993. The I kappa B proteins: multifunctional regulators of Rel/NF-kappa B transcription factors. *Genes & Development,* 7**,** 2064-2070.

BELL, J. K., MULLEN, G. E., LEIFER, C. A., MAZZONI, A., DAVIES, D. R. & SEGAL, D. M. 2003. Leucine-rich repeats and pathogen recognition in Toll-like receptors. *Trends Immunol,* 24**,** 528-33.

BELLINGAN, G. J., CALDWELL, H., HOWIE, S. E., DRANSFIELD, I. & HASLETT, C. 1996. In vivo fate of the inflammatory macrophage during the resolution of inflammation: inflammatory macrophages do not die locally, but emigrate to the draining lymph nodes. *The Journal of Immunology,* 157**,** 2577-2585.

CARE, M. A., COCCO, M., LAYE, J. P., BARNES, N., HUANG, Y., WANG, M., BARRANS, S., DU, M., JACK, A., WESTHEAD, D. R., DOODY, G. M. & TOOZE, R. M. 2014. SPIB and

BATF provide alternate determinants of IRF4 occupancy in diffuse large B cell lymphoma linked to disease heterogeneity. *Nucleic Acids Res,* 42**,** 7591-610.

CHANG, J. J. & ALTFELD, M. 2009. TLR-mediated immune activation in HIV. *Blood,* 113**,** 269-70.

CHANG, J. J., LACAS, A., LINDSAY, R. J., DOYLE, E. H., AXTEN, K. L., PEREYRA, F., ROSENBERG, E. S., WALKER, B. D., ALLEN, T. M. & ALTFELD, M. 2012. Differential regulation of toll-like receptor pathways in acute and chronic HIV-1 infection. *AIDS,* 26**,** 533-41.

CHANG, T. P. & VANCUROVA, I. 2014. Bcl3 regulates pro-survival and pro-inflammatory gene expression in cutaneous T-cell lymphoma. *Biochim Biophys Acta,* 1843**,** 2620-30.

CHAUDHURI, A., YANG, B., GENDELMAN, H. E., PERSIDSKY, Y. & KANMOGNE, G. D. 2008. STAT1 signaling modulates HIV-1–induced inflammatory responses and leukocyte transmigration across the blood-brain barrier. *Blood,* 111**,** 2062-2072.

CHEN, L. F. & GREENE, W. C. 2004. Shaping the nuclear action of NF-kappaB. *Nat Rev Mol Cell Biol,* 5**,** 392-401.

CHIBA, T., INOKO, H., KIMURA, M. & SATO, T. 2013. Role of nuclear IkappaBs in inflammation regulation. *Biomol Concepts,* 4**,** 187-96.

CI, W., POLO, J. M., CERCHIETTI, L., SHAKNOVICH, R., WANG, L., YANG, S. N., YE, K., FARINHA, P., HORSMAN, D. E., GASCOYNE, R. D., ELEMENTO, O. & MELNICK, A. 2009. The BCL6 transcriptional program features repression of multiple oncogenes in primary B cells and is deregulated in DLBCL. *Blood,* 113**,** 5536-48.

COMPAGNO, M., LIM, W. K., GRUNN, A., NANDULA, S. V., BRAHMACHARY, M., SHEN, Q., BERTONI, F., PONZONI, M., SCANDURRA, M., CALIFANO, A., BHAGAT, G., CHADBURN, A., DALLA-FAVERA, R. & PASQUALUCCI, L. 2009. Mutations of multiple genes cause deregulation of NF-kappaB in diffuse large B cell lymphoma. *Nature,* 459**,** 717-21.

DAECKE, J., FACKLER, O. T., DITTMAR, M. T. & KRAUSSLICH, H. G. 2005. Involvement of clathrin-mediated endocytosis in human immunodeficiency virus type 1 entry. *J Virol,* 79**,** 1581-94.

DAVIS, R. E., BROWN, K. D., SIEBENLIST, U. & STAUDT, L. M. 2001. Constitutive Nuclear Factor B Activity Is Required for Survival of Activated B Cell–like Diffuse Large B Cell Lymphoma Cells. *The Journal of Experimental Medicine,* 194**,** 1861-1874.

DELUCA, C., KWON, H., PELLETIER, N., WAINBERG, M. A. & HISCOTT, J. 1998. NF-κB Protects HIV-1-Infected Myeloid Cells from Apoptosis. *Virology,* 244**,** 27-38.

DELVES, P. J. & ROITT, I. M. 2000. The immune system. First of two parts. *N Engl J Med,* 343**,** 37-49.

DING, B. B., YU, J. J., YU, R. Y., MENDEZ, L. M., SHAKNOVICH, R., ZHANG, Y., CATTORETTI, G. & YE, B. H. 2008. Constitutively activated STAT3 promotes cell proliferation and survival in the activated B cell subtype of diffuse large B cell lymphomas. *Blood,* 111**,** 1515-23.

DOITSH, G., CAVROIS, M., LASSEN, K. G., ZEPEDA, O., YANG, Z., SANTIAGO, M. L., HEBBELER, A. M. & GREENE, W. C. 2010. Abortive HIV infection mediates CD4 T cell depletion and inflammation in human lymphoid tissue. *Cell,* 143**,** 789-801.

DYNLACHT, B. D., HOEY, T. & TJIAN, R. Isolation of coactivators associated with the TATA-binding protein that mediate transcriptional activation. *Cell,* 66**,** 563-576.

EBNER, K., BANDION, A., BINDER, B. R., DE MARTIN, R. & SCHMID, J. A. 2003. GMCSF activates NF-kappaB via direct interaction of the GMCSF receptor with IkappaB kinase beta. *Blood,* 102**,** 192-9.

ENGELMAN, A., MIZUUCHI, K. & CRAIGIE, R. 1991. HIV-1 DNA integration: Mechanism of viral DNA cleavage and DNA strand transfer. *Cell,* 67**,** 1211-1221.

FERCH, U., KLOO, B., GEWIES, A., PFANDER, V., DUWEL, M., PESCHEL, C., KRAPPMANN, D. & RULAND, J. 2009. Inhibition of MALT1 protease activity is selectively toxic for activated B cell-like diffuse large B cell lymphoma cells. *J Exp Med,* 206**,** 2313-20.

FIORINI, E., SCHMITZ, I., MARISSEN, W. E., OSBORN, S. L., TOUMA, M., SASADA, T., RECHE, P. A., TIBALDI, E. V., HUSSEY, R. E., KRUISBEEK, A. M., REINHERZ, E. L. & CLAYTON, L. K. 2002. Peptide-Induced Negative Selection of Thymocytes Activates Transcription of an NF-KB Inhibitor. *Molecular Cell,* 9**,** 637-648.

FLANNAGAN, R. S., JAUMOUILLE, V. & GRINSTEIN, S. 2012. The cell biology of phagocytosis. *Annu Rev Pathol,* 7**,** 61-98.

FLORY, E., WEBER, C. K., CHENG, P., HOFFMEYER, A., JASSOY, C. & RAPP, U. R. 1998. Plasma Membrane-Targeted Raf Kinase Activates NF-kB and Human Immunodeficiency Virus Type 1 Replication in T Lymphocytes. *Journal of Virology,* 72**,** 2788-2794.

FREIRE-DE-LIMA, C. G., XIAO, Y. Q., GARDAI, S. J., BRATTON, D. L., SCHIEMANN, W. P. & HENSON, P. M. 2006. Apoptotic cells, through transforming growth factor-beta, coordinately induce anti-inflammatory and suppress pro-inflammatory eicosanoid and NO synthesis in murine macrophages. *J Biol Chem,* 281**,** 38376-84.

GASIUNAS, G., BARRANGOU, R., HORVATH, P. & SIKSNYS, V. 2012. Cas9-crRNA ribonucleoprotein complex mediates specific DNA cleavage for adaptive immunity in bacteria. *Proc Natl Acad Sci U S A,* 109**,** E2579-86.

GEISSMANN, F., JUNG, S. & LITTMAN, D. R. 2003. Blood monocytes consist of two principal subsets with distinct migratory properties. *Immunity,* 19**,** 71-82.

GÉRARDIN, J. A., BAISE, E. A., PIRE, G. A., LEROY, M. P. P. & DESMECHT, D. J. M. 2004. Genomic structure, organisation, and promoter analysis of the bovine (Bos taurus) Mx1 gene. *Gene,* 326**,** 67-75.

GERONDAKIS, S., GROSSMANN, M., NAKAMURA, Y., POHL, T. & GRUMONT, R. 1999. Genetic approaches in mice to understand Rel/NF-kappaB and IkappaB function: transgenics and knockouts. *Oncogene,* 18**,** 6888-95.

GERONDAKIS, S. & SIEBENLIST, U. 2010. Roles of the NF-kappaB pathway in lymphocyte development and function. *Cold Spring Harb Perspect Biol,* 2**,** a000182.

GOHDA, J., MATSUMURA, T. & INOUE, J. I. 2004. Cutting Edge: TNFR-Associated Factor (TRAF) 6 Is Essential for MyD88-Dependent Pathway but Not Toll/IL-1 Receptor Domain-Containing Adaptor-Inducing IFN- (TRIF)-Dependent Pathway in TLR Signaling. *The Journal of Immunology,* 173**,** 2913-2917.

GORANSSON, M., ANDERSSON, M. K., FORNI, C., STAHLBERG, A., ANDERSSON, C., OLOFSSON, A., MANTOVANI, R. & AMAN, P. 2009. The myxoid liposarcoma FUS-DDIT3 fusion oncoprotein deregulates NF-kappaB target genes by interaction with NFKBIZ. *Oncogene,* 28**,** 270-8.

GORDON, S. & TAYLOR, P. R. 2005. Monocyte and macrophage heterogeneity. *Nat Rev Immunol,* 5**,** 953-64.

GOUDEAU, B., HUETZ, F., SAMSON, S., DI SANTO, J. P., CUMANO, A., BEG, A., ISRAEL, A. & MEMET, S. 2003. IkappaBalpha/IkappaBepsilon deficiency reveals that a critical NF-kappaB dosage is required for lymphocyte survival. *Proc Natl Acad Sci U S A,* 100**,** 15800-5.

GRAHAM, F. L. & VAN DER EB, A. J. 1973. A new technique for the assay of infectivity of human adenovirus 5 DNA. *Virology,* 52**,** 456-467.

GREEN, M. R., MONTI, S., RODIG, S. J., JUSZCZYNSKI, P., CURRIE, T., O'DONNELL, E., CHAPUY, B., TAKEYAMA, K., NEUBERG, D., GOLUB, T. R., KUTOK, J. L. & SHIPP, M. A. 2010. Integrative analysis reveals selective 9p24.1 amplification, increased PD-1 ligand expression, and further induction via JAK2 in nodular sclerosing Hodgkin lymphoma and primary mediastinal large B cell lymphoma. *Blood,* 116**,** 3268-77.

GUILLOTON, F., CARON, G., MENARD, C., PANGAULT, C., AME-THOMAS, P., DULONG, J., DE VOS, J., ROSSILLE, D., HENRY, C., LAMY, T., FOUQUET, O., FEST, T. & TARTE, K. 2012. Mesenchymal stromal cells orchestrate follicular lymphoma cell niche through the CCL2-dependent recruitment and polarization of monocytes. *Blood,* 119**,** 2556-67.

GUITER, C., DUSANTER-FOURT, I., COPIE-BERGMAN, C., BOULLAND, M. L., LE GOUVELLO, S., GAULARD, P., LEROY, K. & CASTELLANO, F. 2004. Constitutive STAT6 activation in primary mediastinal large B cell lymphoma. *Blood,* 104**,** 543-9.

GUO, H., GAO, J., TAXMAN, D. J., TING, J. P. & SU, L. 2014. HIV-1 infection induces interleukin-1beta production via TLR8 protein-dependent and NLRP3 inflammasome mechanisms in human monocytes. *J Biol Chem,* 289**,** 21716-26.

HAILFINGER, S., LENZ, G., NGO, V., POSVITZ-FEJFAR, A., REBEAUD, F., GUZZARDI, M., PENAS, E.-M. M., DIERLAMM, J., CHAN, W. C., STAUDT, L. M. & THOME, M. 2009. Essential role of MALT1 protease activity in activated B cell-like diffuse large B cell

lymphoma. *Proceedings of the National Academy of Sciences of the United States of America,* 106**,** 19946-19951.
HAYDEN, M. S. & GHOSH, S. 2011. NF-kappaB in immunobiology. *Cell Res,* 21**,** 223-44.
HAYDEN, M. S. & GHOSH, S. 2012. NF-kappaB, the first quarter-century: remarkable progress and outstanding questions. *Genes Dev,* 26**,** 203-34.
HIROTANI, T., LEE, P. Y., KUWATA, H., YAMAMOTO, M., MATSUMOTO, M., KAWASE, I., AKIRA, S. & TAKEDA, K. 2005. The Nuclear I B Protein I BNS Selectively Inhibits Lipopolysaccharide-Induced IL-6 Production in Macrophages of the Colonic Lamina Propria. *The Journal of Immunology,* 174**,** 3650-3657.
HISCOTT, J., ALPER, D., COHEN, L., LEBLANC, J. F., SPORTZA, L., WONG, A. & XANTHOUDAKIS, S. 1989. Induction of human interferon gene expression is associated with a nuclear factor that interacts with the NF-kappa B site of the human immunodeficiency virus enhancer. *J Virol,* 63**,** 2557-2566.
HISCOTT, J., KWON, H. & GÉNIN, P. 2001. Hostile takeovers: viral appropriation of the NF-kappaB pathway. *Journal of Clinical Investigation,* 107**,** 143-51.
HU, S., XU-MONETTE, Z. Y., TZANKOV, A., GREEN, T., WU, L., BALASUBRAMANYAM, A., LIU, W. M., VISCO, C., LI, Y., MIRANDA, R. N., MONTES-MORENO, S., DYBKAER, K., CHIU, A., ORAZI, A., ZU, Y., BHAGAT, G., RICHARDS, K. L., HSI, E. D., CHOI, W. W., ZHAO, X., VAN KRIEKEN, J. H., HUANG, Q., HUH, J., AI, W., PONZONI, M., FERRERI, A. J., ZHOU, F., SLACK, G. W., GASCOYNE, R. D., TU, M., VARIAKOJIS, D., CHEN, W., GO, R. S., PIRIS, M. A., MOLLER, M. B., MEDEIROS, L. J. & YOUNG, K. H. 2013. MYC/BCL2 protein coexpression contributes to the inferior survival of activated B cell subtype of diffuse large B cell lymphoma and demonstrates high-risk gene expression signatures: a report from The International DLBCL Rituximab-CHOP Consortium Program. *Blood,* 121**,** 4021-31; quiz 4250.
HUTCHINS, A. P., DIEZ, D. & MIRANDA-SAAVEDRA, D. 2013. The IL-10/STAT3-mediated anti-inflammatory response: recent developments and future challenges. *Brief Funct Genomics,* 12**,** 489-98.
IBRAHIM, H. A., AMEN, F., REID, A. G. & NARESH, K. N. 2011a. BCL3 rearrangement, amplification and expression in diffuse large B cell lymphoma. *Eur J Haematol,* 87**,** 480-5.
IBRAHIM, H. A. H., AMEN, F., REID, A. G. & NARESH, K. N. 2011b. BCL3 rearrangement, amplification and expression in diffuse large B cell lymphoma. *European Journal of Haematology,* 87**,** 480-485.
IQBAL, J., NEPPALLI, V. T., WRIGHT, G., DAVE, B. J., HORSMAN, D. E., ROSENWALD, A., LYNCH, J., HANS, C. P., WEISENBURGER, D. D., GREINER, T. C., GASCOYNE, R. D., CAMPO, E., OTT, G., MULLER-HERMELINK, H. K., DELABIE, J., JAFFE, E. S., GROGAN, T. M., CONNORS, J. M., VOSE, J. M., ARMITAGE, J. O., STAUDT, L. M. & CHAN, W. C. 2006. BCL2 expression is a prognostic marker for the activated B cell-like type of diffuse large B cell lymphoma. *J Clin Oncol,* 24**,** 961-8.
JEFFREY, K. L., BRUMMER, T., ROLPH, M. S., LIU, S. M., CALLEJAS, N. A., GRUMONT, R. J., GILLIERON, C., MACKAY, F., GREY, S., CAMPS, M., ROMMEL, C., GERONDAKIS, S. D. & MACKAY, C. R. 2006. Positive regulation of immune cell function and inflammatory responses by phosphatase PAC-1. *Nat Immunol,* 7**,** 274-283.
JINEK, M., CHYLINSKI, K., FONFARA, I., HAUER, M., DOUDNA, J. A. & CHARPENTIER, E. 2012. A Programmable Dual-RNA–Guided DNA Endonuclease in Adaptive Bacterial Immunity. *Science,* 337**,** 816-821.
JUNG, D., GIALLOURAKIS, C., MOSTOSLAVSKY, R. & ALT, F. W. 2006. Mechanism and control of V(D)J recombination at the immunoglobulin heavy chain locus. *Annu Rev Immunol,* 24**,** 541-70.
KARIN, M. 2009. NF-kappaB as a critical link between inflammation and cancer. *Cold Spring Harb Perspect Biol,* 1**,** a000141.
KAYAMA, H., RAMIREZ-CARROZZI, V. R., YAMAMOTO, M., MIZUTANI, T., KUWATA, H., IBA, H., MATSUMOTO, M., HONDA, K., SMALE, S. T. & TAKEDA, K. 2008. Class-specific regulation of pro-inflammatory genes by MyD88 pathways and IkappaBzeta. *J Biol Chem,* 283**,** 12468-77.

KIM, J. A., KIM, S. J., DO, I.-G., JIN, J., NAM, D.-H., KO, Y. H., KIM, K. & SEOG KIM, W. 2011. Hypoxia-associated protein expression in primary central nervous system diffuse large B cell lymphoma: does it predict prognosis? *Leukemia & Lymphoma,* 52**,** 205-213.

KITAMURA, H., KANEHIRA, K., MORIMATSU, K. O. & SAITO, M. 2000. MAIL, a novel nuclear IkB protein that potentiates LPS-induced IL-6 production. *FEBS Letters,* 485**,** 53-56.

KLEIN, U., CASOLA, S., CATTORETTI, G., SHEN, Q., LIA, M., MO, T., LUDWIG, T., RAJEWSKY, K. & DALLA-FAVERA, R. 2006. Transcription factor IRF4 controls plasma cell differentiation and class-switch recombination. *Nat Immunol,* 7**,** 773-82.

KOBAYASHI, S., HARA, A., ISAGAWA, T., MANABE, I., TAKEDA, K. & MARUYAMA, T. 2014. The nuclear IkappaB family protein IkappaBNS influences the susceptibility to experimental autoimmune encephalomyelitis in a murine model. *PLoS One,* 9**,** e110838.

KOHL, N. E., EMINI, E. A., SCHLEIF, W. A., DAVIS, L. J., HEIMBACH, J. C., DIXON, R. A., SCOLNICK, E. M. & SIGAL, I. S. 1988. Active human immunodeficiency virus protease is required for viral infectivity. *Proceedings of the National Academy of Sciences of the United States of America,* 85**,** 4686-4690.

KOIVULA, S., VALO, E., RAUNIO, A., HAUTANIEMI, S. & LEPPA, S. 2011. Rituximab regulates signaling pathways and alters gene expression associated with cell death and survival in diffuse large B cell lymphoma. *Oncol Rep,* 25**,** 1183-90.

KOJIMA, Y., TSURUMI, H., GOTO, N., SHIMIZU, M., KASAHARA, S., YAMADA, T., KANEMURA, N., HARA, T., SAWADA, M., SAIO, M., YAMADA, T., TAKAHASHI, T., TOMITA, E., TAKAMI, T. & MORIWAKI, H. 2006. Fas and Fas ligand expression on germinal center type-diffuse large B cell lymphoma is associated with the clinical outcome. *European Journal of Haematology,* 76**,** 465-472.

KOPPENSTEINER, H., BANNING, C., SCHNEIDER, C., HOHENBERG, H. & SCHINDLER, M. 2012. Macrophage internal HIV-1 is protected from neutralizing antibodies. *J Virol,* 86**,** 2826-36.

KUMAR, H., KAWAI, T. & AKIRA, S. 2011. Pathogen recognition by the innate immune system. *Int Rev Immunol,* 30**,** 16-34.

KUWATA, H., MATSUMOTO, M., ATARASHI, K., MORISHITA, H., HIROTANI, T., KOGA, R. & TAKEDA, K. 2006. IkappaBNS inhibits induction of a subset of Toll-like receptor-dependent genes and limits inflammation. *Immunity,* 24**,** 41-51.

KWON, H., PELLETIE, N., DELUCA, C., GENIN, P., CISTERNAS, S., LIN, R., WAINBERG, M. A. & HISCOTT, J. 1998. Inducible Expression of IkBa Repressor Mutants Interferes with NF-kB Activity and HIV-1 Replication in Jurkat T Cells. *The Journal of Biological Chemistry,* 273**,** 7431-7440.

LAM, L. T., WRIGHT, G., DAVIS, R. E., LENZ, G., FARINHA, P., DANG, L., CHAN, J. W., ROSENWALD, A., GASCOYNE, R. D. & STAUDT, L. M. 2008. Cooperative signaling through the signal transducer and activator of transcription 3 and nuclear factor-{kappa}B pathways in subtypes of diffuse large B cell lymphoma. *Blood,* 111**,** 3701-13.

LATZ, E., SCHOENEMEYER, A., VISINTIN, A., FITZGERALD, K. A., MONKS, B. G., KNETTER, C. F., LIEN, E., NILSEN, N. J., ESPEVIK, T. & GOLENBOCK, D. T. 2004. TLR9 signals after translocating from the ER to CpG DNA in the lysosome. *Nat Immunol,* 5**,** 190-8.

LENZ, G. & STAUDT, L. M. 2010. Aggressive lymphomas. *N Engl J Med,* 362**,** 1417-29.

LENZ, G., WRIGHT, G. W., EMRE, N. C., KOHLHAMMER, H., DAVE, S. S., DAVIS, R. E., CARTY, S., LAM, L. T., SHAFFER, A. L., XIAO, W., POWELL, J., ROSENWALD, A., OTT, G., MULLER-HERMELINK, H. K., GASCOYNE, R. D., CONNORS, J. M., CAMPO, E., JAFFE, E. S., DELABIE, J., SMELAND, E. B., RIMSZA, L. M., FISHER, R. I., WEISENBURGER, D. D., CHAN, W. C. & STAUDT, L. M. 2008. Molecular subtypes of diffuse large B cell lymphoma arise by distinct genetic pathways. *Proc Natl Acad Sci U S A,* 105**,** 13520-5.

LEVY, B. D., CLISH, C. B., SCHMIDT, B., GRONERT, K. & SERHAN, C. N. 2001. Lipid mediator class switching during acute inflammation: signals in resolution. *Nat Immunol,* 2**,** 612-9.

LIEBER, M. R. 2010. The Mechanism of Double-Strand DNA Break Repair by the Nonhomologous DNA End Joining Pathway. *Annual review of biochemistry,* 79**,** 181-211.

LOMAGA, M. A., YEH, W.-C., SAROSI, I., DUNCAN, G. S., FURLONGER, C., HO, A., MORONY, S., CAPPARELLI, C., VAN, G., KAUFMAN, S., VAN DER HEIDEN, A., ITIE, A., WAKEHAM, A., KHOO, W., SASAKI, T., CAO, Z., PENNINGER, J. M., PAIGE, C. J., LACEY, D. L., DUNSTAN, C. R., BOYLE, W. J., GOEDDEL, D. V. & MAK, T. W. 1999. TRAF6 deficiency results in osteopetrosis and defective interleukin-1, CD40, and LPS signaling. *Genes & Development,* 13**,** 1015-1024.

LOSSOS, I. S., CZERWINSKI, D. K., ALIZADEH, A. A., WECHSER, M. A., TIBSHIRANI, R., BOTSTEIN, D. & LEVY, R. 2004. Prediction of survival in diffuse large-B cell lymphoma based on the expression of six genes. *N Engl J Med,* 350**,** 1828-37.

LU, Y. C., YEH, W. C. & OHASHI, P. S. 2008. LPS/TLR4 signal transduction pathway. *Cytokine,* 42**,** 145-51.

LUU, K., GREENHILL, C. J., MAJOROS, A., DECKER, T., JENKINS, B. J. & MANSELL, A. 2014. STAT1 plays a role in TLR signal transduction and inflammatory responses. *Immunol Cell Biol,* 92**,** 761-9.

MAARTENS, G., CELUM, C. & LEWIN, S. R. 2014. HIV infection: epidemiology, pathogenesis, treatment, and prevention. *Lancet,* 384**,** 258-71.

MACKANESS, G. B. 1962. Cellular Resistance to Infection. *The Journal of Experimental Medicine,* 116**,** 381-406.

MANAVALAN, B., BASITH, S., CHOI, Y. M., LEE, G. & CHOI, S. 2010. Structure-function relationship of cytoplasmic and nuclear IkappaB proteins: an in silico analysis. *PLoS One,* 5**,** e15782.

MANKAN, A. K., LAWLESS, M. W., GRAY, S. G., KELLEHER, D. & MCMANUS, R. 2009. NF-kappaB regulation: the nuclear response. *J Cell Mol Med,* 13**,** 631-43.

MANNA, S. K. & AGGARWAL, B. B. 2000. Differential Requirement for p56lck in HIV-tat Versus TNF-Induced Cellular Responses: Effects on NF- B, Activator Protein-1, c-Jun N-Terminal Kinase, and Apoptosis. *The Journal of Immunology,* 164**,** 5156-5166.

MAO, M., BIERY, M. C., KOBAYASHI, S. V., WARD, T., SCHIMMACK, G., BURCHARD, J., SCHELTER, J. M., DAI, H., HE, Y. D. & LINSLEY, P. S. 2004. T lymphocyte activation gene identification by coregulated expression on DNA microarrays. *Genomics,* 83**,** 989-999.

MARSON, A., KRETSCHMER, K., FRAMPTON, G. M., JACOBSEN, E. S., POLANSKY, J. K., MACISAAC, K. D., LEVINE, S. S., FRAENKEL, E., VON BOEHMER, H. & YOUNG, R. A. 2007. Foxp3 occupancy and regulation of key target genes during T-cell stimulation. *Nature,* 445**,** 931-5.

MASSOUMI, R., CHMIELARSKA, K., HENNECKE, K., PFEIFER, A. & FASSLER, R. 2006. Cyld inhibits tumor cell proliferation by blocking Bcl-3-dependent NF-kappaB signaling. *Cell,* 125**,** 665-77.

MEERBREY, K. L., HU, G., KESSLER, J. D., ROARTY, K., LI, M. Z., FANG, J. E., HERSCHKOWITZ, J. I., BURROWS, A. E., CICCIA, A., SUN, T., SCHMITT, E. M., BERNARDI, R. J., FU, X., BLAND, C. S., COOPER, T. A., SCHIFF, R., ROSEN, J. M., WESTBROOK, T. F. & ELLEDGE, S. J. 2011. The pINDUCER lentiviral toolkit for inducible RNA interference in vitro and in vivo. *Proc Natl Acad Sci U S A,* 108**,** 3665-70.

MEYER, R., HATADA, E. N., HOHMANN, H.-P., HAIKER, M., BARTSCH, C., ROETHLISBERGER, U., LAHM, H.-W., SCHLAEGER, E. J., LOON, A. P. G. M. V. & SCHEIDEREIT, C. 1991. Cloning of the DNA-binding subunit of human nuclear factor cB: The level of its mRNA is strongly regulated by phorbol ester or tumor necrosis factor a. *Proceedings of the National Academy of Sciences of the United States of America,* 88**,** 966-970.

MIURA, M., HASEGAWA, N., NOGUCHI, M., SUGIMOTO, K. & TOUMA, M. 2016. The atypical IkappaB protein IkappaB(NS) is important for Toll-like receptor-induced interleukin-10 production in B cells. *Immunology,* 147**,** 453-63.

MOGENSEN, T. H. & PALUDAN, S. R. 2001. Molecular Pathways in Virus-Induced Cytokine Production. *Microbiology and Molecular Biology Reviews,* 65**,** 131-150.

MOSS, J. A. 2013. HIV/AIDS Review. *Radiologic Technology,* 84**,** 247-267.

MURRAY, P. J. & WYNN, T. A. 2011. Protective and pathogenic functions of macrophage subsets. 11**,** 723-737.

NALDINI, L., BLÖMER, U., GALLAY, P., ORY, D., MULLIGAN, R., GAGE, F. H., VERMA, I. M. & TRONO, D. 1996. In Vivo Gene Delivery and Stable Transduction of Nondividing Cells by a Lentiviral Vector. *Science,* 272**,** 263-267.

NOGAI, H., WENZEL, S. S., HAILFINGER, S., GRAU, M., KAERGEL, E., SEITZ, V., WOLLERT-WULF, B., PFEIFER, M., WOLF, A., FRICK, M., DIETZE, K., MADLE, H., TZANKOV, A., HUMMEL, M., DORKEN, B., SCHEIDEREIT, C., JANZ, M., LENZ, P., THOME, M. & LENZ, G. 2013. IkappaB-zeta controls the constitutive NF-kappaB target gene network and survival of ABC DLBCL. *Blood,* 122**,** 2242-50.

OHNO, H., TAKIMOTO, G. & MCKEITHAN, T. 1990. The candidate proto-oncogene bcl-3 is related to genes implicated in cell lineage determination and cell cycle control. *Cell,* 60**,** 991-997.

PARK, K. C., JEONG, J. & KIM, K. I. 2014. Regulation of mIkappaBNS stability through PEST-mediated degradation by proteasome. *Biochem Biophys Res Commun,* 443**,** 1291-5.

PASQUALUCCI, L., COMPAGNO, M., HOULDSWORTH, J., MONTI, S., GRUNN, A., NANDULA, S. V., ASTER, J. C., MURTY, V. V., SHIPP, M. A. & DALLA-FAVERA, R. 2006. Inactivation of the PRDM1/BLIMP1 gene in diffuse large B cell lymphoma. *J Exp Med,* 203**,** 311-7.

PEDERSEN, G. K., ADORI, M., KHOENKHOEN, S., DOSENOVIC, P., BEUTLER, B. & KARLSSON HEDESTAM, G. B. 2014. B-1a transitional cells are phenotypically distinct and are lacking in mice deficient in IkappaBNS. *Proc Natl Acad Sci U S A,* 111**,** E4119-26.

PEDERSEN, G. K., ADORI, M., STARK, J. M., KHOENKHOEN, S., ARNOLD, C., BEUTLER, B. & KARLSSON HEDESTAM, G. B. 2016. Heterozygous Mutation in IkappaBNS Leads to Reduced Levels of Natural IgM Antibodies and Impaired Responses to T-Independent Type 2 Antigens. *Front Immunol,* 7**,** 65.

RITZ, O., ROMMEL, K., DORSCH, K., KELSCH, E., MELZNER, J., BUCK, M., LEROY, K., PAPADOPOULOU, V., WAGNER, S., MARIENFELD, R., BRÜDERLEIN, S., LENNERZ, J. K. & MÖLLER, P. 2013. STAT6-mediated BCL6 repression in primary mediastinal B cell lymphoma (PMBL). *Oncotarget,* 4**,** 1093-1102.

ROSENBAUER, F. & TENEN, D. G. 2007. Transcription factors in myeloid development: balancing differentiation with transformation. *Nat Rev Immunol,* 7**,** 105-17.

ROSENWALD, A., WRIGHT, G., CHAN, W. C., CONNORS, J. M., CAMPO, E., FISHER, R. I., GASCOYNE, R. D., MULLER-HERMELINK, H. K., SMELAND, E. B., GILTNANE, J. M., HURT, E. M., ZHAO, H., AVERETT, L., YANG, L., WILSON, W. H., JAFFE, E. S., SIMON, R., KLAUSNER, R. D., POWELL, J., DUFFEY, P. L., LONGO, D. L., GREINER, T. C., WEISENBURGER, D. D., SANGER, W. G., DAVE, B. J., LYNCH, J. C., VOSE, J., ARMITAGE, J. O., MONTSERRAT, E., LOPEZ-GUILLERMO, A., GROGAN, T. M., MILLER, T. P., LEBLANC, M., OTT, G., KVALOY, S., DELABIE, J., HOLTE, H., KRAJCI, P., STOKKE, T., STAUDT, L. M. & LYMPHOMA/LEUKEMIA MOLECULAR PROFILING, P. 2002. The use of molecular profiling to predict survival after chemotherapy for diffuse large-B cell lymphoma. *N Engl J Med,* 346**,** 1937-47.

ROSENWALD, A., WRIGHT, G., LEROY, K., YU, X., GAULARD, P., GASCOYNE, R. D., CHAN, W. C., ZHAO, T., HAIOUN, C., GREINER, T. C., WEISENBURGER, D. D., LYNCH, J. C., VOSE, J., ARMITAGE, J. O., SMELAND, E. B., KVALOY, S., HOLTE, H., DELABIE, J., CAMPO, E., MONTSERRAT, E., LOPEZ-GUILLERMO, A., OTT, G., MULLER-HERMELINK, H. K., CONNORS, J. M., BRAZIEL, R., GROGAN, T. M., FISHER, R. I., MILLER, T. P., LEBLANC, M., CHIORAZZI, M., ZHAO, H., YANG, L., POWELL, J., WILSON, W. H., JAFFE, E. S., SIMON, R., KLAUSNER, R. D. & STAUDT, L. M. 2003. Molecular diagnosis of primary mediastinal B cell lymphoma identifies a clinically favorable subgroup of diffuse large B cell lymphoma related to Hodgkin lymphoma. *J Exp Med,* 198**,** 851-62.

SAITO, M., GAO, J., BASSO, K., KITAGAWA, Y., SMITH, P. M., BHAGAT, G., PERNIS, A., PASQUALUCCI, L. & DALLA-FAVERA, R. 2007. A signaling pathway mediating downregulation of BCL6 in germinal center B cells is blocked by BCL6 gene alterations in B cell lymphoma. *Cancer Cell,* 12**,** 280-92.

SAMSON, S. I., MEMET, S., VOSSHENRICH, C. A., COLUCCI, F., RICHARD, O., NDIAYE, D., ISRAEL, A. & DI SANTO, J. P. 2004. Combined deficiency in IkappaBalpha and

IkappaBepsilon reveals a critical window of NF-kappaB activity in natural killer cell differentiation. *Blood,* 103**,** 4573-80.

SAVAGE, K. J., MONTI, S., KUTOK, J. L., CATTORETTI, G., NEUBERG, D., DE LEVAL, L., KURTIN, P., DAL CIN, P., LADD, C., FEUERHAKE, F., AGUIAR, R. C., LI, S., SALLES, G., BERGER, F., JING, W., PINKUS, G. S., HABERMANN, T., DALLA-FAVERA, R., HARRIS, N. L., ASTER, J. C., GOLUB, T. R. & SHIPP, M. A. 2003. The molecular signature of mediastinal large B cell lymphoma differs from that of other diffuse large B cell lymphomas and shares features with classical Hodgkin lymphoma. *Blood,* 102**,** 3871-9.

SCANDURRA, M., MIAN, M., GREINER, T. C., RANCOITA, P. M. V., DE CAMPOS, C. P., CHAN, W. C., VOSE, J. M., CHIGRINOVA, E., INGHIRAMI, G., CHIAPPELLA, A., BALDINI, L., PONZONI, M., FERRERI, A. J. M., FRANCESCHETTI, S., GAIDANO, G., MONTES-MORENO, S., PIRIS, M. A., FACCHETTI, F., TUCCI, A., NOMDEDEU, J. F., LAZURE, T., LAMBOTTE, O., UCCELLA, S., PINOTTI, G., PRUNERI, G., MARTINELLI, G., YOUNG, K. H., TIBILETTI, M. G., RINALDI, A., ZUCCA, E., KWEE, I. & BERTONI, F. 2010. Genomic lesions associated with a different clinical outcome in diffuse large B cell lymphoma treated with R-CHOP-21. *British Journal of Haematology,* 151**,** 221-231.

SCHUITEMAKER, H., A.KOOTSTRA, N., A.M.FOUCHIER, R., HOOIBRINK, B. & MIEDEMA, F. 1994. Productive HIV-1 infection of macrophages restricted to the cell fraction with proliferative capacity. *The EMBO Journal,* 13**,** 5929-5936.

SCHUSTER, M., ANNEMANN, M., PLAZA-SIRVENT, C. & SCHMITZ, I. 2013. Atypical IκB proteins – nuclear modulators of NF-κB signaling. *Cell Communication and Signaling,* 11**,** 23-23.

SCHUSTER, M., GLAUBEN, R., PLAZA-SIRVENT, C., SCHREIBER, L., ANNEMANN, M., FLOESS, S., KUHL, A. A., CLAYTON, L. K., SPARWASSER, T., SCHULZE-OSTHOFF, K., PFEFFER, K., HUEHN, J., SIEGMUND, B. & SCHMITZ, I. 2012. IkappaB(NS) protein mediates regulatory T cell development via induction of the Foxp3 transcription factor. *Immunity,* 37**,** 998-1008.

SEN, R. & BALTIMORE, D. 1986. Multiple nuclear factors interact with the immunoglobulin enhancer sequences. *Cell,* 46**,** 705-716.

SHAFFER, A. L., LIN, K.-I., KUO, T. C., YU, X., HURT, E. M., ROSENWALD, A., GILTNANE, J. M., YANG, L., ZHAO, H., CALAME, K. & STAUDT, L. M. 2002. Blimp-1 Orchestrates Plasma Cell Differentiation by Extinguishing the Mature B Cell Gene Expression Program. *Immunity,* 17**,** 51-62.

SHALEM, O., SANJANA, N. E., HARTENIAN, E., SHI, X., SCOTT, D. A., MIKKELSON, T., HECKL, D., EBERT, B. L., ROOT, D. E., DOENCH, J. G. & ZHANG, F. 2014. Genome-scale CRISPR-Cas9 knockout screening in human cells. *Science,* 343**,** 84-87.

SHAROVA, N., SWINGLER, C., SHARKEY, M. & STEVENSON, M. 2005. Macrophages archive HIV-1 virions for dissemination in trans. *EMBO,* 24**,** 2481-2489.

SHIRAKAWA, F. & MIZEL, S. B. 1989. In Vitro Activation and Nuclear Translocation of NF-KB Catalyzed by Cyclic AMP-Dependent Protein Kinase and Protein Kinase C. *Molecular Cell Biology,* 9**,** 2424-2430.

SLACK, J. L., SCHOOLEY, K., BONNERT, T. P., MITCHAM, J. L., QWARNSTROM, E. E., SIMS, J. E. & DOWER, S. K. 2000. Identification of Two Major Sites in the Type I Interleukin-1 Receptor Cytoplasmic Region Responsible for Coupling to Pro-inflammatory Signaling Pathways. *The Journal of Biological Chemistry,* 275**,** 4670-4678.

SMITH, M. F., EIDLEN, D., AREND, W. P. & GUTIERREZ-HARTMANN, A. 1994. LPS-induced expression of the human IL-1 receptor antagonist gene is controlled by multiple interacting promoter elements. *The Journal of Immunology,* 153**,** 3584-3593.

SOUDJA, S. M., CHANDRABOS, C., YAKOB, E., VEENSTRA, M., PALLISER, D. & LAUVAU, G. 2014. Memory-T-cell-derived interferon-gamma instructs potent innate cell activation for protective immunity. *Immunity,* 40**,** 974-88.

SQUARIZE, C. H., CASTILHO, R. M., SRIURANPONG, V., PINTO, D. S., JR. & GUTKIND, J. S. 2006. Molecular cross-talk between the NFkappaB and STAT3 signaling pathways in head and neck squamous cell carcinoma. *Neoplasia,* 8**,** 733-46.

STEWART, S. A., DYKXHOORN, D. M., PALLISER, D., MIZUNO, H., YU, E. Y., AN, D. S., SABATINI, D. M., CHEN, I. S. Y., HAHN, W. C., SHARP, P. A., WEINBERG, R. A. & NOVIN, C. D. 2003. Lentivirus-delivered stable gene silencing by RNAi in primary cells. *Rna,* 9**,** 493-501.

STEWART, S. A., POON, B., SONG, J. Y. & CHEN, I. S. Y. 2000. Human Immunodeficiency Virus Type 1 Vpr Induces Apoptosis through Caspase Activation. *Journal of Virology,* 74**,** 3105-3111.

TAO, Z., FUSCO, A., HUANG, D. B., GUPTA, K., YOUNG KIM, D., WARE, C. F., VAN DUYNE, G. D. & GHOSH, G. 2014. p100/IkappaBdelta sequesters and inhibits NF-kappaB through kappaBsome formation. *Proc Natl Acad Sci U S A,* 111**,** 15946-51.

TOUMA, M., ANTONINI, V., KUMAR, M., OSBORN, S. L., BOBENCHIK, A. M., KESKIN, D. B., CONNOLLY, J. E., GRUSBY, M. J., REINHERZ, E. L. & CLAYTON, L. K. 2007. Functional Role for Iκ BNS in T Cell Cytokine Disruption. *The Journal of Immunology,* 179**,** 1681-1692.

TOUMA, M., KESKIN, D. B., SHIROKI, F., SAITO, I., KOYASU, S., REINHERZ, E. L. & CLAYTON, L. K. 2011. Impaired B cell development and function in the absence of IkappaBNS. *J Immunol,* 187**,** 3942-52.

TRINH, D. V., ZHU, N., FARHANG, G., KIM, B. J. & HUXFORD, T. 2008. The Nuclear IκB Protein IκBζ Specifically Binds NF-κB p50 Homodimers and Forms a Ternary Complex on κB DNA. *Journal of Molecular Biology,* 379**,** 122-135.

TSUCHIYA, S., YAMABE, M., YAMAGUCHI, Y., KOBAYASHI, Y., KONNO, T. & TADA, K. 1980. Establishment and characterization of a human acute monocytic leukemia cell line (THP-1). *International Journal of Cancer,* 26**,** 171-176.

UEMATSU, S. & AKIRA, S. 2007. Toll-like receptors and Type I interferons. *J Biol Chem,* 282**,** 15319-23.

WANG, N., LIANG, H. & ZEN, K. 2014. Molecular mechanisms that influence the macrophage m1-m2 polarization balance. *Front Immunol,* 5**,** 614.

WIDMER, U., MANOGUE, K. R., CERAMI, A. & SHERRY, B. 1993. Genomic cloning and promoter analysis of macrophage inflammatory protein (MIP)-2, MIP-1 alpha, and MIP-1 beta, members of the chemokine superfamily of proinflammatory cytokines. *The Journal of Immunology,* 150**,** 4996-5012.

WRIGHT, G., TAN, B., ROSENWALD, A., HURT, E. H., WIESTNER, A. & STAUDT, L. M. 2003. A gene expression-based method to diagnose clinically distinct subgroups of diffuse large B cell lymphoma. *Proceedings of the National Academy of Sciences of the United States of America,* 100**,** 9991-9996.

WU, Z., ZHANG, X., YANG, J., WU, G., ZHANG, Y., YUAN, Y., JIN, C., CHANG, Z., WANG, J., YANG, X. & HE, F. 2009. Nuclear protein IkappaB-zeta inhibits the activity of STAT3. *Biochem Biophys Res Commun,* 387**,** 348-52.

YAMAMOTO, M., YAMAZAKI, S., UEMATSU, S., SATO, S., HEMMI, H., HOSHINO, K., KAISHO, T., KUWATA, H., TAKEUCHI, O., TAKESHIGE, K., SAITOH, T., YAMAOKA, S., YAMAMOTO, N., YAMAMOTO, S., MUTA, T., TAKEDA, K. & AKIRA, S. 2004. Regulation of Toll/IL-1-receptor-mediated gene expression by the inducible nuclear protein IκBζ. *Nature,* 430**,** 218-222.

YAMASAKI, S., ISHIKAWA, E., SAKUMA, M., HARA, H., OGATA, K. & SAITO, T. 2008. Mincle is an ITAM-coupled activating receptor that senses damaged cells. *Nat Immunol,* 9**,** 1179-88.

YAMAZAKI, S., MUTA, T. & TAKESHIGE, K. 2001. A novel IkappaB protein, IkappaB-zeta, induced by proinflammatory stimuli, negatively regulates nuclear factor-kappaB in the nuclei. *J Biol Chem,* 276**,** 27657-62.

YANG, Y., SHAFFER, A. L., 3RD, EMRE, N. C., CERIBELLI, M., ZHANG, M., WRIGHT, G., XIAO, W., POWELL, J., PLATIG, J., KOHLHAMMER, H., YOUNG, R. M., ZHAO, H., YANG, Y., XU, W., BUGGY, J. J., BALASUBRAMANIAN, S., MATHEWS, L. A., SHINN, P., GUHA, R., FERRER, M., THOMAS, C., WALDMANN, T. A. & STAUDT, L. M. 2012. Exploiting synthetic lethality for the therapy of ABC diffuse large B cell lymphoma. *Cancer Cell,* 21**,** 723-37.

12. Appendix

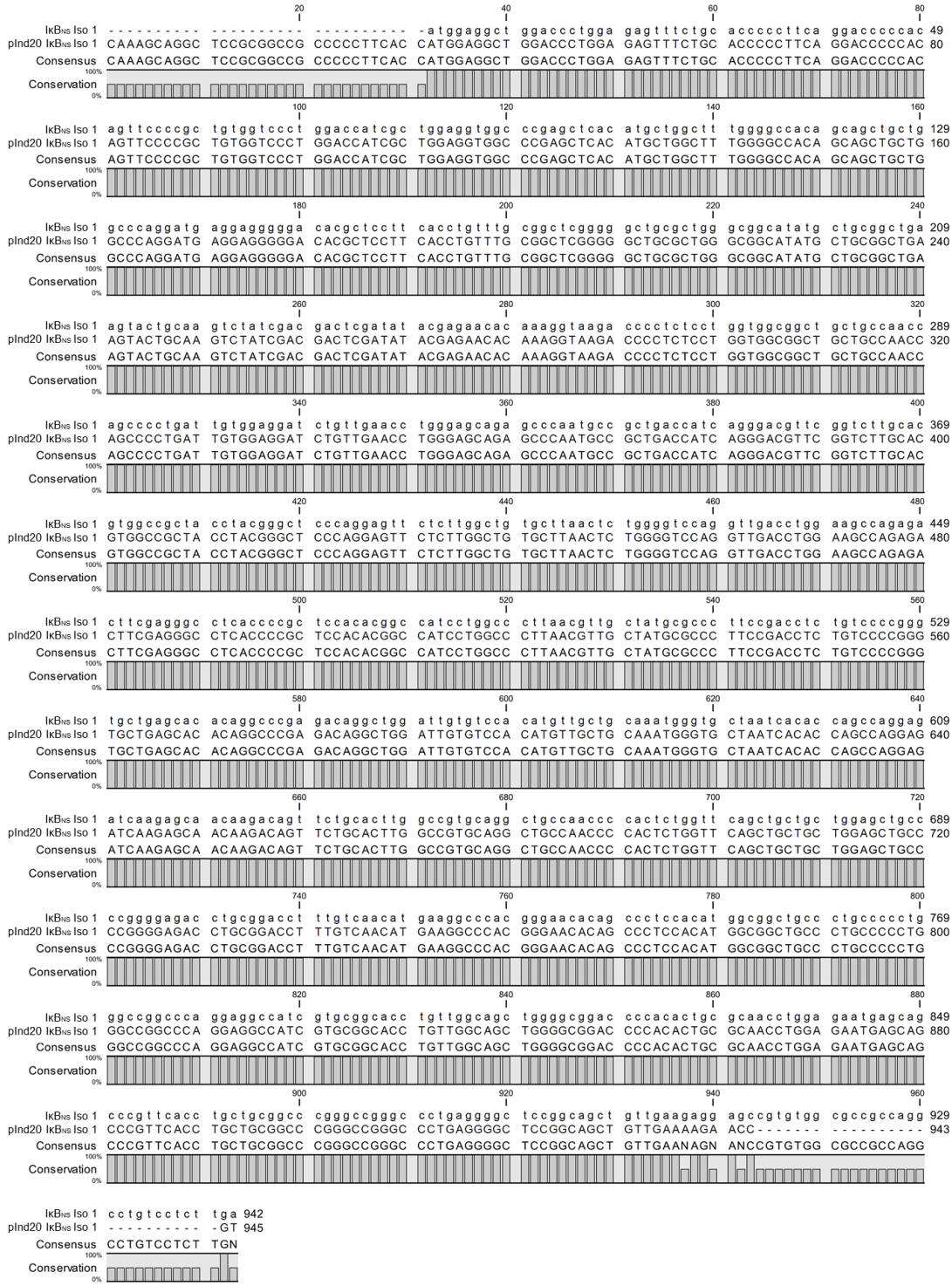

Figure 12.1: Alignment of a reference sequence of IκB$_{NS}$ isoform 1 and the sequencing result of the pInd20 IκB$_{NS}$ isoform 1 clone later used for our experiment.

The sequence starts 31 bases upstream from the start codon of IκB$_{NS}$ isoform 1. From the start codon, it is 100 % identical to the IκB$_{NS}$ isoform 1 reference sequence until base 936 of the plasmid sequence. Since this sequencing method is only reliable until approximately 900 bp from the start of the sequencing, we can assume that the sequence inserted into the plasmid is indeed IκB$_{NS}$ isoform 1.

13. Personal contribution and affidavit

This work was conducted in the laboratory of molecular medicine of the interfaculty institute for biochemistry under the support of my supervisor Prof. Dr. Klaus Schulze-Osthoff.

All experiments were performed by myself and all figures were made by myself. The figures in the introduction part were based on the sources cited in the legends.

Hereby I declare that I prepared the MD Thesis: "The role of $I\kappa B_{NS}$ regulator of NFκB in macrophages and diffuse large B cell lymphomas" on my own and with no other sources and aids than quoted.

Tübingen, 03.07.2018

Ronald Keller

14. Acknowledgment

First of all, I would like to thank Prof. Dr. Klaus Schulze-Osthoff for the opportunity to work in the laboratory of molecular medicine of the interfaculty institute for biochemistry, his help during the application for the IZKF and his thorough corrections during the fabrication of this thesis.

I especially like to thank Sebastian Lorscheid for his constant support and tutoring during the whole time.

Huge thanks also go to Dr. Stephan Hailfinger for his help in the design of the DLBCL-related experiments and to Dr. Daniela Kramer for her help in the design of the macrophage-related experiments.

Moreover, I like to thank my family and friends for their support and especially my parents Petra and Wolfgang Keller for always having been there for me.

I want to give special thanks to my partner Juliane Nitsch for intense discussions and helpful suggestions throughout the whole time.

Furthermore, I thank my fellow students in the IZKF-Promotionskolleg for discussions, ideas and help.

Tübingen, 03.07.2018

Ronald Keller